
# Intelligent Control System Design for Energy Conservation in Commercial Buildings

Hao Huang

School of Mechanical Engineering

Faculty of Engineering, Mathematical and Computer Sciences

The University of Adelaide

South Australia, 5005

Australia

A thesis submitted in fulfilment of the requirements for the degree of

Doctor of Philosophy

February 22, 2016

# Abstract

This thesis focuses on the development of model predictive control (MPC) strategies for reducing energy consumption in air-conditioned buildings. It is well known that the building sector is responsible for 40 per cent of the world's energy usage and 33 per cent of all greenhouse emissions. As a result of global environmental issues and decreasing energy resources, there is strong motivation to develop more efficient control strategies for Heating, Ventilation, and Air Conditioning (HVAC) systems in buildings. The existing HVAC control strategies are not energy or cost efficient, which results in energy waste, high on-peak electricity demand and poor thermal comfort in buildings.

Previous works have shown that MPC can be utilised as a supervisory controller to achieve energy saving while maintaining the indoor thermal comfort in buildings. However, most of the past studies were focused on small residential buildings or mid-size commercial buildings. It is highly desired to improve the existing MPC strategies to make them more reliable and applicable for large commercial buildings. This thesis extends the previous works by addressing the following challenges when dealing with the large buildings. Firstly, HVAC plants and the thermal dynamics of buildings are inherently nonlinear. Accurate modelling of these components is difficult due to the limited number of sensors that are usually installed and the paucity of prior knowledge of the system. There is a need to develop models that are capable of effectively handling the nonlinearity to achieve better modelling accuracy. Secondly, in large commercial buildings with adjacent large open spaces, the effects of thermal coupling between differently

controlled spaces play a crucial role. This significance of the interaction between zones has seldom been discussed before and requires more thorough investigation. Thirdly, although load shifting function of MPC have been proven to be effective in achieving cost savings in buildings with a considerable thermal mass, it is demanding to investigate the application value of these strategies in lightweight commercial buildings. Finally, given the presence of uncertainties, these models may not be able to predict the indoor temperature accurately, which may lead to poor control performance and even instability in operation of the MPC strategy. The existing robust control approaches are generally too conservative, and may not be suitable for use in real-world buildings.

In this study, the advantages of neural networks (NNs) will be exploited to address the challenges outlined above. NNs are known as universal approximators, meaning that they can model any continuous functions with any desired degree of accuracy. In particular, the NNs will be used to conduct modelling work, generate control rule, and improve the performance of classical MPC. The major contributions of this thesis are presented in four chapters, with each based on an individual scientific paper.

*Paper-1* presents a systematic modelling method for air handling units (AHUs) and thermal zone using a recursive NN (RNN). As the major novelty, a cascade NN structure is developed, which enables the thermal dynamics modelling of both interior zones and perimeter zones within investigated building. This approach allows accurate prediction of both supply air temperature and zone temperature prediction, making it suitable for predictive control design.

Continuing with the first paper, *Paper-2* introduces a multi-input, multi-output (MIMO) model, which effectively models the convective heat exchange between open spaces within multi-zone commercial buildings. The proposed model allows closed-loop prediction for several adjacent zones simultaneously by considering their thermal interaction. A NN-based optimal start-stop control method is also developed in this paper to demonstrate the energy saving potential enabled by using the proposed predictive model.

The NN models provide accurate prediction results, but they are in general difficult to optimise under an MPC framework. *Paper-3* presents a hybrid MPC (HMPC), which combines the classic MPC with an inverse NN model. With the HMPC, the classical MPC based on linearised building model optimises the supplied cooling energy. The inverse NN model compensates the nonlinearity associated with the AHU process and generates more accurate control inputs. Simulations and experiments demonstrate the feasibility of the proposed method in achieving energy and cost reductions while maintaining good indoor thermal comfort in the investigated large commercial building.

The MPC formulation in *Paper-3* does not take the system uncertainty into account. In reality, however, the modelled building energy systems are always affected by uncertainties, so that the modelling errors become inevitable which cause control performance degradation to the MPC. *Paper-4* considers the application of a robust MPC (RMPC) to handle the system uncertainty within buildings. In particular, an uncertainty estimator is developed based on the previously presented RNN model to provide uncertainty bound to the conventional closed-loop min-max RMPC. The newly developed bound estimator reduces the conservatism of the RMPC and achieves improved control performance.

In conclusion, the research work presented in this thesis has made important contributions to the research of intelligent model predictive control for air-conditioning systems in commercial buildings. The methodologies developed in this thesis can be utilised for other buildings or for the control of other dynamic systems.

# Declarations

I certify that this work contains no material which has been accepted for the award of any other degree or diploma in my name, in any university or other tertiary institution and, to the best of my knowledge and belief, contains no material previously published or written by another person, except where due reference has been made in the text. In addition, I certify that no part of this work will, in the future, be used in a submission in my name, for any other degree or diploma in any university or other tertiary institution without the prior approval of the University of Adelaide and where applicable, any partner institution responsible for the joint-award of this degree.

I give consent to this copy of my thesis when deposited in the University Library, being made available for loan and photocopying, subject to the provisions of the Copyright Act 1968.

The author acknowledges that copyright of published works contained within this thesis resides with the copyright holder(s) of those works.

I also give permission for the digital version of my thesis to be made available on the web, via the Universitys digital research repository, the Library Search and also through web search engines, unless permission has been granted by the University to restrict access for a period of time.

SIGNED: . . . . . DATE: . . . . . .

# Acknowledgements

First of all, I would like to extend my sincere gratitude to my supervisor, Dr Lei Chen who brought me into the interesting research filed. He has provided me with tremendous guidance and support during the PhD journey. His wisdom and diligence have helped me to overcome all the difficulties and to keep me on the right track. He has also encouraged me to engage in various activities to promote my research, from which I benefited a lot.

I would like to express my gratitude to Associate Professor Eric Hu who supervised me on a weekly basis. Eric has provided precious resources and great ideas in this study. He has also given me great encouragement which helped me to go through the hardest period of my research .

I would like to thank Dr Moterza Mohammadzaheri who was co-supervising this project during the first year of my PhD. He was always willing to share his experience and knowledge with the others, from where I have learned a lot.

In particular, I am grateful to Professor Robert Bidmead for his suggestions that have greatly inspired me and opened my eyes in conducting my research. I cannot go that far to implement my idea without his kind suggestions.

I feel very fortunate to have the opportunity to study and work in the School of Mechanical Engineering, University of Adelaide. I have received precious feedback and suggestions from other academic staff, who had illustrated me and helped me from many aspects. Also, many thanks to Ms Dorothy Missingham and Ms Alison-Jane Hunter for running the terrific writing workshop which improves my writing and speaking.

I would like to thank my PhD colleagues: Yangkun Zhang, Boyin Ding, Difang Tan, Da Sun and Fangtai Tan for those joyful time spending at the lab. I am grateful to Mr Yu Ouyang for his suggestions from industry point of view. His advice has helped me to conquer practical problems in the most effective way.

I would like to acknowledge Adelaide Airport Limited for providing financial support and experimental data for this study. Also, I show my great appreciation to Johnson Controls Australia Pty Ltd staff members: Trevor McGrath, Anthony Underwood and Dave Furniss, who had offered technical help and support in setting up the experiment platform and conducting experiment at T-1 building. Without their help and patience, the filed test could never be finished.

Finally, but foremost, I would like to express my great love and appreciation to my parents, who gave birth to me and supported me in my study. My eternal appreciation goes to my beloved wife, Fu Xie, who had gone through so much tough time with me. Her accompaniment, love and support have always been the energy of finishing my study.

# List of Publications

This thesis is submitted as a portfolio of publications either published or submitted for publication by peer-reviewed journals according to the 'Academic Program Rules' of the University of Adelaide. The papers included in this thesis are all closely related to the field of the research of this work. This thesis is based on the following papers, which are referred to by their Arabic numerals:

**Paper-1** Huang H., Chen L., Mohammadzaheri M., Hu E., "A New Zone Temperature Predictive Modeling for Energy Saving in Buildings", In Procedia Engineering, vol. 49, pp. 142 - 151, 2012.

**Paper-2** Huang H., Chen L., Hu E., "A neural network-based multi-zone modelling approach for predictive control system design in commercial buildings", In Energy and Buildings, vol. 97, pp. 86 - 97, 2015.

**Paper-3** Huang H., Chen L., Hu E., "A new model predictive control scheme for energy and cost savings in commercial buildings: An airport terminal building case study", In Building and Environment, vol. 89, pp. 203 - 216, 2015.

**Paper-4** Huang H., Chen L., Hu E., "Reducing energy consumption for buildings under system uncertainty through robust MPC with adaptive bound estimator", *Submitted to Building and Environment*, 2015.

The following conference papers are of close relevance to the present work and are included in the appenices.

**2013** Huang H., Chen L., M. Mohammadzaheri., Hu E., Chen ML., "Multi-zone temperature prediction in a commercial building using artificial neural network model", In Control and Automation (ICCA), 2013 10th IEEE International Conference on, pp. 1896-1901, 2013.

**2014** Huang H., Chen L., Hu E., "Model predictive control for energy-efficient buildings: An airport terminal building study", In Control Automation (ICCA), 11th IEEE International Conference on, pp. 1025-1030, 2014.

**2015** Huang H., Chen L., Hu E., "A hybrid model predictive control scheme for energy and cost savings in commercial buildings: Simulation and experiment", In American Control Conference (ACC), 2015, pp. 256-261, 2015.

# Nomenclature

$C_z$ capacitance associated with the fast-dynamic masses (kJ/°C)

$C_w$ capacitance associated with the slow-dynamic masses (kJ/°C)

$C_a$ specific heat of air (kJ/kg°C)

$C_{cw}$ the overall thermal capacity of the chilled water and metal body of cooling coil (kJ/°C)

$C_{pw}$ specific heat capacity of chilled water (kJ/°C)

$CO_2$ carbon dioxide concentration (ppm)

$D_{out}$ outdoor air damper opening level (%)

$A$ area of the solid surface ($m^2$)

$f_w$ chilled water flow rate (l/s)

$f_{cw}$ chilled water flow rate (l/s)

$H_r$ relative humidity (%)

$T$ thermal node temperature (°C)

$T_c$ chilled water temperature (°C)

$T_{sp}$ set point temperature (°C)

$T_{oc}$ temperature constraints during occupied hours (°C)

$T_{uc}$ temperature constraints during unoccupied hours (°C)

$T_{cwo}$ outflow water temperature (°C)

$T_{ao}$ discharge (outflow) air temperature (°C)

$T_{cwr}$ return chilled water temperature (°C)

$T_{cws}$ supply chilled water temperature (°C)

$T_{ai}$ temperature of the air going into the cooling coil (°C)

$m_w$ water mass-flow rate of the cooling coil (kg/s)

$\dot{m}$ mass flow rate of the supplied air (kg/s)

$P_c$ power consumption of cooling energy consumed by the cooling coils (kW)

$P_f$ power consumption of supply fan (kW)

$Q_{chil}$ cooling load of the building (kW)

$Q_f$ supplied free-cooling energy (kW)

$Q_c$ supplied cooling coil energy (kW)

$Q_s$ heat gain generated by solar radiation (W)

$Q_p$ heat gain generated by occupancy (W)

$Q_{leak}$ heat gain caused by the leakage of the zone (W)

$R$ thermal resistance associated with walls, window or floor (°C/W)

$R_c$ convective heat transfer coefficient between adjacent zones (°C/W)

$R_w$ convective heat transfer coefficient associated with the air node and surface of the wall (°C/W)

$R_{win}$ convective heat transfer coefficient through window (°C/W)

$R_f$ convective heat transfer coefficient associated with the floor (°C/W)

$S_r$ global horizontal irradiation (W/m$^2$)

U overall heat transfer coefficient (kJ/m$^2$K)

$h$ convective heat transfer coefficients per unit area (W/m$^2$K)

$V_c$ chilled water valve opening level (%)

$V_{cw}$ chilled water valve opening level (%)

$V_z$ volume of the zone (m$^3$)

$\Delta t$ sampling time of the building data (s)

$n_a, n_b$ orders of the input variable

$r$ order of the system

$n_k$ time delay of the input variable

$f$ nonlinear neural network function

$\rho$ density of the air (kg/m$^3$)

$k$ time delay of the input variable

$w$ uncertainty

## *Subscripts*

$i$ indices for zones

sa supply air

r return air

out outdoor air

w walls and ceiling

g windows

f floor

N prediction horizon

k time step

cws supply chilled water

cwr return chilled water

### *Abbreviations*

COP Coefficient of Performance of the chiller plant

MPC Model Predictive Control

HMPC Hybrid Model Predictive Control

MIMO Multi-input, Multi-output

HVAC Heating, Ventilating, and Air Conditioning

BMS Building Management System

AHU Air Handling Units

CAV Constant Air Volume

VAV Variable Air Volume

ANN Artificial Neural Network

RNN Recurrent Neural Network

RMPC Robust MPC

ARMPC Adaptive Robust MPC

SMPC Stochastic MPC

BC Baseline Control

RC Resistance Capacitance

OSSC Optimal Start-Stop Control

TOU Time-of-Use

LTI Linear Time Invariant

PMV Predicted Mean Vote index

NARX Nonlinear Autoregressive models with exogenous input

ARMAX Autoregressive Moving Averagemodel with exogenous inputs

# Contents

# List of Figures

# List of Tables

# Chapter 1

# Introduction

## 1.1 Motivation

Buildings account for about 40 per cent of global energy consumption and are also responsible for 33 per cent of carbon emissions [1]. About 50 per cent of the end energy usage in buildings is related to their heating, ventilation and air conditioning (HVAC) systems. For these reasons, any efficiency improvements made to HVAC systems can significantly contribute to the reduction of energy consumption and greenhouse gas emissions.

Many countries have set long-term building energy saving targets for the development of 'greener' and more sustainable buildings. For example, in the United States (US), the California Public Utilities Commission plans to achieve reductions of 60-70 per cent of commercial building energy usage by 2030 [2]. In China, the Building Energy Conservation Plan in the Twelfth Five-Year Period sets goals of reducing 81.2 Mtoe of building energy consumption by the end of 2015 [3]. In Australia, the Equipment Energy Efficiency Committee has set a ten year strategy to improve the energy performance of HVAC systems by 20 per cent [4]. Achieving these goals requires both zero-carbon technology for future buildings as well as a reduction in the energy consumed by existing buildings. A rapid, and economic way to reduce energy consumption is to retrofit existing buildings

by implementing more advanced control algorithms.

Typical commercial HVAC control uses interconnected proportional-integral-derivative (PID) loops [5], ON/OFF control [6] or rule-based control (RBC) [7, 8] to regulate the local actuators. Their main task is to track the set point of the actuators designated by the building management systems (BMS). A typical example is the regulation of indoor temperature using chilled (hot) water valves to track the specified set-point. Despite the fact that fine-tuned local controllers can provide good set point tracking and modest disturbance rejection, they cannot provide optimal solutions when a building's overall performance is considered. This is because local controllers regulate thermal comfort by using the currently measured indoor temperature, but do not consider any information on ambient weather changes, the dynamics of the physical building and its real-time occupancy. Due to the existence of building thermal mass, HVAC systems governed by the current control rules usually respond to indoor temperature changes with significant time-delays. This causes both over-cooling and over-heating, which are two of the main causes for energy waste in public buildings.

Therefore, it is better to have a supervisory controller, which considers environmental factors and optimises the overall performance of the HVAC system. Basic supervisory functions include scheduling of cooling and heating systems, component sequencing and operational mode switching. The main goal is to provide a comfortable environment for the building's occupants with minimum energy input or operating cost [9]. For example, to avoid high electricity demand charges, a load-shifting control can be used by specifying different set point temperatures at different time of the day. Despite the popular use of BMSs in the HVAC industry, the energy saving potential achievable by applying supervisory control has not been fully exploited yet. In existing buildings, a night setback technique is used to achieve energy saving by relaxing the setpoint temperature during unoccupied hours. However, this strategy does not maximise the energy saving potential of the building system and can even cause thermal discomfort [10].

The need for the development of supervisory control motivates the investigation of Model Predictive Control (MPC). MPC is a control method that is able to solve constrained multivariable control problems and deal with multivariable coupling systems. It uses mathematical models to predict the future evolution of a dynamic process to optimise the control signal. At each sampling time, it solves a constrained optimisation problem over a finite future horizon, then applies the first input to the system. When a new step starts, it repeats the optimisation process using the new measurement [11]. The benefits of applying MPC to achieve energy savings in buildings come from several aspects, which are:

- The indoor temperature does not always need to be kept at a fixed value, because comfortable temperature is indicated by a temperature range [12]. By setting up constrained optimisation problems, MPCs allow the indoor temperature to vary within a specific thermal comfort range, without causing any violations.
- The most critical disturbances affecting building systems, such as occupancy and weather change can be predicted and easily incorporated into the MPC.
- By using the buildings' thermal mass, it is possible to shift the cooling (or heating) load from peak hours to off-peak hours, thereby reducing the total electricity bill and demand costs.
- Occupants' schedules have relatively fixed patterns and can also be predicted in advance, and can be formulated as time-varying constraints in the MPC to meet the occupants' actual demands.

## 1.2 Research Objectives

For the development of an MPC, the selection of the predictive models is the most crucial step , since it affects the computational speed and accuracy of the control algorithm. These

models are required to capture the dynamics of the HVAC building in a building: such as the building's physical properties, interactions between zones, the dynamics of the HVAC components, and influences from occupants and weather conditions. MPC should have good prediction accuracy, be robust against disturbance and simple in structure. Once such a model is made available, it can be used to optimise energy usage while maintaining good thermal comfort. MPC algorithms based on linear models are most commonly used. In such cases the resulting optimisation problem is a convex one, which guarantees global solutions can be obtained. Unfortunately, since building systems are inherently nonlinear and uncertain, linear models may result in poor closed-loop control performance, and even cause instability.

Intelligent models, such as neural networks (NN), provide more accurate results for the modelling of building energy systems [13, 14]. In particular, the NN models in recursive forms always demonstrate good control performance in the presence of uncertainty, thus are more suitable for modelling dynamic systems as compared to the static NNs. However, such models always require a large amount of experimental data to be trained with, which is not always available at the building sites. Moreover, there is not a fast or reliable optimisation algorithm to handle these types of models under the MPC framework.

Research on the application of MPC for building system control has attracted increasing attention from the control community. However, more research effort is still needed to develop an MPC that is more implementable and stable. To conclude, the main challenges of implementing MPC in real-world buildings are:

- Classical MPCs are based on linear, differentiable models, while building energy systems are always modelled as nonlinear systems. This is because air-conditioned buildings' processes, such as the operation of the cooling coil and outdoor air damper, contain static nonlinearity and cannot be accurately modelled by using first-principle models. Also, the simplified models for cooling and heating energy

are expressed in bilinear forms, which often results in non-convex optimisation problems that are hard to solve [7, 15, 16].

- The development of an MPC requires a thermal dynamic model to perform long-term predictions. This prediction model is subject to errors because a buildings thermal dynamics are affected by a number of disturbances, such as outdoor temperature, solar radiation, internal heat gain and the occupants' behaviours. The problem becomes even harder to solve when several spaces of a building are considered simultaneously, in that heat transfer from the neighbouring zones becomes another source of uncertainty.

- HVAC faults, such as wrong sensor readings, stuck air dampers and improper control settings or algorithms cause inaccurate monitoring and control of air-handling units (AHUs). These faults directly cause improper control of airflow and cooling (heating) energy and a waste of energy. It is therefore important to guarantee proper monitoring and control of the systems before the MPC is developed and tested [17, 18].

- Since physical buildings are influenced by a number of uncertainties, these models cannot always perform indoor temperature prediction precisely, which causes deterioration in control performance. This motivates the use of robust MPC. It is usually assumed that uncertainty is bound to be Gaussian distributed and known a priori in the previous robust MPC (RMPC) studies. These approaches are not suitable for dealing with real-world buildings, which are affected by time-varying and non-Gaussian distributed uncertainty [19, 20].

Motivated by the need for reducing energy consumption while maintaining thermal comfort in commercial buildings, this thesis investigates an advanced control strategy for HVAC systems. The objective building is an airport terminal controlled by a modern BMS system. The overall aim is to develop a robust, cost-effective and implementable MPC

strategy for commercial HVAC plants, including the strategies for the local AHUs, chiller and boiler. Throughout the thesis, the advantages of both classical MPC and intelligent approaches will be investigated to address the above challenges. In particular, the thesis makes the following contributions:

- Developing a systematic approach for the modelling of building heating and cooling energy systems. Recursive neural network (RNN) models are employed for the modelling of the AHUs and thermal zone processes. In particular, a cascade NN structure is proposed, which enable the model to predict indoor temperaure in both perimeter and interior zones inside large commercial buildings.

- Developing a multi-input, multi-output (MIMO), neural network modelling method for multi-zone buildings. This modelling approach is especially designed for buildings with wide open space, where the thermal coupling between the adjacent space is a major source of uncertainty. The model is subsequently employed in the design of a simple and effective optimal start-stop control algorithm for reducing energy consumption within the investigated building.

- Presenting a hybrid model predictive control (HMPC) for building energy systems. In the hybrid structure, a resistance-capacitance (RC) model is built to represent the thermal dynamics of the thermal zone. The system nonlinearities associated with the AHUs processes are handled by feedback linearisation. An inverse NN model is developed to perform a nonlinear mapping between the linearised control input and the actual control command. The proposed HMPC also improves the efficiency of the existing economizer control. A simulation study is conducted to demonstrate the advantages of MPC over the baseline control method in achieving energy and cost savings. The potential benefits of conducting pre-cooling in lightweight commercial building is also investigated in a real-time experiment.

- Designing a robust MPC with uncertainty bound estimator for building energy sys-

tems, so that the expected electricity cost is minimised while guaranteeing thermal comfort. The proposed uncertainty bound estimator models the system uncertainties by comparing the difference between the nominal model and the previously presented RNN model. The proposed estimator computes the possible uncertainty bound, and solves the resulting min-max robust optimisation problem using the tightened constraint sets.

.

# References

[1] L. Pérez-Lombard, J. Ortiz, and C. Pout, "A review on buildings energy consumption information," *Energy and Buildings*, vol. 40, no. 3, pp. 394–398, 2008.

[2] Z. Stakeholders, "Zero net energy commercial building action plan," tech. rep., 2011.

[3] C. Securities, "Market opportunities under energy convervation special plan during twelfth five-year plan period," *Beijing: Cinda Securities Co,.Ltd*, 2013.

[4] "National strategy on energy efficiency," tech. rep., Council of Australian Governments (COAG), 2009.

[5] Y. Ma, A. Kelman, A. Daly, and F. Borrelli, "Predictive control for energy efficient buildings with thermal storage: Modeling, stimulation, and experiments," *Control Systems, IEEE*, vol. 32, pp. 44–64, Feb 2012.

[6] M. Avci, M. Erkoc, A. Rahmani, and S. Asfour, "Model predictive HVAC load control in buildings using real-time electricity pricing," *Energy and Buildings*, vol. 60, no. 0, pp. 199 – 209, 2013.

[7] F. Oldewurtel, A. Parisio, C. N. Jones, D. Gyalistras, M. Gwerder, V. Stauch, B. Lehmann, and M. Morari, "Use of model predictive control and weather forecasts for energy efficient building climate control," *Energy and Buildings*, vol. 45, no. 0, pp. 15 – 27, 2012.

[8] J. Široký, F. Oldewurtel, J. Cigler, and S. Prívara, "Experimental analysis of model predictive control for an energy efficient building heating system," *Applied Energy*, vol. 88, no. 9, pp. 3079 – 3087, 2011.

[9] S. Wang and Z. Ma, "Supervisory and optimal control of building hvac systems: A review," *HVAC&R Research*, vol. 14, no. 1, pp. 3–32, 2008.

[10] M. Garcia-Sanz and J. Florez, "Adaptive optimum start-up and shut-down time controllers for heating systems based on a robust gradient method," *Control Theory and Applications, IEE Proceedings*, vol. 141, pp. 323–328, Sep 1994.

[11] S. Qin and T. A. Badgwell, "A survey of industrial model predictive control technology," *Control Engineering Practice*, vol. 11, no. 7, pp. 733 – 764, 2003.

[12] ASHRAE, *Thermal environmental conditions for human occupancy.* American Society of Heating, Refrigerating, and Air-Conditioning Engineers, 2013.

[13] N. Morel, M. Bauer, M. El-Khoury, and J. Krauss, "Neurobat, a predictive and adaptive heating control system using artificial neural networks," *Solar Energy Journal*, vol. 21, pp. 161–201, 2001.

[14] P. Ferreira, A. Ruano, S. Silva, and E. Conceiçâo, "Neural networks based predictive control for thermal comfort and energy savings in public buildings," *Energy and Buildings*, vol. 55, no. 0, pp. 238 – 251, 2012.

[15] Y. Ma, J. Matusko, and F. Borrelli, "Stochastic model predictive control for building

HVAC systems: complexity and conservatism," *Control Systems Technology, IEEE Transactions on*, vol. 23, no. 1, pp. 101–116, 2015.

[16] S. Goyal and P. Barooah, "A method for model-reduction of nonlinear building thermal dynamics," in *American Control Conference (ACC), 2011*, pp. 2077–2082, June 2011.

[17] S. C. Bengea, P. Li, S. Sarkar, S. Vichik, V. Adetola, K. Kang, T. Lovett, F. Leonardi, and A. D. Kelman, "Fault-tolerant optimal control of a building HVAC system," *Science and Technology for the Built Environment*, vol. 21, no. 6, pp. 734–751, 2015.

[18] S. Wang and Y. Chen, "Fault-tolerant control for outdoor ventilation air flow rate in buildings based on neural network," *Building and Environment*, vol. 37, no. 7, pp. 691 – 704, 2002.

[19] A. Domahidi, F. Ullmann, M. Morari, and C. Jones, "Learning near-optimal decision rules for energy efficient building control," in *Decision and Control (CDC), 2012 IEEE 51st Annual Conference on*, pp. 7571–7576, Dec 2012.

[20] Y. Ma, G. Anderson, and F. Borrelli, "A distributed predictive control approach to building temperature regulation," in *American Control Conference (ACC), 2011*, pp. 2089–2094, 2011.

# Chapter 2

# Literature Review

With the fast development of computational technology, the costs of data storage, processing, and modelling have significantly decreased over recent years. This makes the design and implementation of more complex control techniques for advanced building HVAC control strategies more feasible. In general, advanced HVAC control strategies can be classified into those based on classical MPC theory and those on intelligent control theory. Although these two methods have been widely discussed in the literature, a critical review is still needed in order to address the following problems:

1. How is MPC connected to the concept of supervisory control?
2. What are the main challenges when implementing MPC at real buildings?
3. What are the pros and cons of the classic MPC and intelligent control methods and how to make a selection between them?

## 2.1 Early Studies on Supervisory Control

The idea of applying MPC for building energy control originates from the idea of the supervisory control strategy. The main task of supervisory control is to determine the set

point values for local controllers. Its main purpose is to seek the minimum energy input or operating cost to provide satisfactory indoor environmental conditions by considering varying weather conditions as well as HVAC characteristics [1]. Most HVAC systems are equipped with some types of energy conservation technologies, for example, the active thermal storage system [2, 3], chiller sequence control [4], variable speed control for the pump and supply fan [5], blind control [6] and economizer control [7]. These control strategies are usually pre-programmed into the BMS and configured by the HVAC vendors to suit specific buildings. Supervisory control is able to re-organise these conservation strategies to achieve a more significant energy reduction.

The night setback strategy is a commonly used supervisory approach in intermittently occupied buildings to achieve basic savings. It simply turns on the cooling (or heating) systems before the occupants arrive at the building and turns them off before they leave. However, operational schedules determined by the night setback strategy are fixed, and are not adaptive to the varying weather conditions. This could even result in energy waste and thermal comfort violations. A straightforward way of achieving energy savings is to use an optimal start-stop control method [8–10]. The optimal start-stop control is an 'advanced' version of night setback strategy. On different days, it schedules the cooling (heating) systems smartly so that indoor temperature can be maintained with a comfortable range only during occupancy.

The optimal start-stop control has been investigated by several studies. For example, Seem et al. [8] compared seven different methods for predicting the optimal return time from night setback under a simulation environment. They found that a quadratic equation related to the initial room temperature could predict the optimal return time properly. Sun et al. [4] developed a simplified building model to predict the cooling load, and decide the optimal number of operating chillers and their pre-cooling time. Yang et al. [11] built a backpropagation-based NN model to determine optimal start time for a heating system in a building. The proposed NN model uses room temperature, outdoor air temperature

and their varying rates as the inputs to predict the temperature rising time. Ben-Nakhi et al. [12] applied a general regression NN to optimise air conditioning setback schedule in public buildings. Simulation shows that the NN can accurately predict the temperature setback time with a good robustness.

Although the optimal start-stop control can be used together with the night setback to reduce the total energy consumption, this method still results in high utility costs, as it uses a fixed temperature set point during occupied hours. One way to reduce the utility costs is using the buildings' thermal mass to perform load shifting (e.g., by shifting the cooling load from expensive peak hours to cheap off-peak hours). This method schedules the set point to a lower value during the unoccupied hours and then releases it during the occupied hours. This control strategy results in lower operational costs, even though the total cooling or heating load may increase. Using building thermal mass to reduce the operating costs for cooling has four benefits [13]:

1. It can reduce mechanical cooling using cooler morning ambient air to perform free-cooling;

2. It uses much cheaper off-peak electricity energy to perform precooling;

3. The demand costs can be greatly reduced by shifting the peak load;

4. The coefficient of performance (COP) of the chiller plant can be improved using more favourable part-load and ambient conditions.

This load shifting (or precooling strategy) was first proposed by Braun [13] and forms the basic concept for many of the MPC frameworks being investigated. In this work, it is shown that 10% to 50% of energy costs can be achieved using the precooling strategy. In general, more cost savings can be achieved when higher ratios of peak to off-peak rates and more free cooling are available. To achieve more significant savings, Lee and Braun [14] developed and compared three ways to optimise the set-point temperature for

limiting demand in buildings. In these methods, the set-points are set to the lower comfort limit before the start of occupancy. The temperature set-point is then adjusted during the discharge period to save more energy. The result shows that the set-point trajectories that are optimised using demand limiting have a logarithmic shape.

Although the above-mentioned supervisory control technologies have been proven effective in reducing energy or utility costs, they have rarely been implemented in real-world buildings. This is because these control strategies are dependent on several factors, such as building thermal capacitance, weather conditions, electricity rate structure and occupancy schedule. Simply scheduling the set point with a specific pattern can cause thermal comfort violation or even more energy waste. A systematic optimisation framework is required to take into account all these factors. Further, the embedded hardware system has a limited computational capability which makes the real-time implementation of these control methods problematic [15]. With the fast development of computational technology in recent years, the implementation of a supervisory control is becoming more realistic nowadays. This is why MPC has garnered increasing attention in recent years.

## 2.2 Classical Model Predictive Control

### 2.2.1 Building Models

The essence of MPC is to optimise a predicted state trajectory, so the process model is the heart of an MPC controller. Building energy system is a complicated combination of different factors, such as HVAC equipment, building envelop, thermal mass, weather conditions, occupants, their behaviours, and so on. Therefore, thermal dynamic models to predict the building states, component models to predict the dynamics of each HVAC component (fan, pump, valve, etc.), energy model to predict energy consumption and operational costs, weather forecast models to predict environmental disturbance (outdoor temperature, solar radiation, etc.), and occupancy models to predict the internal heat gain

and occupancy status are necessary.

The choice of the model is crucial. When it comes to implementation, linear models are more preferable, because they allow convex optimisation to be conducted. As the energy term of a simplified building model is bilinear, feedback linearisation is always applied to linearise the nonlinear models at the desired operating point [16, 17]. In summary, the building models used for classical MPC can be categorised into three groups.

#### Detailed physical model

In the HVAC engineering society, energy simulation programmes, such as EnergyPlus [18] TRNSYS [19], and ESP-r [20] are commonly used. These models are built based on heat transfer, fluid mechanics and other engineering sciences to model building temperatures, airflows and energy use; These detailed physical models can achieve very high modelling accuracy, but they often require excessive parameter tuning and simulation. Moreover, these models are generally complicated in size and can quickly lead to computationally intractable optimisation problems. Therefore, detailed physical models are usually developed to evaluate the performance of the new control approaches [10, 21, 22].

#### RC model

Simplified physical models are often referred to as a thermal resistance capacitance (RC) network. The RC model uses an interconnection of thermal resistances and capacitances to represent the heat transfer phenomenon between the air node, walls, windows, ceilings, and furniture. The identification process of RC models depends on the measured data, but still keeps its physical structure. Thus, they have better generalisation ability than the black box models [23]. More importantly, the RC models are explicit and can be converted into linear time invariant (LTI) models. This make the convex optimisation problem applicable [24]. For these reasons, RC models have been commonly applied in various research groups [2, 6, 25]. Past research has proven that high-order RC models

achieve limited benefits over the low-order RC models; thus, reduced order RC models are preferable to use control purposes [16, 26]. There are also several drawbacks to use the RC models. For example, buildings' thermal dynamics are nonlinear, but the structure of RC models is linear; Additionally, several disturbance sources affecting the building are not predictable and cannot be included with the model. These factors all affect the prediction accuracy of the RC model.

#### Statistical model

Statistical models include autoregressive exogenous (ARX), autoregressive moving average exogenous (ARMAX), OE, BoxJenkins (BJ) [27], MPC relevant identification (MRI) [24], and subspace models [28]. Most of these models are differentiable and therefore suitable for control design. Statistical models are easy to build since they do not use any prior knowledge on the physical systems, which can greatly reduce the costs of model development. In addition, because most of the statistical models are in regression forms, they can guarantee a certain degree of accuracy. For this reason, statistic models have recently been applied in several implementation studies [17, 29, 30]. However, due to their linear nature, large errors sometimes occur when the degree of uncertainty and nonlinearity are significant. Additionally, they cannot be easily modified to include other disturbance models or be analysed .

### 2.2.2 Deterministic Model Predictive Control

The MPC refers to a class of control algorithms that utilise a process model to predict the future states of a plant and optimise the inputs over the prediction, while taking into account various types of constraints. The MPC method is perhaps the only advanced control technique (more advanced compared to the PID control method) that has been widely applied in the industry. The related fields include petroleum refineries, chemicals, food processing, automotive, and aerospace applications [31, 32]. The way an HVAC sys-

tem operates resembles an industrial process; it processes the energy through the boiler, chiller, and AHUs. Therefore, the MPC has the potential of becoming an alternative control approach for building systems.

If the nominal prediction equals to the real system outputs, the MPC is referred to as a deterministic MPC (DMPC). Considering an LTI model, the DMPC can be formulised as a linear programming or a quadratic programming problem. The basic idea of DMPC is to solve the following optimisation at each time step:

$$\min_{u} \sum_{j=0}^{j=N-1} l(x_{k+j|k}, u_{k+j|k}, d_{k+j|k}), \tag{2.1}$$

subject to:

$$\begin{aligned} x_{k+j+1|k} &= f(x_{k+j|k}, u_{k+j|k}, d_{k+j|k}), \quad \forall j = 0, ..., N-1 \\ y_{k+j+1|k} &= g(x_{k+j|k}, u_{k+j|k}, d_{k+j|k}), \quad \forall j = 0, ..., N \\ u_{k+j|k} &\in \mathbb{U}, \quad \forall j = 1, ..., N \\ y_{k+j|k} &\in \mathbb{Y}, \quad \forall j = 0, ..., N \end{aligned} \tag{2.2}$$

where the double indices $k+j|k$ denotes the prediction value at time $k+j$ made at time $k$, $N$ is the prediction horizon, $x$ is the system state of the building, such as zone temperatures, relative humidity, $CO_2$ concentrations and surface temperature of the building envelop. Moreover, $u$ denotes a vector of the control inputs applied to the building system, for supervisory control purposes, $u$ could be the set point for chilled water temperature, supply air temperature, or zone temperature. Additionally, $y$ is the output of the system, and $d$ denotes disturbance variables, such as outdoor temperatures, solar radiations, internal heat gain generated by occupants, and electrical devices. The function $f$ denotes the function which allows one to predict the future building states based on the initial states, control inputs, and future disturbances. In classical control, $f$ is usually a state space model derived from differential equations. Further, $\mathbb{X}$ and $\mathbb{U}$ denote the constraints of the states and inputs, respectively, and $l_k$ denotes the cost function.

Various types of supervisory control strategies can be easily integrated into the MPC framework. For example, the optimal start-stop control function can be realised by applying time-varying constraints in Eq. (2.2), such as that in [2, 5, 16, 28, 33]. The load shifting function can be realised by adding penalty coefficients on the time-varying electricity price to the cost function $l_k$, such as that in [30, 34].

There have been several attempts to validate the energy saving potential of MPC, through both simulation and experimental study.

In an experimental study conducted by Široký et al. [35], two conference rooms of a building are modelled as an RC network. The cost function penalises the desired temperature tracking error and temperature difference between supply and return water heater circuits. The MPC designates the set-point temperature for each room, which demonstrates 17% in energy savings over the conventional controller.

In a simulation study [5], a bilinear building model is built in which parameters are obtained using historical building data. The optimisation problem is formulised as a linear programming problem, which minimises total heating power and peak airflow. Compared with the baseline controller, MPC reduces the peak air flow rate and total energy consumption by 33.3% and 73.2%, respectively.

In an experimental study [36], MPC is developed to control a cooling system of the HVAC at the University of California at Merced. A series of simplified models are developed for chillers, cooling towers, thermal storage tanks and building envelop. They employ a strategy called moving window block to solve the optimisation problem. The results show about a 19.1% improvement of the system COP over the baseline controller.

Ma et al. [30] presented an economic MPC to optimise set-points of HVAC systems for achieving load shifting and operational cost reduction. The experimental study shows that under a time-of-use electricity rate structure, the cooling load for HVAC systems was successfully shifted from peak hours to off-peak hours. This operation reduces both the demand cost and the total electricity bill.

When MPC is used as a supervisory controller, the total energy or cost can be reduced by solving optimisation problems. The saving opportunity comes from many aspects, such as more efficient use of free cooling energy, reduced peak electricity usage, and better thermal constraint satisfaction. Even the simplest linear MPC can achieve a certain degree of savings. Unfortunately, building dynamics are always involved with uncertainty, due to occupants' behaviours and weather forecast errors. These factors cannot always be accurately represented by the linear models. In this context, we investigate the following two problems: What happens if model-plant mismatch exists? What happens if the modelling errors are not uniformly distributed?

### 2.2.3 Robust MPC

The DMPC assumes nominal prediction to be the same as the real systems. However, obtaining deterministic control decisions on the future states of a real system is not possible, as the buildings' dynamics are highly uncertain and dependent on the accuracy of disturbance forecasting. In addition, the parameters of building models are not always correct and are subject to measurement noise. The feedback nature of the MPC allows the controller to reject a small degree of uncertainty, but not for systems with large uncertainties. The uncertainty should be considered in order to guarantee control stability. Two methods, RMPC and stochastic MPC (SMPC) have been investigated to solve the problem.

In RMPC, the uncertainty is assumed to be bound, so that the constraints are tightened in order to achieve constraint satisfaction for all possible realisations of the uncertainty along the horizon. The most commonly applied RMPC is minmax RMPC, which minimises the worst-case performance as follows:

$$\min_{u} \max_{w} \sum_{j=0}^{j=N-1} l(x_{k+j|k}, u_{k+j|k}, d_{k+j|k}, w_{k+j|k}), \tag{2.3}$$

where $w \in \mathbb{W}$ denotes unknown, bounded uncertainty. Open-loop minmax MPC is highly

conservative and can result in infeasibility and instability problems [37]. The reason is that the open loop control does not take into account that the information on the future disturbance will be contained in the future measured state trajectory. A more commonly considered form is the closed-loop MPC [37]. In closed-loop MPC, the future control inputs are usually parameterised as affine functions of future measured states and decision variables. A RMPC constructed in such a way is less conservative than an open-loop one because of feedback prediction, but the affine structure of states and control input result in challenging non-convex problem. This problem can be further solved by using min-max MPC with disturbance feedback, which directly parameterises the control input sequence into the uncertainty [38–41].

Although RMPC can guarantee stability and recursive feasibility, it is required that the uncertainty bound of RMPC should be designed in advance which is not always possible. Improper choice of an uncertainty bound would cause thermal comfort violation (too small) or energy waste to the system (too wide). More often than not, the bound is chosen to be as wide as possible in order to cover the occurrence of high uncertainty with low probability of occurrence. If possible, it is better to obtain a smaller uncertainty bound which could result in less conservative solutions. This can be achieved using an uncertainty bound estimator [42] or a comparison model [43].

### 2.2.4 Stochastic MPC

Stochastic MPC (SMPC) provides an alternative method to solve the uncertainty problem with the least control performance loss [44]. In SMPC, the expected value of the cost function is optimised:

$$\min_{\mu} E[\sum_{j=0}^{j=N-1} l(x_{k+j|k}, u_{k+j|k}, d_{k+j|k}, w_{k+j|k})], \tag{2.4}$$

where $E$ denotes the expected value of the cost. Moreover, SMPC also uses the chance constraints instead of deterministic ones to achieve more savings:

$$P(x_{k+j|k}) \geqslant 1-\alpha, \tag{2.5}$$

where $P$ denotes the probability of the event. Under such a formulation, the constraints only need to be satisfied with a certain level of probability, and therefore could result in less conservative solutions. SMPC has been studied in building energy control [17, 45–47]. In these studies, the occupancy prediction errors and weather forecast errors are often modelled as uncertainties.

Oldewurtel et al. [46] proposed an SMPC to regulate building temperature. In this work, the weather forecast error is assumed to be Gaussian distributed and is modelled by an autoregressive model. Chance constraints are used in the optimisation problem to improve the energy efficiency of the method.

Mady et al. [45] used a building occupancy model to improve mean energy efficiency while minimising expected discomfort. The occupancy pattern is modelled as a Markov chain probability function. The experimental results show the advantage of the SMPC as compared to the MPC with fixed occupancy schedules.

To consider cases that are more realistic, where the buildings are subject to non-Gaussian disturbance, Ma et al. [17] proposed another stochastic MPC framework. In this work, the uncertainties caused by occupation and weather prediction error were learned from historical data and modelled as finitely supported probability distribution functions. To make the SMPC computationally tractable, a feedback linearisation is used to transform the chance constraints to deterministic ones.

In summary, SMPC interprets the constraints probabilistically, which can result in less violation probability so that can result in less conservative solutions. However, SMPC problems are hard in general and can only be solved approximately or by imposing specific problem structures, e.g., assuming the uncertainty is bounded or uniformly distributed. More research efforts are needed to handle the cases where the uncertainty

is more significant and difficult to identify, which usually happens in real-world building sites.

### 2.2.5 Dealing with Thermal Coupling

Commercial buildings typically consist of a number of zones that interact with each other through convective or conductive heat transfer. The temperature in each zone is measured by a sensor and controlled by an individual AHU or a variable air volume (VAV) terminal. When MPC is employed to control these sub-zones, local models and objective functions are usually designed for each individual subsystem, without considering the interactions among the local systems. If the interaction between the adjacent zones is mild, satisfied control performance can be achieved using the feedback signals. Nevertheless, for the buildings where the zones are highly interactive, ignoring the interactions between subsystems may lead to a significant loss in control performance. Moreover, as the number of controlled zones increases, the number of decision variables involved that must be optimised increases rapidly. This not only makes the optimisation problem intractable but also the implementation work difficult.

The convective heat transfer coefficient is determined by a number of variables, such as the airflow rate between the adjacent zones and the distance between the temperature sensors. Generally speaking, the time constant related to the convective heat transfer between two zones increases with the physical distance between them [48] . Currently, convection heat transfer between zones can be analysed using Computational Fluid Dynamics (CFD) simulation [49]. However, CFD models are computationally complex, and cannot be directly used to achieve control purpose, so they are more often to conduct control analysis [50]. Therefore, the development of more reliable and simple mathematical models is needed. Goyal et al. [48] modelled the inter-zone convection of a building with reduced order RC networks. They found that when the convection effects are considered, the temperature predicted by the RC model is more accurate than the model that only

considers the conductive heat transfer.

Distributed control provides a solution for managing energy distribution within multi-zone buildings. Distributed MPC has been studied by a number of researchers [17, 25, 51, 52]. Most of these methods were based on the classic MPC method. Moroan [33] concluded that a distributed MPC that considers the thermal coupling among zones outperforms the MPC that does not consider thermal interaction. The effects of neighbouring rooms seem to be negligible compared to the effects of opening windows and doors and the supplied thermal energy.

Ma et al. [34] developed a distributed MPC based on dual decomposition. This technique distributes the computational load of a centralised MPC to a set of VAV box embedded controllers, making the implementation of the control algorithm possible. In [53], a primal-dual active-set method is proposed for the DMPC to reduce the communication delays between the controllers. This method is shown to generate much less communication delay than other proposed distributed algorithms.

Despite of the past works, some underlying questions must be answered: How significant is thermal interaction for the control development? Do we need to consider it when designing the predictive controller? These problems seem to be more significant for large commercial buildings, in which coupling effect become a more significant factor due to jointing of many separated zones.

## 2.3 Intelligent Control

### 2.3.1 Neural Network Modelling

Intelligent models include (NN) [54–57], fuzzy systems [58, 59], adaptive neuron-fuzzy systems [60], genetic and evolutionary algorithms [61, 62] and support vector machine [63]. In this thesis, we focus on NNs. An attractive feature of NNs is they are able to learn complicated nonlinear relationships between input and output variables. NNs have been

used to predict the cooling load, electricity usage or indoor temperature as a function of time varying input variables in the building [64–66]. To improve the generalisation ability of NNs, different categories of NN models have been applied to building systems, such as the recursive NN [67, 68], adaptive NN [69], reinforcement learning NN [70], and deep learning NN [71].

Past research has compared the NN model against several other models, including the detailed physical model [72], time-series ARX model [64], RC model [57], and several other intelligent models [56]. It has been found that the ANN outperforms these models in terms of prediction accuracy. For example, Ruano et al. [73] incorporated a multiple objective genetic algorithm (MOGA) with radial basis function NN to build a temperature prediction model for a school building. Three objectives were set for the MOGA, which aim to reduce model complexity and improve model performance and model validity. The model was used for long-range prediction and achieved more accurate prediction results than a physical model.

### 2.3.2 Neural Network Based Control

In some studies, the NN models are used for supervisory control to achieve energy savings. The principle of this control method is similar to the classical MPC. The difference is that the nonlinear neural model is used for prediction. To handle these models, nonlinear optimisation approaches such as sequential quadratic programming (SQP), are often used to compute the gradients of the predicted output trajectory [74]. Computational intelligence algorithms, such as the evolutionary algorithm [75], particle swarm optimisation [76], and discrete branch and bound approaches [54] can also be used to optimise NN models.

Massie [3] developed an optimal NN controller to minimise the total energy consumption of building HVAC systems by controlling a commercial ice storage system. The supervisory controller consists of a training network and a predictor network. The training

network adjusts the weights of the network and passes them to the predictor network. The predictor network can then modify its weights and finds values for the chiller setpoint temperature and ice tank valve position to minimise overall operating cost.

In [77], a multi-layer perceptron NN is employed to model a multi-zone HVAC system. A firefly algorithm is applied to solve the constrained, NN based optimisation model, which provides set point for the supply air temperature and the supply air static pressure. Ferreira et al. [54] developed an ANN-based model predictive control for a campus building. The energy usage is optimised by using a discrete branch and bound approach. Yang et al. [70] implemented a reinforcement learning control method for LowEx Building systems, in which the controller learns from previous operations to be adaptive to the changing environment.

By reviewing the above work, it can be seen that, if the building systems have a high degree of nonlinearity, the NN model predictive control could provide a more accurate prediction trajectory as compared with classical MPC. Their self-learning ability also makes them adapt to the changing environment. However, when online implementation is considered, the reliability and computational speed of the optimisation algorithms become a problem.

For this reason, it is worthwhile to investigate the application of other types of NN control methods for building energy control. An example is NN based feedback linearisation [78–80]. This algorithm firstly linearises the NN model into affine, linear equations. The linear optimisation method can then be applied based on the nonlinear prediction results. This algorithm transforms a nonlinear optimisation problem into a linear one; thus, it is less computationally expensive and more suitable for online optimisation. Additionally, since the RNN can maintain good modelling accuracy in the presence of uncertainty, it can be also be used as an uncertain compensator for the first principle models [81, 82]. These features make the NN suitable for the design of a hybrid MPC. Although these methods have been demonstrated in a number of applications [81, 83–85], it is still worthwhile to

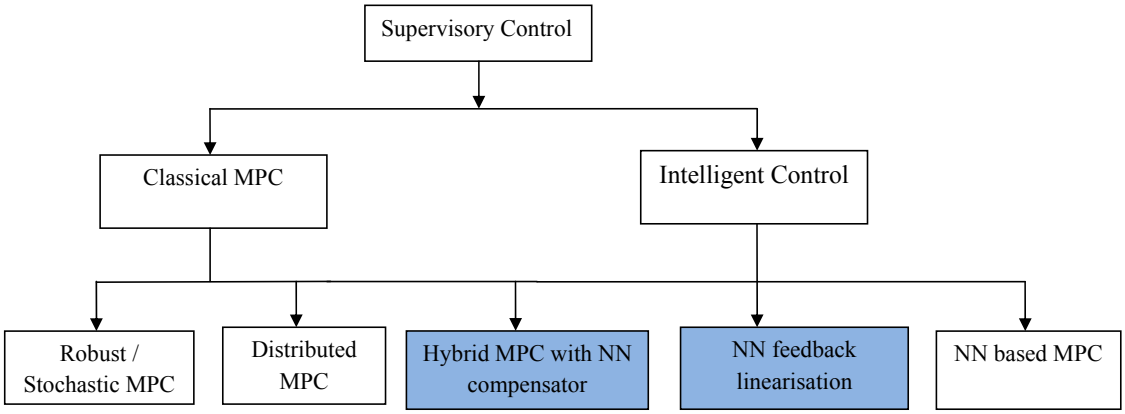


Figure 2.1: Summary of supervisory control strategies for HVAC systems.

investigate the application value of these types of methods on building energy control.

After reviewing different supervisory control strategies, the connection between the supervisory control and two categories of predictive control methods is identified and illustrated in Fig. 2.1. The blue section illustrates the research methodology that has not been exploited yet.

## 2.4 Review Summary and Research Gaps

The literature review has elucidated the great progress made in the application of MPC for building energy management in the last decade. Despite this, the online implementation of such a technology in real-world commercial buildings is still challenging. How to deal with uncertainty and relax the computational burden are two major obstacles for the implementation of MPC. Another challenge comes from the fact that the thermal dynamics of buildings and HVAC systems differ greatly from one to another; therefore, there is no universal method that can be applied to all building types. Specifically, the following research gaps have been identified in this thesis:

- While simplified RC models dominate MPC related studies, the reliability of using

RC models for large commercial buildings still requires more investigation. This is because the past case studies primarily investigated small and mid-size buildings, such as offices and conference rooms [2, 86]. The thermal zones in these buildings have a relatively fixed occupancy pattern and are well isolated so that the dynamic is more comprehensive. However, the reliability of RC models for thermal zones with more complex dynamics, such as large buildings with wide-open space and frequent change of occupancy, is still unknown. More expensive modelling approaches, such as NN model, may provide a better modelling accuracy to such problems. However, the trade-off of using NN models for predictive control requires further investigation.

- The past building modelling works based on the NN models were mostly constrained to single zone studies. The effects of heat transfer between the adjacent zones, especially convective, have rarely been considered in the past. This assumption may be correct if the walls provide sufficient insulation, but not for the zones where convective heat transfer between each other is significant. A model that is able to accommodate the thermal interaction between adjacent zones within the multi-zone building is therefore needed.

- Although NN models have been employed for load prediction and supervisory control [12, 54, 68], the use of the models for building energy optimisation poses a challenge. The reason is that nonlinear optimisation or computational intelligence algorithms needed for handling NN models may result in multiple local minima and high computational complexity. A less expensive solution is to integrate the NN model into the classical MPC, so that the uncertainty of the building can be handled separately. However, this method has not been employed for building energy control yet.

- The load shifting strategy under the MPC framework has been proven to be effective

in achieving cost savings [2, 30]. However, the application value of such strategies for light-weighted commercial buildings with wide-open space lacks experimental verification.

- The RMPC and SMPC were previously investigated to handle model uncertainty within buildings. Both methods require extracting stochastic properties of the historical data to reduce performance bound and conservatism. To deal with the non-Gaussian distributed uncertainties in the investigated building, it is necessary to devise a way that provides uncertainty bounds to the RMPC, so that less performance loss will be occurred with the use of RMPC.

# References

[1] S. Wang and Z. Ma, "Supervisory and optimal control of building HVAC systems: A review," *HVAC&R Research*, vol. 14, no. 1, pp. 3–32, 2008.

[2] Y. Ma, A. Kelman, A. Daly, and F. Borrelli, "Predictive control for energy efficient buildings with thermal storage: Modeling, stimulation, and experiments," *Control Systems, IEEE*, vol. 32, pp. 44–64, Feb 2012.

[3] D. D. Massie, "Optimization of a building's cooling plant for operating cost and energy use," *International Journal of Thermal Sciences*, vol. 41, no. 12, pp. 1121 – 1129, 2002.

[4] Y. Sun, S. Wang, and G. Huang, "Model-based optimal start control strategy for multi-chiller plants in commercial buildings," *Building Services Engineering Research and Technology*, vol. 31, no. 2, pp. 113–129, 2010.

[5] M. Maasoumy and A. Sangiovanni-Vincentelli, "Total and peak energy consumption minimization of building HVAC systems using model predictive control," *Design Test of Computers, IEEE*, vol. 29, pp. 26–35, Aug 2012.

[6] T. O. T. Gyalistras D, *Final report: Use of weather and occupancy forecasts for optimal building climate control (OptiControl)*. Zurich, Switzerland: Terrestrial Systems Ecology ETH, 2010.

[7] J. Seem and J. House, "Development and evaluation of optimization-based air economizer strategies," *Applied Energy*, vol. 87, no. 3, pp. 910 – 924, 2010.

[8] M. Garcia-Sanz and J. Florez, "Adaptive optimum start-up and shut-down time controllers for heating systems based on a robust gradient method," *Control Theory and Applications, IEE Proceedings*, vol. 141, pp. 323–328, Sep 1994.

[9] J. Flòrez and G. Barney, "Adaptive control of central heating systems: part 1: optimum start time control," *Applied Mathematical Modelling*, vol. 11, no. 2, pp. 89 – 95, 1987.

[10] A. Garnier, J. Eynard, M. Caussanel, and S. Grieu, "Low computational cost technique for predictive management of thermal comfort in non-residential buildings," *Journal of Process Control*, vol. 24, no. 6, pp. 750 – 762, 2014.

[11] I.-H. Yang, M.-S. Yeo, and K.-W. Kim, "Application of artificial neural network to predict the optimal start time for heating system in building," *Energy Conversion and Management*, vol. 44, no. 17, pp. 2791 – 2809, 2003.

[12] A. E. Ben-Nakhi and M. A. Mahmoud, "Energy conservation in buildings through efficient A/C control using neural networks," *Applied Energy*, vol. 73, no. 1, pp. 5 – 23, 2002.

[13] J. E. Braun, "Reducing energy costs and peak electrical demand through optimal control of building thermal storage," *ASHRAE Transactions*, vol. 96, pp. 876–887, 1990.

[14] K. ho Lee and J. E. Braun, "Development of methods for determining demand-limiting setpoint trajectories in buildings using short-term measurements," *Building and Environment*, vol. 43, no. 10, pp. 1755 – 1768, 2008.

[15] G. E. Kelly, "Control system simulation in north america," *Energy and Buildings*, vol. 10, no. 3, pp. 193 – 202, 1988.

[16] S. Bengea, V. Adetola, K. Kang, M. J. Liba, D. Vrabie, R. Bitmead, and S. Narayanan, "Parameter estimation of a building system model and impact of estimation error on closed-loop performance," in *Decision and Control and European Control Conference (CDC-ECC), 2011 50th IEEE Conference on*, pp. 5137–5143, 2011.

[17] Y. Ma, J. Matusko, and F. Borrelli, "Stochastic model predictive control for building HVAC systems: Complexity and conservatism," *Control Systems Technology, IEEE Transactions on*, vol. 23, no. 1, pp. 101–116, 2015.

[18] D. B. Crawley, L. K. Lawrie, F. C. Winkelmann, W. Buhl, Y. Huang, C. O. Pedersen, R. K. Strand, R. J. Liesen, D. E. Fisher, M. J. Witte, and J. Glazer, "Energyplus: creating a new-generation building energy simulation program," *Energy and Buildings*, vol. 33, no. 4, pp. 319 – 331, 2001.

[19] "Thermal energy system specialists, transient system simulation tool." `http://www.trnsys.com`, 2015.

[20] "Esp-r." `http://www.esru.strath.ac.uk/Programs/ESP-r.htm,`, 2015.

[21] C. D. Corbin, G. P. Henze, and P. May-Ostendorp, "A model predictive control optimization environment for real-time commercial building application," *Journal of Building Performance Simulation*, vol. 6, no. 3, pp. 159–174, 2013.

[22] M. Sourbron, C. Verhelst, and L. Helsen, "Building models for model predictive control of office buildings with concrete core activation," *Journal of Building Performance Simulation*, vol. 6, no. 3, pp. 175–198, 2013.

[23] J. E. Braun and N. Chaturvedi, "An inverse gray-box model for transient building load prediction," *HVAC Research*, vol. 8, no. 1, pp. 73–99, 2002.

[24] S. Prívara, J. Cigler, Z. Váňa, F. Oldewurtel, C. Sagerschnig, and k. . Eva Žáčeková, "Building modeling as a crucial part for building predictive control," *Energy and Buildings*, vol. 56, no. 0, pp. 8 – 22, 2013.

[25] J. Cai and J. E. Braun, "A generalized control heuristic and simplified model predictive control strategy for direct-expansion air-conditioning systems," *Science and Technology for the Built Environment*, vol. 21, no. 6, pp. 773–788, 2015.

[26] S. Goyal and P. Barooah, "A method for model-reduction of nonlinear building thermal dynamics," in *American Control Conference (ACC), 2011*, pp. 2077–2082, June 2011.

[27] G. Mustafaraj, J. Chen, and G. Lowry, "Development of room temperature and relative humidity linear parametric models for an open office using BMS data," *Energy and Buildings*, vol. 42, no. 3, pp. 348 – 356, 2010.

[28] S. Pívara, J. Široký, L. Ferkl, and J. Cigler, "Model predictive control of a building heating system: The first experience," *Energy and Buildings*, vol. 43, no. 23, pp. 564 – 572, 2011.

[29] S. C. Bengea, P. Li, S. Sarkar, S. Vichik, V. Adetola, K. Kang, T. Lovett, F. Leonardi, and A. D. Kelman, "Fault-tolerant optimal control of a building HVAC system," *Science and Technology for the Built Environment*, vol. 21, no. 6, pp. 734–751, 2015.

[30] J. Ma, S. J. Qin, and T. Salsbury, "Application of economic MPC to the energy and demand minimization of a commercial building," *Journal of Process Control*, vol. 24, no. 8, pp. 1282 – 1291, 2014.

[31] S. Qin and T. A. Badgwell, "A survey of industrial model predictive control technology," *Control Engineering Practice*, vol. 11, no. 7, pp. 733 – 764, 2003.

[32] M. LAwrynczuk, "A family of model predictive control algorithms with artificial neural networks," *Int. J. Appl. Math. Comput. Sci.*, vol. 17, pp. 217–232, June 2007.

[33] P.-D. Moroan, R. Bourdais, D. Dumur, and J. Buisson, "Building temperature regulation using a distributed model predictive control," *Energy and Buildings*, vol. 42, no. 9, pp. 1445 – 1452, 2010.

[34] Y. Ma, G. Anderson, and F. Borrelli, "A distributed predictive control approach to building temperature regulation," in *American Control Conference (ACC), 2011*, pp. 2089–2094, 2011.

[35] J. Široký, F. Oldewurtel, J. Cigler, and S. Prívara, "Experimental analysis of model predictive control for an energy efficient building heating system," *Applied Energy*, vol. 88, no. 9, pp. 3079 – 3087, 2011.

[36] Y. Ma, F. Borrelli, B. Hencey, B. Coffey, S. Bengea, and P. Haves, "Model predictive control for the operation of building cooling systems," *Control Systems Technology, IEEE Transactions on*, vol. 20, pp. 796 –803, may 2012.

[37] P. Scokaert and D. Mayne, "Min-max feedback model predictive control for constrained linear systems," *IEEE Trans. Autom. Cont*, vol. 43, no. 8, pp. 1136–1142, 1998.

[38] J. Löfberg, *Minimax Approaches to Robust Model Predictive Control*. No. 812 in Linköping Studies in Science and Technology. Dissertations, 2003.

[39] P. J. Goulart, E. C. Kerrigan, and J. M. Maciejowski, "Optimization over state feedback policies for robust control with constraints," *Automatica*, vol. 42, no. 4, pp. 523 – 533, 2006.

[40] S. Lucia, J. A. Andersson, H. Brandt, M. Diehl, and S. Engell, "Handling uncertainty in economic nonlinear model predictive control: A comparative case study," *Journal of Process Control*, vol. 24, no. 8, pp. 1247 – 1259, 2014.

[41] F. Oldewurtel, C. Jones, and M. Morari, "A tractable approximation of chance constrained stochastic mpc based on affine disturbance feedback," in *Decision and Control, 2008. CDC 2008. 47th IEEE Conference on*, pp. 4731–4736, Dec 2008.

[42] A. Richards and J. How, "Robust model predictive control with imperfect information," in *American Control Conference, 2005. Proceedings of the 2005*, pp. 268–273, June 2005.

[43] H. Fukushima and R. R. Bitmead, "Robust constrained predictive control using comparison model," *Automatica*, vol. 41, no. 1, pp. 97 – 106, 2005.

[44] L. Blackmore and M. Ono, "Convex chance constrained predictive control without sampling."

[45] C. R. Alie El-Din Mady, Gregory M. Provan and K. N. Brown, "Stochastic model predictive controller for the integration of building use and temperature regulation," *Proceedings of the Twenty-Fifth AAAI Conference on Artificial Intelligence*, pp. 1371 – 1376, 2011.

[46] F. Oldewurtel, A. Parisio, C. N. Jones, D. Gyalistras, M. Gwerder, V. Stauch, B. Lehmann, and M. Morari, "Use of model predictive control and weather forecasts for energy efficient building climate control," *Energy and Buildings*, vol. 45, no. 0, pp. 15 – 27, 2012.

[47] Y. Ma and F. Borrelli, "Fast stochastic predictive control for building temperature regulation," in *American Control Conference (ACC), 2012*, pp. 3075–3080, June 2012.

[48] S. Goyal, C. Liao, and P. Barooah, "Identification of multi-zone building thermal interaction model from data," in *Decision and Control and European Control Conference (CDC-ECC), 2011 50th IEEE Conference on*, pp. 181–186, Dec 2011.

[49] Z. Zhai and Q. Y. Chen, "Numerical determination and treatment of convective heat transfer coefficient in the coupled building energy and CFD simulation," *Building and Environment*, vol. 39, no. 8, pp. 1001 – 1009, 2004. Building Simulation for Better Building Design.

[50] D. Kim, J. Braun, E. Cliff, and J. Borggaard, "Development, validation and application of a coupled reduced-order CFD model for building control applications," *Building and Environment*, vol. 93, Part 2, pp. 97 – 111, 2015.

[51] H. Scherer, M. Pasamontes, J. Guzmn, J. lvarez, E. Camponogara, and J. Normey-Rico, "Efficient building energy management using distributed model predictive control," *Journal of Process Control*, vol. 24, no. 6, pp. 740 – 749, 2014.

[52] D. K. J. H. Vamsi Putta, Guangwei Zhu and J. E. Braun, "A distributed approach to efficient model predictive control of building HVAC systems," *International High Performance Buildings Conference*, pp. 1–6, 2012.

[53] S. Koehler, C. Danielson, and F. Borrelli, "A primal-dual active-set method for distributed model predictive control," in *American Control Conference (ACC), 2015*, pp. 4759–4764, July 2015.

[54] P. Ferreira, A. Ruano, S. Silva, and E. Conceiçâo, "Neural networks based predictive control for thermal comfort and energy savings in public buildings," *Energy and Buildings*, vol. 55, no. 0, pp. 238 – 251, 2012.

[55] A. Kusiak and G. Xu, "Modeling and optimization of HVAC systems using a dynamic neural network," *Energy*, vol. 42, no. 1, pp. 241–250, 2012. cited By (since 1996)8.

[56] A. Kusiak and M. Li, "Cooling output optimization of an air handling unit," *Applied Energy*, vol. 87, no. 3, pp. 901 – 909, 2010.

[57] H. Huang, L. Chen, and E. Hu, "A neural network-based multi-zone modelling approach for predictive control system design in commercial buildings," *Energy and Buildings*, vol. 97, no. 0, pp. 86 – 97, 2015.

[58] M. Mohammadzaheri, S. Grainger, and M. Bazghaleh, "Fuzzy modeling of a piezoelectric actuator," *International Journal of Precision Engineering and Manufacturing*, vol. 13, pp. 663–670, 2012.

[59] M. Killian, B. Mayer, and M. Kozek, "Effective fuzzy black-box modeling for building heating dynamics," *Energy and Buildings*, vol. 96, pp. 175 – 186, 2015.

[60] K. Li, H. Su, and J. Chu, "Forecasting building energy consumption using neural networks and hybrid neuro-fuzzy system: A comparative study," *Energy and Buildings*, vol. 43, no. 10, pp. 2893 – 2899, 2011.

[61] R. Parameshwaran, R. Karunakaran, C. V. R. Kumar, and S. Iniyan, "Energy conservative building air conditioning system controlled and optimized using fuzzy-genetic algorithm," *Energy and Buildings*, vol. 42, no. 5, pp. 745 – 762, 2010.

[62] G. Platt, J. Li, R. Li, G. Poulton, G. James, and J. Wall, "Adaptive HVAC zone modeling for sustainable buildings," *Energy and Buildings*, vol. 42, no. 4, pp. 412 – 421, 2010.

[63] J. Liang and R. Du, "Model-based fault detection and diagnosis of HVAC sys-

tems using support vector machine method," *International Journal of Refrigeration*, vol. 30, no. 6, pp. 1104 – 1114, 2007.

[64] G. Mustafaraj, G. Lowry, and J. Chen, "Prediction of room temperature and relative humidity by autoregressive linear and nonlinear neural network models for an open office," *Energy and Buildings*, vol. 43, no. 6, pp. 1452 – 1460, 2011.

[65] T. Lu and M. Viljanen, "Prediction of indoor temperature and relative humidity using neural network models: model comparison," *Neural Computing and Applications*, vol. 18, no. 4, pp. 345–357, 2009.

[66] S. Karatasou, M. Santamouris, and V. Geros, "Modeling and predicting building's energy use with artificial neural networks: Methods and results," *Energy and Buildings*, vol. 38, no. 8, pp. 949 – 958, 2006.

[67] N. Morel, M. Bauer, M. El-Khoury, and J. Krauss, "Neurobat, a Predictive and Adaptive Heating Control System Using Artificial Neural Networks," *Solar Energy Journal*, vol. 21, pp. 161–201, 2001.

[68] S. Karatasou, M. Santamouris, and V. Geros, "Modeling and predicting building's energy use with artificial neural networks: Methods and results," *Energy and Buildings*, vol. 38, no. 8, pp. 949 – 958, 2006.

[69] J. Yang, H. Rivard, and R. Zmeureanu, "On-line building energy prediction using adaptive artificial neural networks," *Energy and Buildings*, vol. 37, no. 12, pp. 1250 – 1259, 2005.

[70] L. Yang, Z. Nagy, P. Goffin, and A. Schlueter, "Reinforcement learning for optimal control of low exergy buildings," *Applied Energy*, vol. 156, pp. 577 – 586, 2015.

[71] P. Romeu, F. Zamora-Martnez, P. Botella-Rocamora, and J. Pardo, "Time-series forecasting of indoor temperature using pre-trained deep neural networks," vol. 8131

of *Lecture Notes in Computer Science*, pp. 451–458, Springer Berlin Heidelberg, 2013.

[72] A. H. Neto and F. A. S. Fiorelli, "Comparison between detailed model simulation and artificial neural network for forecasting building energy consumption," *Energy and Buildings*, vol. 40, no. 12, pp. 2169 – 2176, 2008.

[73] A. Ruano, E. Crispim, E. Conceicäo, and M. Lúcio, "Prediction of building's temperature using neural networks models," *Energy and Buildings*, vol. 38, no. 6, pp. 682 – 694, 2006.

[74] C. M. S. Mokhtar S. Bazaraa, Hanif D. Sherali, *Nonlinear Programming: Theory and Algorithms*. New York: Wiley, April 2006.

[75] K. Deb, A. Pratap, S. Agarwal, and T. Meyarivan, "A fast and elitist multiobjective genetic algorithm: Nsga-ii," *Trans. Evol. Comp*, vol. 6, pp. 182–197, Apr. 2002.

[76] X. He, Z. Zhang, and A. Kusiak, "Performance optimization of HVAC systems with computational intelligence algorithms," *Energy and Buildings*, vol. 81, pp. 371 – 380, 2014.

[77] Y. Zeng, Z. Zhang, and A. Kusiak, "Predictive modeling and optimization of a multi-zone HVAC system with data mining and firefly algorithms," *Energy*, vol. 86, pp. 393 – 402, 2015.

[78] H. Deng, H.-X. Li, and Y. hu Wu, "Feedback-linearization-based neural adaptive control for unknown nonaffine nonlinear discrete-time systems," *Neural Networks, IEEE Transactions on*, vol. 19, pp. 1615–1625, Sept 2008.

[79] A. Yeildirek and F. Lewis, "Feedback linearization using neural networks," *Automatica*, vol. 31, no. 11, pp. 1659 – 1664, 1995.

[80] M. Mohammadzaheri, L. Chen, and S. Grainger, "A critical review of the most popular types of neuro control," *Asian Journal of Control*, vol. 14, no. 1, pp. 1–11, 2012.

[81] F.-J. Lin, H.-J. Shieh, L.-T. Teng, and P.-H. Shieh, "Hybrid controller with recurrent neural network for magnetic levitation system," *Magnetics, IEEE Transactions on*, vol. 41, pp. 2260–2269, July 2005.

[82] D. C. Psichogios and L. H. Ungar, "A hybrid neural network-first principles approach to process modeling," *AIChE Journal*, vol. 38, no. 10, pp. 1499–1511, 1992.

[83] Y.-S. Yang and X.-F. Wang, "Adaptive H ∞ tracking control for a class of uncertain nonlinear systems using radial-basis-function neural networks," *Neurocomputing*, vol. 70, no. 46, pp. 932 – 941, 2007.

[84] D. O. Pedro, Jimoh, "Neural network based feedback linearization control of a servo-hydraulic vehicle suspension system," *International Journal of Applied Mathematics and Computer Science*, vol. 21, no. 1, pp. 137–147, 2011.

[85] H. A. te Braake, E. J. van Can, J. M. Scherpen, and H. B. Verbruggen, "Control of nonlinear chemical processes using neural models and feedback linearization," *Computers & Chemical Engineering*, vol. 22, no. 78, pp. 1113 – 1127, 1998.

[86] M. Maasoumy, M. Razmara, M. Shahbakhti, and A. S. Vincentelli, "Handling model uncertainty in model predictive control for energy efficient buildings," *Energy and Buildings*, vol. 77, no. 0, pp. 377 – 392, 2014.

# Chapter 3

# Methodology

In order to address the research gaps mentioned in the literature, the details of the methods that will be undertaken during the study are described in the following subsections. Fig. 3.1 illustrates the overview of the methodology adopted for this project. The developed research methodology is formulated in four articles, with each paper aiming to fulfil some research gaps and to achieve the corresponding research objective. Detailed descriptions of the linkages between these papers and the main achievement will be demonstrated in the latter sections. In the following sections, the aspects of building control that this thesis focuses on will be introduced.

## 3.1 Research Building

This thesis focuses on the Terminal-1 (T1) building at Adelaide Airport, South Australia. The T-1 is the main terminal for domestic and international flights, which is approximately 750 metres end to end and has a total floor area of approximately 75,000 $m^2$. The energy review shows that the annual electricity bill recorded in the T-1 building is about 1 million dollars. About 40% of this energy consumption relates to HVAC systems. Different from other airport terminals, the T-1 building has no flights during the night, so the HVAC

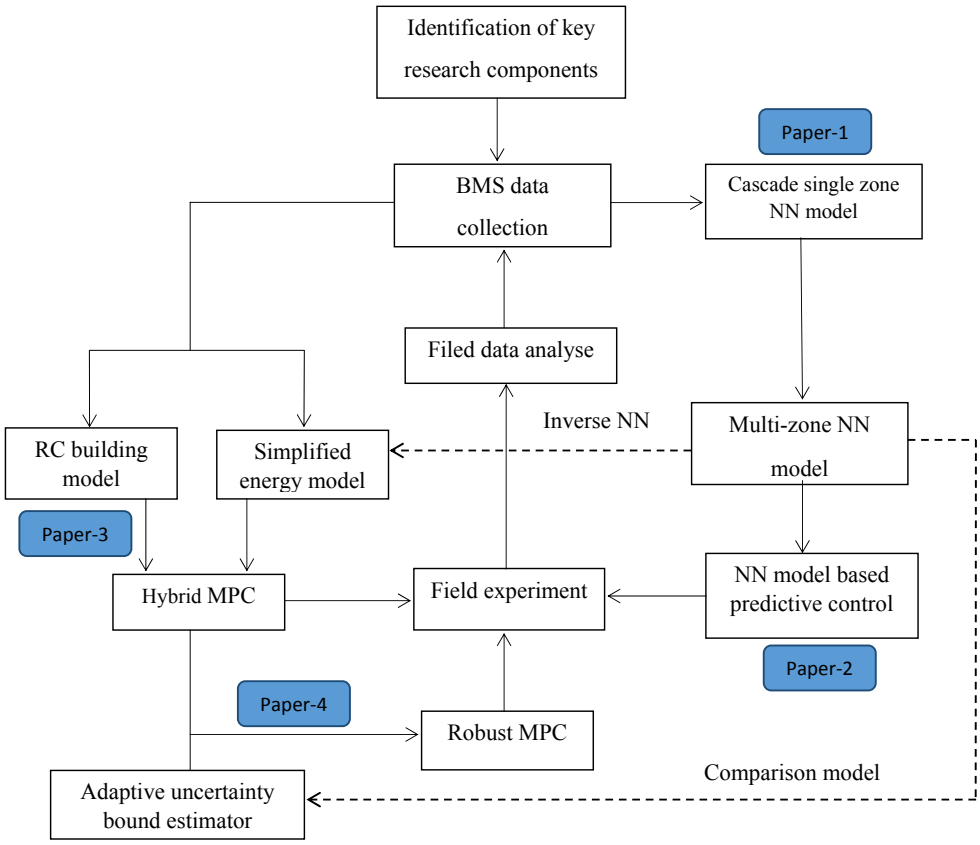


Figure 3.1: Summary of research methodology applied in this study and their link with the papers

system of this building has a relatively long period of night setback. Comfort requirements only need to be met when occupants are present, (e.g., when a flight is approaching and passengers are checking in). The comfort constraints can be relaxed when there is no flight. These unique properties make the building a good research vehicle for testing the proposed control strategies.

## 3.2 Thermal Comfort

The main function of HVAC systems is to provide a comfortable indoor environment for the occupants. The predicted mean vote (PWV) is the most commonly applied model to indicate occupants' thermal comfort. The PMV model was developed by P. O. Fanger using heat balance equations and empirical studies about skin temperature to define comfort [1]. PMV is calculated based on temperature, relative humidity, mean radiant temperature, air velocity, and individual factors such as metabolism rate and clothing insulation. When using PMV for the indication of thermal comfort, zero is the ideal value, representing thermal neutrality. The comfort zone is defined by the combinations of the six parameters for which the PMV is within the range of [-0.5, 0.5].

The nonlinear characteristics of PMV make the implementation of MPC difficult, as linear constraints cannot be directly applied under the nonlinear model framework. For this reason, thermal comfort is more commonly indicated by operative temperature bounded by upper and lower temperature values [2, 3]. According to ASHRAEs Standard 55, comfort temperature should be ranged from 20-23 °C in the winter and 23- 26°C in the summer [4]. Additionally, a minimum ventilation rate must be met when the space is occupied to maintain a reasonable level of carbon dioxide concentration. The actual comfort requirement might be more specific than this. For the investigated study, it is required that the indoor temperature be kept at 22 °C in the summer and 21.5 °C in the winter. Therefore, the aim is to keep the temperature closed to the set point value for most of the time during the occupancy. However, the temperature is allowed to vary between the upper and lower comfort range during the transitional period between occupied and un-occupied hours. To conclude, the thermal comfort is indicated by dry bulb temperature and carbon dioxide concentration in this study.

## 3.3 Occupancy Prediction

Occupant prediction is an important parameter for the design of predictive controls within building systems. Not only because it represents a major source of internal heat gain, but also because it is a constraint describing the occupants's comfort requirements. The energy saving potential for predictive controllers has been demonstrated in a number of studies [5, 6]. Because the occupancy is highly uncertain and expensive to measure, it is often modelled as a stochastic variable [7]. Several approaches have been used for occupancy prediction. For example, Ma et al. [8] built a thermal model during unoccupied hour. They use the difference between the prediction and the real data during occupied hour to model the load profile. Maasoumy et al. [8] used the measurement of carbon dioxide concentration to indicate the level of occupancy within the building. Liao and Barrooah [9] developed an agent-based model to simulate the behaviour of the occupants within the building.

To make it simple, in this study, the occupancy schedules are assumed to be perfectly predicted. This schedule is set according to the actual working hours and the flight schedule, which can be easily obtained from the BMS database. The thermal load brought by the occupancy will be indicated using $CO_2$ concentration, which is similar to [10].

## 3.4 Energy Price

Most of the existing buildings use the night-setback strategy, which turns on the HVAC systems before occupation and turns them off before the occupied hours are over. This strategy usually causes unnecessarily long operational hours. If the dynamic electricity price is not utilised, the optimisation only minimises the energy costs, which could reduce the AHU operational hours [11]. On the other hand, while advanced electricity pricing methods, such as time-of-use (TOU) rates, critical-peak-pricing (CPP), and real-time pricing (RTP) are applied by utilities, it is possible for the end users to reduce both the peak

electricity and demand costs [12, 13]. In this study, we employed the TOU rate in Adelaide, South Australia, as the criterion to investigate the energy and cost saving potential of MPC.

## 3.5 Energy and Cost Saving Evaluation Methods

Evaluating the energy saving potential of the proposed control strategies can be realised by both simulation and experiment. For simulation, two methods are often employed. The first one is to conduct a closed-loop simulation using the control model obtained from the measured data and then to compare the results produced by the MPC with the baseline controller. The parameters of the models are sometimes perturbed to make the simulation more realistic [14]. This approach allows one to make a comparison between the existing control strategy and the developed one straightforwardly. However, this requires an accurate model to be built, otherwise the simulation result will deviate a lot from the true value, and the comparison becomes meaningless. The second method is to test the advanced control algorithm on high fidelity models [15]. For example, using the TRNSYS model together with the Matlab optimisation toolbox to perform the simulation [16]. However, the high fidelity model can hardly model the uncertainty presented at the real buildings, which could make the simulation un-realistic.

In this thesis, we choose the first approach for simulation purposes. Alternatively, we use a well-trained recursive NN model as the reference model during the simulation. Since the recursive NN can capture uncertainty of the building systems and achieve better indoor temperature accuracy than the control model (usually a control oriented model), it can often generate a control result that is closer to the experimental study.

The control methods proposed in this thesis have also been validated by experimental studies. During the experiment, the optimal set-point was generated by conducting closed-loop simulation one day ahead of the experimental day. The new set-point values are then sent to the BMS. Making comparisons between the experimental method with the

existing control method is achieved by choosing the days on which weather patterns and occupancy profiles were similar to the experimental day. This method was previously adopted in [17], which allows a easy comparison to be made between baseline control and the proposed control method.

## 3.6 Linkage Between Papers

This section deals with authors' results related to the thesis. This thesis is not written in a conventional way but its core lies in four reviewed papers, which are included here with a brief comment on how the particular paper contributes to the thesis. The novelty and uniqueness of this research are presented in the following papers:

*Paper-1* introduces a systematic NN modelling method for large commercial buildings using BMS data. In particular, we present a novel cascade RNN model, which uses neighbouring zone temperatures as an input to perform indoor temperature prediction. The method results in single-zone prediction results with enhanced prediction accuracy. This method also makes it possible to model both interior and perimeter zones of large commercial buildings with good accuracy. This method can also be used to evaluate the degree of coupling between zones.

Although the NN model proposed in *Paper-1* establishes a connection between adjacent zones, it cannot be directly applied to perform long-term prediction for multiple zones. This is because the neighbouring zone temperatures are only known to the current step, but the future ones are unknown and dependent upon their coupling status. *Paper-2* validates and improves the outcomes of the method proposed in *Paper-1*. It presents a multi-zone NN model that is capable of predicting thermal dynamics of several adjacent zones simultaneously. The developed model is the first recursive MIMO model which models the convective thermal interaction between adjacent zones. This method is especially suitable for the modelling of the thermal zones which are wide open, adjacent, but controlled by different AHUs. By comparing simulation results, we prove that this ap-

proach produces better prediction results than using single-zone models. Moreover, based on the model, a simple and effective optimal start-stop control method is developed for the investigated building. The energy saving potential of applying this method to achieve energy saving is proved. Moreover, the proposed multi-zone model provides a more correct optimal control result, due to its enhanced prediction accuracy.

The NN based predictive control presented in *Paper-2* is rule based but does not provide any global optimised solutions. To take into account more factors, such as time-varying electricity price, free-cooling and the thermal storage ability of the building, a more systematic optimisation framework is needed. To achieve this, a hybrid MPC (HMPC) is presented in *Paper-3*. The HMPC employs a low-complexity RC model as a control oriented model, which is linearised using feedback linearisation. Linear programming is applied to solve the optimisation problem, and an inverse NN is employed to map the nonlinear relationship between the actual control command and the linearised control output. Simulations and experiments were conducted, which demonstrate the effectiveness of this strategy in achieving energy and cost savings within commercial buildings.

The HMPC introduced in *Paper-3* deals with the uncertainty associated with the nonlinear HVAC process, but it does not consider the uncertainty related to the building process. Because the simplified RC model used for building dynamics modelling is linear, time-invariant, it inevitably results in modelling errors, which cause degradation to the performance of the MPC. This is particularly true for the experimental zones, which are affected by a high degree of uncertainty, and accurate modelling results are hard to obtain. Therefore, *Paper-4* mainly concerns the design of a RMPC to handle system uncertainties and to guarantee constraints satisfaction. In particular, this paper proposes an adaptive uncertainty bound estimator for robust MPC. The estimator is built upon the RNN model introduced in *Paper-2* and *Paper-3*. This approach makes it possible to handle the non-Gaussian uncertainty effectively. The results show this method is able to obtain better constraints satisfaction with the least performance loss.

Finally, Chapter 8 summarise the main findings in this thesis, and discusses the topics for further research.

# References

[1] R. Z. Freire, G. H. Oliveira, and N. Mendes, "Predictive controllers for thermal comfort optimization and energy savings," *Energy and Buildings*, vol. 40, no. 7, pp. 1353 – 1365, 2008.

[2] Y. Ma, A. Kelman, A. Daly, and F. Borrelli, "Predictive control for energy efficient buildings with thermal storage: Modeling, stimulation, and experiments," *Control Systems, IEEE*, vol. 32, pp. 44–64, Feb 2012.

[3] I. Hazyuk, C. Ghiaus, and D. Penhouet, "Optimal temperature control of intermittently heated buildings using model predictive control: Part II control algorithm," *Building and Environment*, vol. 51, no. 0, pp. 388 – 394, 2012.

[4] A. Standard, "Thermal environmental conditions for human occupancy," 2004.

[5] S. S. Kwok and E. W. Lee, "A study of the importance of occupancy to building cooling load in prediction by intelligent approach," *Energy Conversion and Management*, vol. 52, no. 7, pp. 2555 – 2564, 2011.

[6] F. Schildbach, D. Sturzenegger, and M. Morari, "Importance of Occupancy Information for Building Climate Control," *Applied Energy*, vol. 101, p. 521532, Jan. 2013.

[7] C. R. Alie El-Din Mady, Gregory M. Provan and K. N. Brown, "Stochastic model predictive controller for the integration of building use and temperature regulation," *Proceedings of the Twenty-Fifth AAAI Conference on Artificial Intelligence*, pp. 1371 – 1376, 2011.

[8] Y. Ma, J. Matusko, and F. Borrelli, "Stochastic model predictive control for building hvac systems: Complexity and conservatism," *Control Systems Technology, IEEE Transactions on*, vol. 23, no. 1, pp. 101–116, 2015.

[9] C. Liao and P. Barooah, "An integrated approach to occupancy modeling and estimation in commercial buildings," in *American Control Conference (ACC), 2010*, pp. 3130–3135, June 2010.

[10] M. Maasoumy and A. Sangiovanni-Vincentelli, "Total and peak energy consumption minimization of building HVAC systems using model predictive control," *Design Test of Computers, IEEE*, vol. 29, pp. 26–35, Aug 2012.

[11] H. Huang, L. Chen, and E. Hu, "A neural network-based multi-zone modelling approach for predictive control system design in commercial buildings," *Energy and Buildings*, vol. 97, no. 0, pp. 86 – 97, 2015.

[12] W. Surles and G. P. Henze, "Evaluation of automatic priced based thermostat control for peak energy reduction under residential time-of-use utility tariffs," *Energy and Buildings*, vol. 49, pp. 99 – 108, 2012.

[13] J. Ma, S. J. Qin, and T. Salsbury, "Application of economic MPC to the energy and demand minimization of a commercial building," *Journal of Process Control*, vol. 24, no. 8, pp. 1282 – 1291, 2014. Economic nonlinear model predictive control.

[14] S. Bengea, V. Adetola, K. Kang, M. J. Liba, D. Vrabie, R. Bitmead, and S. Narayanan, "Parameter estimation of a building system model and impact of estimation error on closed-loop performance," in *Decision and Control and European Control Conference (CDC-ECC), 2011 50th IEEE Conference on*, pp. 5137–5143, 2011.

[15] C. D. Corbin, G. P. Henze, and P. May-Ostendorp, "A model predictive control op-

timization environment for real-time commercial building application," *Journal of Building Performance Simulation*, vol. 6, no. 3, pp. 159–174, 2013.

[16] G. P. Henze, D. E. Kalz, S. Liu, and C. Felsmann, "Experimental analysis of model-based predictive optimal control for active and passive building thermal storage inventory," *HVAC&R Research*, vol. 11, no. 2, pp. 189–213, 2005.

[17] Y. Ma, A. Kelman, A. Daly, and F. Borrelli, "Predictive control for energy efficient buildings with thermal storage: Modeling, stimulation, and experiments," *Control Systems, IEEE*, vol. 32, pp. 44–64, Feb 2012.

# Chapter 4

# Modelling of Building Energy Systems

This chapter is based on the following paper:

*Full citation*: Huang H., Chen L., Mohammadzaheri M., Hu E., "A New Zone Temperature Predictive Modeling for Energy Saving in Buildings", In Procedia Engineering, vol. 49, pp. 142 - 151, 2012.

The above paper was written at the early stage of the study. Some modifications have been made to make the knowledge more complete.

*Contributions of this chapter*: In this chapter, the capability of the RNN in modelling the nonlinear AHU plants and thermal dynamics of the investigated building is demonstrated. As a major novelty, the developed RNN model uses neighbouring zone temperatures as inputs to perform temperature prediction in the investigated zone. This method results in improved prediction accuracies by considering the thermal coupling.

# Statement of Authorship

| | |
|---|---|
| Title of Paper | A new zone temperature predictive modelling for energy saving in buildings |
| Publication Status | ☑ Published ☐ Accepted for Publication<br>☐ Submitted for Publication ☐ Unpublished and Unsubmitted w ork w ritten in manuscript style |
| Publication Details | Huang H., Chen L., Mohammadzaheri M., and Hu E., (2012), A new zone temperature predictive modelling for energy saving in buildings, Procedia Engineering Vol. 49C pp. 144-153. |

## Principal Author

| | |
|---|---|
| Name of Principal Author (Candidate) | Hao Huang |
| Contribution to the Paper | Developed theory, collected data, developed models and wrote the manuscript. |
| Overall percentage (%) | 60% |
| Certification: | This paper reports on original research I conducted during the period of my Higher Degree by Research candidature and is not subject to any obligations or contractual agreements with a third party that would constrain its inclusion in this thesis. I am the primary author of this paper. |
| Signature | Date 15/10/15 |

## Co-Author Contributions

By signing the Statement of Authorship, each author certifies that:

i. the candidate's stated contribution to the publication is accurate (as detailed above);
ii. permission is granted for the candidate in include the publication in the thesis; and
iii. the sum of all co-author contributions is equal to 100% less the candidate's stated contribution.

| | |
|---|---|
| Name of Co-Author | Lei Chen |
| Contribution to the Paper | Supervised research, helped with data collection and edited manuscript |
| Signature | Date 15/10/15 |

| | |
|---|---|
| Name of Co-Author | Morteza Mohammadzaheri |
| Contribution to the Paper | Supervised research, helped to evaluate and edit the manuscript |
| Signature | Date 18/10/15 |

| | |
|---|---|
| Name of Co-Author | Eric Hu |
| Contribution to the Paper | Supervised research , helped to evaluate and edit manuscript |
| Signature | Date 15/10/15 |

**Abstract**

Currently in most buildings, the heating, ventilation and air conditioning (HVAC) systems are controlled by the present temperature in the buildings. If the predictions for future indoor temperature in the building or a zone were available, the building management system (BMS) could use both present and future temperatures to control HVAC systems to optimise the energy usage of the buildings. Therefore, a lot of research effort has been devoted to develop accurate temperature prediction models using various approaches, e.g., traditional thermodynamic, simplified physical model, artificial neural networks (ANN), and fuzzy logic approaches. When a sufficient amount of historical data of the building is available, the ANN approach is thought to be the most cost-effective one. Most of the previous studies of ANN modelling of building temperature, have either focused on single zone studies or assumed that the thermal coupling between the zones are insignificant. In this study, a more realistic multi-zone scenario in a large building is proposed in the development of the ANN temperature predictive model. Different from the previous studies, the coupled effects between zones caused by heat transfer are modelled using several ANN models in cascade forms. The accuracies of the models were validated using experimental data, which shows that the ANN models are very suitable to be used for the modelling of the AHUs process. More importantly, it is found that considering the temperatures of the neighbouring zones can achieve more accurate results as compared with the single-zone model, which indicates the importance of the thermal coupling during the control design.

## 4.1 Introduction

Heating, ventilation and air conditioning (HVAC) systems in commercial buildings account for almost 50% of electricity bills for the buildings. An effective way to achieve energy efficiency in HVAC systems is to implement supervisory control systems to optimise the set points and operating modes of local control components [1]. In recent years,

the supervisory control system design has benefitted greatly from the widespread use of building management systems (BMS). BMS provides operators with a platform to monitor and record the HVAC conditions, as well as to tune the local control parameters with ease. To make the most efficient use of BMS for supervisory control systems design, online predictive models with the ability to predict both the long-term and short-term dynamic behaviours of HVAC systems are needed. The predictive model should be accurate within a wide operating range and be suited to model both perimeter and interior zones of the building, by considering both the internal heat gain and varying ambient environment. This dynamic model can be used for energy-efficiency control, such as model predictive control (MPC) for building energy control [2–5].

In this paper, we focus on the investigation of the thermal zone process. Thermal zone is referred to as an area in which the sensible temperature and relative humidity are regulated by a single air handling unit (AHU) or a variable air volume box. The BMS uses a series of PID controllers in cascaded form to regulate the indoor temperatures, each associated with a particular zone. Zone thermal dynamics modelling is a challenging task for a list of reasons. Firstly, a building's operational environment is a time-varying system, influenced by a variety of uncertainties. The change of occupancy level, weather conditions and operational mode will affect the temperatures of zones inside a building. Furthermore, HVAC system itself has several coupled control processes that cannot be treated independently. For example, the AHU process suffers from process-gain and time-delay variation due to the chilled water temperature change and flow-rate fluctuation [6]. Moreover, there are many nonlinear control variables such as temperature, humidity and damper actions, which cannot be accurately modelled using the first principle models. Lastly, the coupling effects between the adjacent zones are always unknown and hard to model.

For achieving such a modelling task, energy and mass balance integral-differential equations are often employed. The parameters in the equations are with physical signif-

icance and can well represent the main characteristics of the systems. However, tuning a detailed physical model requires extensive efforts and time consuming. On the other hand, simplified physical models derived from grey-box modelling methods cannot always provide enough modelling accuracy. Recently, intelligent modelling technologies, such as artificial neural network (ANN) models, have been extensively used for HVAC zone temperature prediction. It has been shown in several studies that ANN models are suitable for the modelling of nonlinear HVAC systems and buildings' thermal dynamics [7–11]. For example, Ruano et al. [8] built an adaptive radial basis function neural network model to predict the temperature in a school building, with the result revealing better performance than the multi-node physically based model. Using feedforward neural networks, Lu and Viljanen [7] constructed a nonlinear autoregressive with external input (NNARX) model to predict both indoor temperature and relative humidity. Based on this study, Mustafaraj et al. [10] developed both a linear ARX model and a neural network-based NNARX model using BMS data to predict the thermal behaviour of an open office. Besides pure modelling works, the ANN models have also been applied to control applications. For example, an online ANN controller was developed and used in [2] to control a commercial ice storage of an HVAC system. The controller determined the hourly set-points for the chiller plant in order to minimize the total cost over a 24-hour period. In another study, a back propagation-based ANN model was developed to determine the rising time for a heating system in a building [12]. The similar model structure was later used in [13] to increase the thermal comfort level of occupants and reduce energy consumption by reducing temperature overshoot and undershoot phenomena in an air conditioning system.

However, most of the existing studies had either focused on single-zone examination or assumed that the interaction within the buildings were negligible [10, 14]. This assumption may be true for the rooms that are well insulated, but not the zones with wide open space, such as a public hall. In real-life buildings, thermal characteristics of the

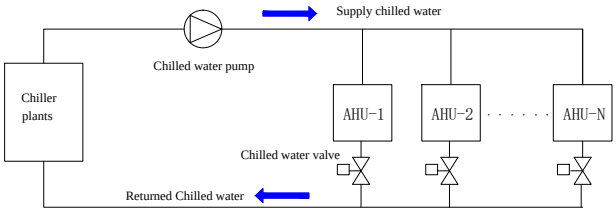


Figure 4.1: Schematic of the chiller plant.

zones are very different from one to another, and are correlated. It is therefore necessary to develop a method suitable for multi-zone modeling, so that they can be used to predict zone temperature at any locations of a building. When a model predictive control is considered, the effect of this thermal coupling will be lumped into the uncertainty terms, which will increase the degree of uncertainty within the model and deteriorate its performance. Investigating the effects of this thermal coupling therefore becomes important.

The paper starts by analysing the physical principle of the AHU plant and thermal zone process. Afterwards, the thermal dynamics models for them will be modelled by using RNN models. In particular, this research proposes a cascade NN structure which enables modelling of temperature dynamics in both perimeter and interior zones of a large commercial building.

## 4.2 System Description

### 4.2.1 AHU Model

In this section, some first principles models for the HVAC plants and thermal zones are built and analysed. The purpose is to illustrate the complexity of the building modelling problem. The HVAC system investigated in the case study has three chillers to provide chilled water. The strategy of starting a new chiller is determined by the common chilled water return temperature in the primary loop. If this temperature is above a threshold

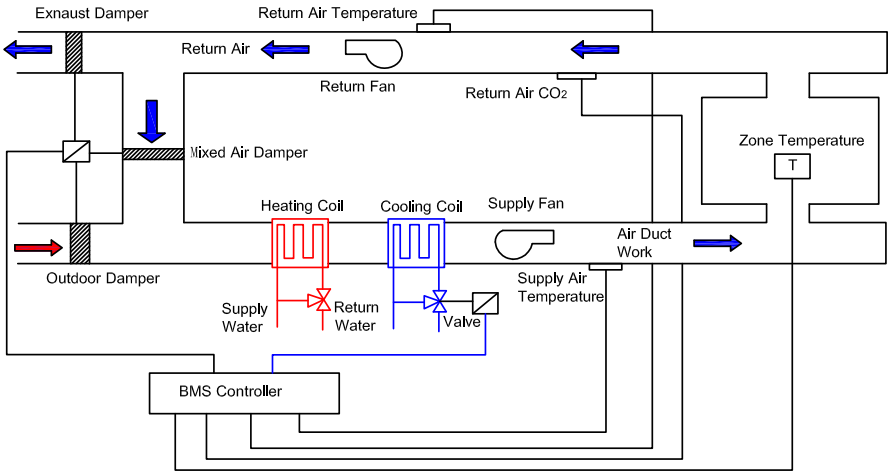


Figure 4.2: Schematic of the AHU. The arrows indicate the direction of the air flow inside the duct.

value of 12°C for more than five minutes, the BMS will enable a new chiller. Fig. 4.1 shows the schematic diagram of a chiller plant: chilled water is transmitted from the chiller plants to the cooling coils at individual AHUs through control of variable speed water pumps.

At the subsystem level, several AHUs are running in parallel to serve different zones. Fig. 4.2 shows the schematic diagram of a constant air volume (CAV) air-handling unit. It consists of a cooling coil, a heating coil, water valves, fans and air dampers. The return air is partially recirculated through the mixed air damper and partially exhausted through the exhaust damper. On the other side, the fresh air enters the circuit through the outdoor air damper and then mixed with the return air. These three dampers are controlled to regulate the percentage of return air and outdoor air used for conditioning the space. When ambient temperature is sufficient low, the outdoor air damper will be open to allow more cool air to come in. If we assume that no frictional losses occur across the converging section, the

relationship among the return air, outdoor air and mixed air can be depicted as [15]:

$$m_r C_a T_r + m_{out} C_a T_{out} = m_m C_a T_m, \tag{4.1a}$$

$$m_r + m_o = m_m, \tag{4.1b}$$

where $m_r$ and $T_r$ are mass flow rate and temperature of the return air, respectively, $m_{out}$ and $T_{out}$ are mass flow rate and temperature of the outdoor air, respectively, $m_m$ and $T_m$ are mass flow rate and temperature of the mixed air, respectively, and $C_a$ is specific heat of air. The mixed air passes through the cooling coil in which heat exchange happens. It is assumed that the cooling coil is well mixed, so that the outflow water temperature is the same as the mean temperature of the water inside the coil. The energy balance on the water and air side of the cooling coil can therefore be expressed as:

$$C_{cw}\frac{dT_{cwo}}{dt} = m_w C_p(T_{cws} - T_{cwo}) - UA(T_{cwo} - T_{sa}), \tag{4.2a}$$

$$C_a\frac{dT_{sa}}{dt} = UA(T_{cwo} - T_{sa}) - \dot{m}C_a(T_{sa} - T_{ai}), \tag{4.2b}$$

where $C_{cw}$ is the overall thermal capacity of the chilled water and coil body, $T_{cwo}$ is outflow water temperature, $T_{ao}$ is discharge (outflow) air temperature, $m_w$ is water mass flow rate, U is overall heat transfer coefficient, A is effective surface of the coil, $C_a$ is the specific heat capacity of the supplied air, and $T_{ai}$ is the temperature of the air going into the cooling coil. The chilled water temperature and flow rate vary according to the cooling load of the entire building, which causes disturbance to the AHU process.

The control input to the system is $m_w$ regulated by the opening level of chilled water valve in percentage. The chilled water valve is simply controlled proportionally by the difference between measured zone temperature and setpoint temperature to maintain the desired zone temperature value. The water valve also has static nonlinearity, which is caused by the water pressures around the installed valve in the pipe network. It can be

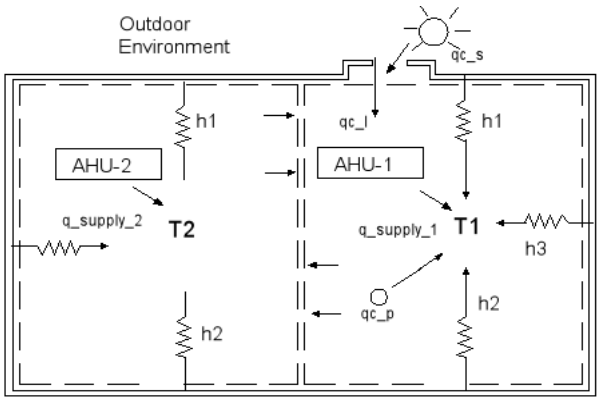


Figure 4.3: Analytical model for calculating zone temperatures.

seen that the main factors affecting the supply air temperature are return air temperature, outdoor air temperature, return chilled water temperature, chilled water flow rate, valve opening level and damper opening level. Eq. (4.2a) is bilinear in structure, because of the multiplication of chilled water temperature and chilled water flow rate.

### 4.2.2 Thermal Zone Process

It is assumed that there is a big room that is divided into two zones and the temperature in each zone is uniform, as shown in Fig. 4.3. It can be seen that the temperatures of the zones depend on the surface temperature of the walls, heat transfer coefficient of the walls, outdoor temperature, flow rate of the supply air, supply air temperature, solar gain and neighbouring zone temperature etc. The temperature distribution in each zone is assumed to be uniform, the density of the air and air flow rates are both assumed to be constant. Energy and mass balance governing equation of the zone can be written as [15]:

$$\begin{aligned} C_z\frac{dT_z}{dt} = \dot{m}_1 C_a(T_{sa}-T_z) + U_R A_R(T_R-T_z) + U_g A_g(T_{out}-T_z) + U_w A_w(T_w-T_z) \\ +\dot{m}_2 C_a(T_n-T_z) + Q_r + Q_p + Q_{leak}, \end{aligned} \tag{4.3a}$$

$$C_w \frac{dT_z}{dt} = U_w A_w (T_z - T_w) + U_w A_w (T_{out} - T_w), \tag{4.3b}$$

$$C_R \frac{dT_R}{dt} = U_R A_R (T_z - T_R) + U_R A_R (T_{out} - T_R), \tag{4.3c}$$

where $C_z$ is the overall thermal capacity of the zone, $T_z$ and $T_n$ are zone temperature and neighbouring zone temperature, respectively, $T_{out}$ is outdoor temperature, $T_{sa}$ is supply air temperature, $T_w$ is mean temperature of inside surface of the walls, $\dot{m}_1$ and $\dot{m}_2$ are mass flow rate of the supply air and the air between investigated zone and its neighbouring zone, $U_w$, $U_g$ and $U_R$ denote the overall heat transfer coefficient of surface of the walls, window and roof, respectively, $A_w$, $A_R$ and $A_g$ denote area of the wall, roof and window, respectively, $Q_r$, $Q_p$ and $Q_{leak}$ stand for heat gain from solar radiation, occupants and leakage of the zones, respectively. Eq. (4.3) illustrates that the rate of temperature change in the investigated zone is related to the dynamic variables such as the temperatures of supply air, wall surface, outdoor air and neighbouring zone. The convective heat transfer between zones can be expressed as:

$$R_f = \alpha d R_v C_v \tag{4.4}$$

where $\alpha$ denotes the constant of proportionality, $d$ denotes the distance between the two temperature sensors, $R_v$ denotes resistance per unit distance, and $C_v$ denotes the capacitance between the zones.

## 4.3 Recurrent NN

It can be seen that both simplified AHU model and thermal zone models are nonlinear in nature and affected by uncertainties. Therefore, NN model could be a better method to perform the modelling task. Feedforward neural network is a static network, and if without tapped delay term, it is unable to represent a dynamic system. On the other hand, the RNN has an internal feedback loop, so it can store information for latter use. Their

abilities to deal with time-varying input or output through their own natural temporal operation are of particular interests of researchers [16]. The RNN can always demonstrate good control performance in the presence of uncertainty, and is more suitable for dynamical systems as compared with the FNN.

Nonlinear autoregressive with exogenous inputs (NARX) model is used to express the RNN structure. A multiple inputs, single output nonlinear system used for one-step-ahead prediction has the following form:

$$\hat{y}(k) = f[\phi(k), w] + e(k), \tag{4.5}$$

$$\begin{aligned} \phi(k) = [&y(k-1)...y(k-n_a), u_1(k-d_1)...u_1(k-n_b- \\ &d_1+1), ..., u_i(t-d_i)...u_i(k-n_i-d_i+1)]^T, \end{aligned} \tag{4.6}$$

where $\hat{y}$ denotes the predicted outputs, $i$ denotes the number of input variables, $d$ is the delay time of input variables, $k$ is time step, $n_a$ to $n_i$ are the orders of input variables, $f$ is the NN function, $w$ is the weighting factor, and $e$ is modelling error. The output variable is predicted one step ahead, as a function of past values of both input variable $u$ and output variable $y$. The delay time is an inherent property of the input variable, which can be obtained from the physical characteristics of the dynamic system. The orders of inputs variables, expressed by $n_i$ , reflects the persistence of dynamics within the system [17].

### 4.3.1 Multi-layer Perceptions Neural Network

ANNs are mathematical models inspired by biological NNs. They mimic a human neuron system, to acquire learning ability. Learning from historical data, the networks adjust the connection weights among the neurons according to learning rules, so that trained networks can generate correct outputs. The most attractive feature of NNs is that they are capable of approximating any measurable functions to any desired degree of accuracy

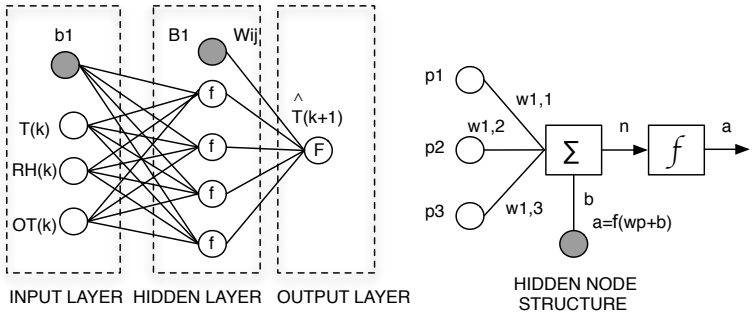


Figure 4.4: (left): The structure of a feed-forward neural network model; (right): the structure of a hidden node in the ANN.

[18]. Multi-layer perceptions (MLPs) are the most commonly used NNs in control [19]. The structure of an ANN is illustrated in Fig. 4.4. The first layer of MLP is a set of sensory units containing the information from all input variables. The second layer is a hidden layer containing a certain number of neurons. Each neuron has a sum operator and an activation function, which perform nonlinear transformation. The hidden layer uses a logistic sigmoid function as the activation function. A NN with three layers of neurons was employed. The network function is expressed with the following equation:

$$\hat{y}(t) = F\sum_{i=1}^{n_u} W_{j,u} f(\sum_{i=1}^{n_h} w_{u,i}\varphi_i(k) + b_{u,0}) + B_{j,0}, \tag{4.7}$$

$$f(x) = \frac{1}{1+exp(-x)}, \tag{4.8}$$

where $u$ denotes the inputs to the network, $w_{u,j}$ is the weighting vector from the hidden neurons to the output layer, $W_{j,u}$ represents the matrix containing the weights from the external inputs to the hidden units, $b_{u,0}$ and $B_{j,0}$ are the bias of the hidden units and the output layer, respectively, and the scalars $n_u$ and $n_h$ denote the number of units in the input layerand hidden layer, respectively. $\varphi_i(k)$ indicates the vector that contains the regression of the Eq. (4.6) at time step $k$, $f$ is sigmoid function expressed by Eq. (4.8), and $F$ uses a linear function, and j = 1 as only one out put is considered. The weight vector $w$ and bias

vector $b$ at the hidden layer were initialised using the Nguyen-Widrow method to keep the trained model more consistent. Levenberg-Marquardt was employed to train the NN, which minimises mean square error (MSE). The transfer function $f$ in the hidden layer can also be a linear one, which makes the NN model linear as well.

## 4.4 Data Preparation

ANN modelling was started by choosing the relevant input candidatures and storing them in a matrix for preparation. Since some of the candidature variables selected above may be correlated, noisy and have no significant relationships with the outputs, a suitable input variable selection criterion is needed. To address the problem, a simple linear forward selection criterion is used in this study to obtain the best ANN model structure as well as to investigate the relevance of each input variable [17]. Using this method, the initial candidate variables are chosen based on the prior knowledge of the system. The performance of the model is then maximised by changing the orders of input variables and number of hidden layers. The remaining candidature variables are then added on top of the previous ones, after the last optimisation process is finished. The candidate variables that fail to improve the performance of the ANN model are abandoned and others will be preserved .

The experiment started by choosing a combination with three inputs: zone temperature ($T_z$), outdoor temperature ($T_{out}$) and supplied cooling energy ($Q_u$). The delay times of variables were estimated by observing the historical data and were used to re-arrange the input variables. The data preparation method used in [20] was employed in this study.

After considering the delay, the data matrix can be rewritten as:

$$\overbrace{\begin{bmatrix} T_z(r) & \cdots & T_z(r-n_a+1) & T_{out}(r) & \cdots & T_{out}(r-n_b+1) & Q_u(r) & \cdots & Q_u(r-n_c+1) \\ \vdots & \vdots & \vdots & \vdots & \vdots & \vdots & \vdots & \vdots & \vdots \\ T_z(n) & \cdots & T_z(n-n_a+1) & T_{out}(n) & \cdots & T_{out}(n-n_b+1) & Q_u(n) & \cdots & Q_u(n-n_c+1) \end{bmatrix}}^{input}, \tag{4.9}$$

$$\overbrace{\begin{bmatrix} T_z(r+1)) \\ \vdots \\ T_z(n+1) \end{bmatrix}}^{output}, \tag{4.10}$$

where $r$ is the order of the system, which is equal to the maximum order of input and output variables. Eq. (4.9) was later expanded to include more input variable candidates for NN training in order to obtain the best model structure. For example, when 31 days' data are used for training, with $n_a = 3, n_b = 2, n_c = 1$, the data can be prepared in the following way:

$$Data = \overbrace{\begin{bmatrix} T_3 & T_2 & T_1 & T_{out,3} & T_{out,2} & Q_{r,3} & Q_{u,3} \\ T_4 & T_3 & T_2 & T_{out,2} & T_{out,1} & Q_{r,2} & Q_{u,2} \\ \vdots & \vdots & \vdots & \vdots & \vdots & \vdots & \vdots \\ T_{4464} & T_{4463} & T_{4462} & T_{out,4464} & T_{out,4463} & Q_{r,4464} & Q_{u,4464} \end{bmatrix}}^{input}, \overbrace{\begin{bmatrix} T_4 \\ T_5 \\ \vdots \\ T_{4465} \end{bmatrix}}^{output}. \tag{4.11}$$

## 4.5 Cascade MPC for Multi-zone Building

The thermal dynamics of a multi-zone building can be represented by an interconnected system of several zones. Fig. 4.6 shows the layout of the experimental areas used in

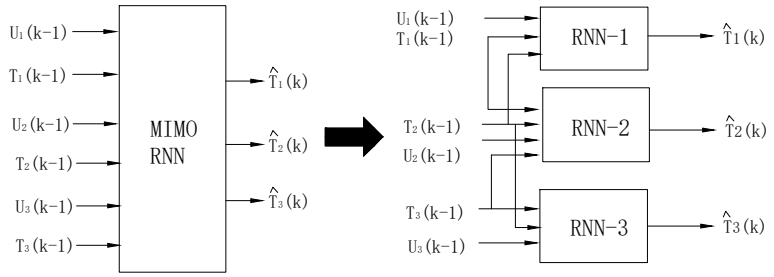


Figure 4.5: Structure of cascade RNN for multi-zone modelling.

this study. It has both perimeter zones which are directly connected to the ambient environment, and interior zones which are only connected to the perimeter zones. Obviously, outdoor temperature and solar radiation affect the external zones through convection, conduction and radiation but have negligible effects on the interior zones. Considering this fact, a multi-zone temperature prediction follows the following rules:

1. To predict the temperature of the perimeter zone, the weather inputs, such as outdoor temperature and solar radiation must be considered.

2. To predict the interior zone temperatures, weather inputs can be ignored but temperature of the perimeter zone should be considered.

3. When several zones are considered together, external zone temperatures must be predicted first and then used as a input to predict interior zone temperatures.

A MIMO model with the structure as shown in Fig. 4.5 is used to express the dynamic behaviour of a three-zone process, where $u_1$ to $u_3$ are the input variables, $T_1$ to $T_3$ are measured zone temperatures and $T_3$ is the predicted zone temperature. Following the rules set above, the MIMO model can be decoupled into three individual multiple-inputs, single-output (MISO) models. Each MISO model represents the thermal characteristic of a single zone, but still maintains connection with its neighbouring zones. The availability of this method on a real building will be tested in the following sections.

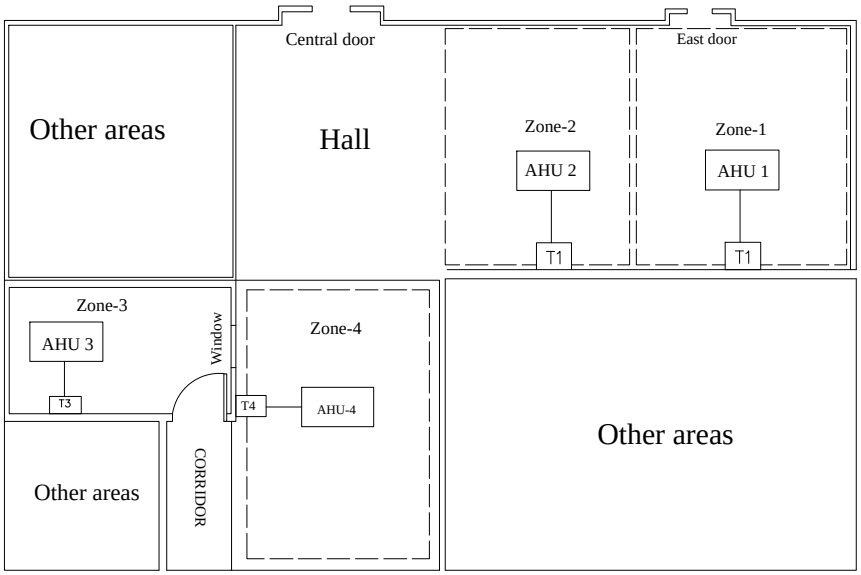


Figure 4.6: Layout of the experimental zones.

## 4.6 Data Gathering

The experimental data used in this study were collected from a commercial HVAC system at the Terminal One of Adelaide Airport through the BMS. To address the problem, thermal zones located at two different locations of the building were selected for experimental purposes: one is located at the perimeter zone (Zone-1) and the other located at the interior zone (Zone-3). Fig. 4.6 shows the general layout of the selected zones. Zone-1 is only adjacent to Zone-2 without any wall built between them. Zone-3 is an office room, located in the central part of the building (Zone-3). This room is adjacent to a spacious hall (Zone-4) but separated by a wall. The experiment data were collected on typical summer days in January 2011. The data set were divided into two groups. The first 20 days' data were used for model training, and remaining days' data were used for model validation.

Table 4.1 lists a series of variables based on the analytical models presented in the previous section. These include controllable variables related to the HVAC system, and

Table 4.1: Input variables definition.

| Variables | Description | Unit |
|---|---|---|
| **HVAC process** | | % |
| $V_c$ | Chilled water valve opening level | $l/s$ |
| $Q_u$ | Supplied cooling energy | $kJ$ |
| $f_{cw}$ | Chilled water flow rate | °C |
| $T_c$ | Chilled water temperature | °C |
| $D_{out}$ | Outdoor air damper opening level | % |
| **Zone process** | | |
| $T_{out}$ | Outdoor temperature | °C |
| $T_n$ | Neighbouring zone temperature | °C |
| $T_z$ | Objective zone temperature | °C |
| $T_r$ | Return air temperature | °C |
| $S_r$ | Global horizontal irradiation | $W/m^2$ |

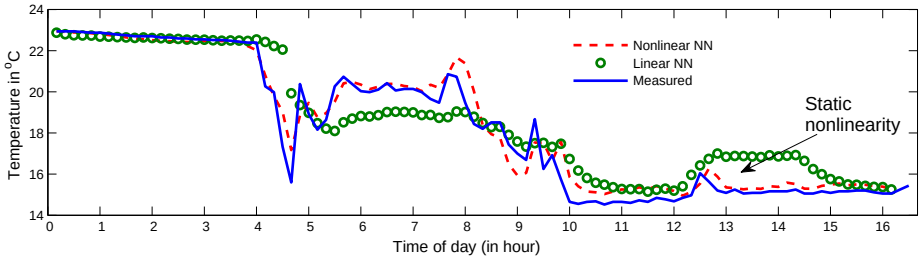


Figure 4.7: Comparison between linear and nonlinear NN models.

uncontrollable variables indicating the thermal conditions of the internal and external environment. The data are scaled between -1 and 1, before it is fed into the NN for training to avoid the dominant effects of certain variables. The algorithm used to scale the inputs into [-1,1] is:

$$x' = \frac{(y_{max} - y_{min})(x - x_{min})}{x_{max} - x_{min}} + y_{min}, \tag{4.12}$$

where $x'$ and $x$ denote the number before and after normalisation, $y_{max} = 1$ and $y_{min} = -1$ are the maximum and minimum values of specified range, $x_{max}$ and $x_{min}$ are the maximum and minimum values of the data set to be scaled, respectively. Every time the neural network function is used, the output values of the network should be reversed to obtain the real system output.

We build two groups of RNN models in this section. The models in the first group model the AHU process. At first, the prediction result of the linear NN is compared with the nonlinear NN to investigate the nonlinearity of the AHU plant. Afterwards, the significance of the chilled water temperature is also investigated. The second group of models are used for indoor temperature prediction in Zones 1 and 3, respectively. In particular, we investigate the influence of the neighbouring zone temperature on the prediction accuracy of the investigated zone.

Table 4.2: Simulation results when different models are used.

| | RMSE (in °C) | NMSE (in °C) |
|---|---|---|
| AHU model-1 | 1.53 | 73% |
| AHU model-2 | 1.21 | 80% |
| AHU model-3 (Linear NN) | 1.55 | 47% |
| Zone-1 model-1 | 0.54 | 75% |
| Zone-1 model-2 | 0.45 | 86% |
| Zone-3 model-1 | 0.27 | 62% |
| Zone-3 model-2 | 0.17 | 89% |

Table 4.3: Different model structures

| *Model type* | *Model structure* |
|---|---|
| AHU-1 model-1 | $f(T_r(k), D_{out}(k), V_c(k)), T_{out}(k-1), T_{out}(k), T_{cw}(k), T_{cw}(k-1))$ |
| AHU-1 model-2 | $f(T_r(k), D_{out}(k), V_c(k)), T_{out}(k-1), T_{out}(k))$ |
| AHU-1 model-3 (linear) | $f(T_r(k), D_{out}(k), V_c(k)), T_{out}(k-1), T_{out}(k), T_{cw}(k), T_{cw}(k-1))$ |
| Zone-1 model-1 | $f(T_1(k-2), T_1(k-1), T_1(k), T_{out}(k-1), T_{out}(k), Q_u(k), S_r(k))$ |
| Zone-1 model-2 | $f(T_1(k-2), T_1(k-1), T_1(k), T_{out}(k-1), T_{out}(k), Q_u(k), S_r(k), T_2(k))$ |
| Zone-3 model-1 | $f(T_3(k-2), T_3(k-1), T_3(k), T_{out}(k-1), T_{out}(k), Q_u(k), S_r(k))$ |
| Zone-3 model-2 | $f(T_3(k-2), T_3(k-1), T_3(k), T_{out}(k-1), T_{out}(k), Q_u(k)), S_r(k), T_4(k))$ |

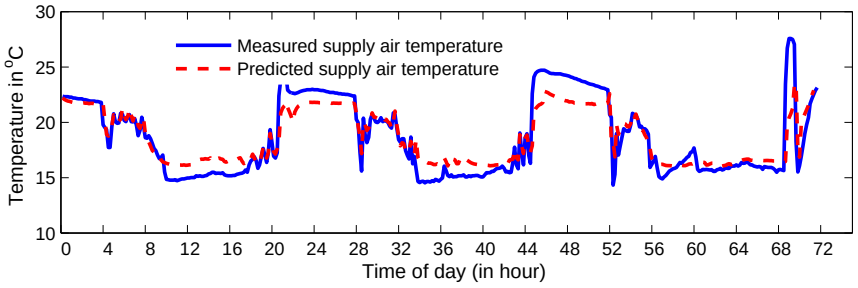


Figure 4.8: AHU model without considering chilled water temperature.

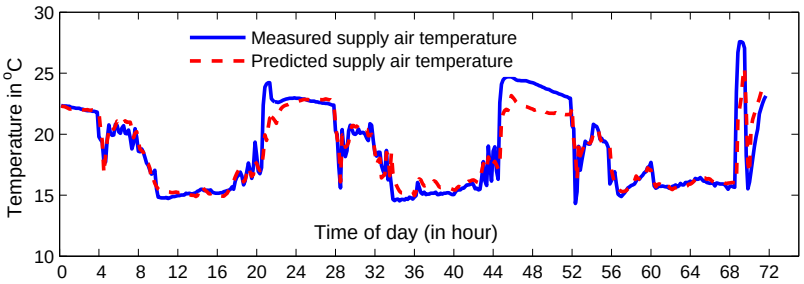


Figure 4.9: AHU model considering chilled water temperature.

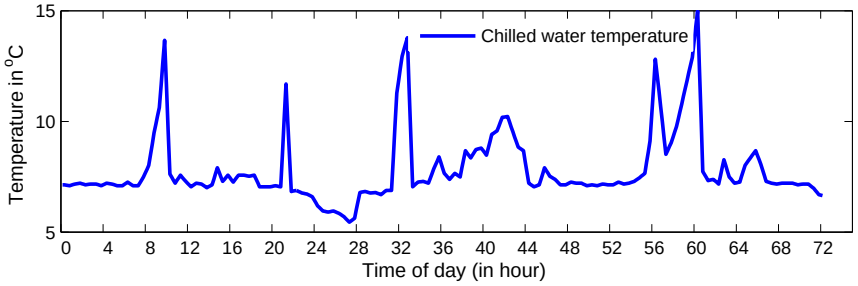


Figure 4.10: Chilled water temperature

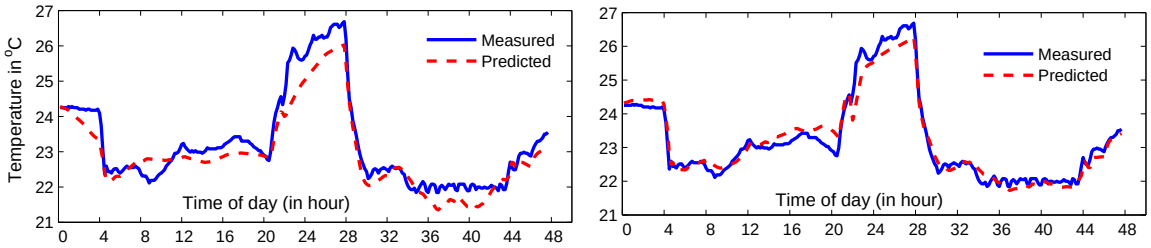


Figure 4.11: Prediction results for Zone-1; Left: Neighbouring zone temperature was not used; Right: Neighbouring zone temperature was used.

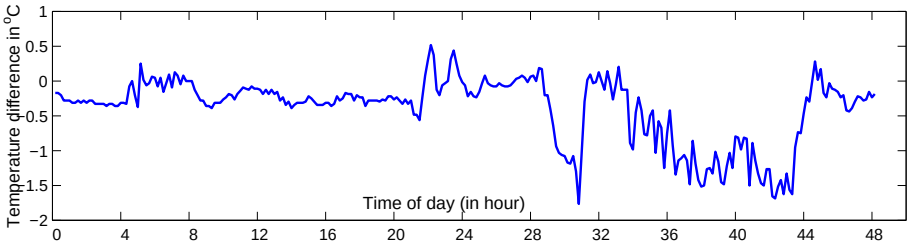


Figure 4.12: Temperature difference between Zone-1 and Zone-2.

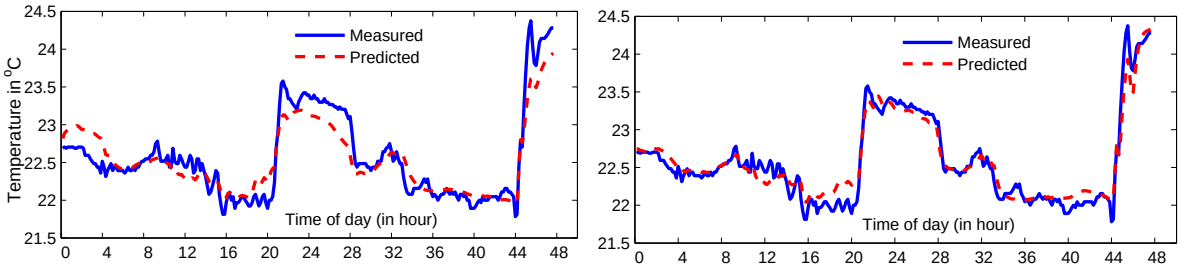


Figure 4.13: Prediction results for Zone-3; Left: Neighbouring zone temperature was not used; Right: Neighbouring zone temperature was used.

## 4.7 Validation Results and Discussion

After the training process, the obtained models should be validated. An important concern when training the NN model is to avoid the phenomenon of over-fitting. Over-fitting means the model performs well during the training process, but generates large errors during the testing process. To avoid this phenomenon, the trained models were always validated using another set measured data, which were different from the training data. During the validation, the measured output data were only used at the first step. Starting from the second step, the predicted outputs are used as the input variables for the prediction. This is called multiple-steps-ahead prediction. In general, the performance of the predictive model degrades as the step size increases. In this study, one-day-ahead prediction was selected. The best neural network structure (in terms of input orders, hidden layer number) was chosen based on relative mean squared error (RMSE) and normalised

mean squared error (NMSE). The obtained final model structures are listed in Table 4.3. The following observations have been made:

- The overall simulation result is reported in Table 4.2. It clearly shows that a substantial reduction in prediction error was achieved when the chilled water temperature was considered by the AHU model. It also demonstrates that the nonlinear model outperforms the linear one. The prediction accuracies in Zone 1 and 3 were also improved after their neighbouring zone temperatures were considered as inputs.

- A comparison between the plots of the predictive supply air temperature trajectory is illustrated in Fig. 4.7. It can be seen that the nonlinear NN model outperforms the linear ARX model considerably. The nonlinear NN model has a NMSE of 80%, which is much higher than the linear ARX model (47%) . This result proves that there are some nonlinearities in the AHU process that are captured by the nonlinear NN model.

- According to Fig. 4.8, when the first AHU model was considered, an obvious temperature error was generated. This error was successfully eliminated (as shown in Fig. 4.9) when the second AHU model, in which chilled water temperature was used as a variable, was used. This indicates that the operating status of the local AHUs are closely related to the operating status of the chiller plant. This is especially true for the system installed with multiple chillers, whose staging up and down causes fluctuation to the chilled water temperature. From Fig. 4.10, it can be seen that the chiller staging up caused the chilled water temperature to raise from 7 °C to 14 °C and then back to 7 °C at 9:00 am. This effects of this change on the supply air temperatures at the local AHUs can be modelled by the RNN with very a good prediction accuracy.

- Fig. 4.11 and 4.13 compare the prediction results when the neighbouring zone temperature was considered as an input or not. Interestingly, it shows that when the

neighbouring zone temperature was employed as an input for the NN model, the prediction accuracies for both Zone-1 and 2 were improved. This indicates that both conductive and convective heat transfer influence the dynamics of the investigated zone, and the heat transfer phenomenon can be well presented by the proposed cascade NN model. Fig. 4.11 also shows that there was a persistent prediction error happened on the second day. During the same period of time, there was a big temperature difference between Zone-1 and 2, as shown in Fig. 4.12. This clearly indicates the relationship between the prediction error and temperature difference between the adjacent zones.

## 4.8 Conclusions

In this paper, a series of RNN models have been built to model the thermal dynamics of the AHU plant and thermal zone process, and validated using BMS data. It is found that the RNN is capable of modelling the nonlinear AHU process with a good prediction accuracy. Moreover, we used a cascade NN model to identify the thermal connection between adjacent zones. It was found that the temperature of the investigated zone can be predicted more accurately, when the neighbouring zone temperature is employed as an input. This proposed method enables the temperature prediction for both perimeter and interior zones. The proposed model can be utilised for achieving energy savings in buildings. For instance, the operating hours and set point temperature for individual AHUs can be re-scheduled based on the prediction result, while taking the constraints such as occupant hours and time-based electricity price into account. Since there are always a large number of AHUs inside large buildings, a significant amount of energy saving is possible when the same strategy is applied on each of them. In further studies, the RNN model will be used to design predictive control strategies.

# References

[1] S. Wang and Z. Ma, "Supervisory and optimal control of building HVAC systems: A review," *HVAC&R Research*, vol. 14, no. 1, pp. 3–32, 2008.

[2] D. D. Massie, "Optimization of a building's cooling plant for operating cost and energy use," *International Journal of Thermal Sciences*, vol. 41, no. 12, pp. 1121 – 1129, 2002.

[3] T. Chow, G. Zhang, Z. Lin, and C. Song, "Global optimization of absorption chiller system by genetic algorithm and neural network," *Energy and Buildings*, vol. 34, no. 1, pp. 103 – 109, 2002.

[4] F. Oldewurtel, A. Parisio, C. N. Jones, D. Gyalistras, M. Gwerder, V. Stauch, B. Lehmann, and M. Morari, "Use of model predictive control and weather forecasts for energy efficient building climate control," *Energy and Buildings*, vol. 45, no. 0, pp. 15 – 27, 2012.

[5] Y. Ma, F. Borrelli, B. Hencey, B. Coffey, S. Bengea, and P. Haves, "Model predictive control for the operation of building cooling systems," *Control Systems Technology, IEEE Transactions on*, vol. 20, pp. 796 –803, may 2012.

[6] X. Xu, S. Wang, and G. Huang, "Robust MPC for temperature control of air-conditioning systems concerning on constraints and multitype uncertainties," *Building Services Engineering Research and Technology*, vol. 31, no. 1, pp. 39–55, 2010.

[7] T. Lu and M. Viljanen, "Prediction of indoor temperature and relative humidity using neural network models: model comparison," *Neural Computing and Applications*, vol. 18, pp. 345–357, 2009.

[8] A. Ruano, E. Crispim, E. ConceiA, and M. LAcio, "Prediction of building's temper-

ature using neural networks models," *Energy and Buildings*, vol. 38, no. 6, pp. 682 – 694, 2006.

[9] S. Patil, H. Tantau, and V. Salokhe, "Modelling of tropical temperature by auto regressive and neural network models," *Biosystems Engineering*, vol. 99, no. 3, pp. 423 – 431, 2008.

[10] G. Mustafaraj, G. Lowry, and J. Chen, "Prediction of room temperature and relative humidity by autoregressive linear and nonlinear neural network models for an open office," *Energy and Buildings*, vol. 43, no. 6, pp. 1452 – 1460, 2011.

[11] A. Mechaqrane and M. Zouak, "A comparison of linear and neural network arx models applied to a prediction of the indoor temperature of a building," *Neural Comput. Appl.*, vol. 13, pp. 32–37, Apr. 2004.

[12] I.-H. Yang, M.-S. Yeo, and K.-W. Kim, "Application of artificial neural network to predict the optimal start time for heating system in building," *Energy Conversion and Management*, vol. 44, no. 17, pp. 2791 – 2809, 2003.

[13] J. W. Moon and J.-J. Kim, "Ann-based thermal control models for residential buildings," *Building and Environment*, vol. 45, no. 7, pp. 1612 – 1625, 2010.

[14] G. Platt, J. Li, R. Li, G. Poulton, G. James, and J. Wall, "Adaptive HVAC zone modeling for sustainable buildings," *Energy and Buildings*, vol. 42, no. 4, pp. 412 – 421, 2010.

[15] B. Tashtoush, M. Molhim, and M. Al-Rousan, "Dynamic model of an hvac system for control analysis," *Energy*, vol. 30, no. 10, pp. 1729 – 1745, 2005.

[16] C.-C. Ku and K. Lee, "Diagonal recurrent neural networks for dynamic systems control," *Neural Networks, IEEE Transactions on*, vol. 6, pp. 144–156, Jan 1995.

[17] G. D. Robert May and H. Maier, "Review of input variable selection methods for artificial neural networks artificial neural networks," in *Artificial Neural Networks - Methodological Advances and Biomedical Applications* (K. Suzuki, ed.), 2011.

[18] K. Hornik, M. Stinchcombe, and H. White, "Multilayer feedforward networks are universal approximators," *Neural Networks*, vol. 2, no. 5, pp. 359 – 366, 1989.

[19] M. Mohammadzaheri, L. Chen, and S. Grainger, "A critical review of the most popular types of neuro control," *Asian Journal of Control*, vol. 14, no. 1, pp. 1–11, 2012.

[20] A. Mirsephai, M. Mohammadzaheri, L. Chen, and B. O'Neill, "An artificial intelligence approach to inverse heat transfer modeling of an irradiative dryer," *International Communications in Heat and Mass Transfer*, vol. 39, no. 1, pp. 40 – 45, 2012.

# Chapter 5

# Multi-zone Modelling and Control

This chapter is based on the following paper:

*Full citation*: Huang H., Chen L., Hu E., "A neural network-based multi-zone modelling approach for predictive control system design in commercial buildings", In Energy and Buildings, vol. 97, pp. 86 - 97, 2015.

*Contribution of this chapter*: Continuing with the previous chapter, this paper proposes a MIMO model for indoor temperature prediction in multi-zone buildings. An optimal start-stop controller is also built based on the model, which demonstrates great energy saving potential.

# Statement of Authorship

| | |
|---|---|
| Title of Paper | A neural network-based multi-zone modelling approach for predictive control system design in commercial buildings, Energy and Buildings |
| Publication Status | ☑ Published ☐ Accepted for Publication<br>☐ Submitted for Publication ☐ Unpublished and Unsubmitted work written in manuscript style |
| Publication Details | Huang H., Chen L., and Hu E., (2015), A neural network-based multi-zone modelling approach for predictive control system design in commercial buildings, Energy and Buildings, Vol. 97, 2015, Pages 86-97. doi: 10.1016/j.enbuild.2015.03.045 |

## Principal Author

| | |
|---|---|
| Name of Principal Author (Candidate) | Hao Huang |
| Contribution to the Paper | Developed theory, process data, conduct experiment, wrote manuscript and acted as the corresponding author. |
| Overall percentage (%) | 60% |
| Certification: | This paper reports on original research I conducted during the period of my Higher Degree by Research candidature and is not subject to any obligations or contractual agreements with a third party that would constrain its inclusion in this thesis. I am the primary author of this paper. |
| Signature | Date 15/10/15 |

## Co-Author Contributions

By signing the Statement of Authorship, each author certifies that:

i. the candidate's stated contribution to the publication is accurate (as detailed above);
ii. permission is granted for the candidate in include the publication in the thesis; and
iii. the sum of all co-author contributions is equal to 100% less the candidate's stated contribution.

| | |
|---|---|
| Name of Co-Author | Lei Chen |
| Contribution to the Paper | Supervised research, helped with data collection and experiment setup, and reviewed manuscript |
| Signature | Date 15/10/15 |

| | |
|---|---|
| Name of Co-Author | Eric Hu |
| Contribution to the Paper | Supervised research, helped to edit manuscript. |
| Signature | Date 15/10/15 |

**Abstract**

Predictive control techniques for heating, ventilation and air conditioning (HVAC) systems have been paid an increasing attention in recent years. Such methods rely on building models to accurately predict indoor temperature and make optimal control decisions. Obtaining building models is challenging, as buildings thermal dynamics are nonlinear, have long time delays, and contain uncertainties. Previous studies on building modelling work mostly focused on small-scale buildings and single-zone cases. They do not accommodate some important features of real-world commercial buildings, such as the effects of thermal coupling between adjacent zones. This paper presents an artificial neural network (ANN) model-based system identification method to model multi-zone buildings. The proposed model considers the energy input from mechanical cooling, ventilation, weather change, and in particular, the convective heat transfer between the adjacent zones. The testing of the temperature history shows that the proposed ANN model captures the thermal interactions between the zones reasonably well, therefore achieves more accurate prediction results than a single-zone model. Based on the model, a simple and effective model-based predictive control method is developed, with the results showing that comfortable temperature can be maintained with reduced energy consumption.

## 5.1 Introduction

Buildings are responsible for 40 per cent of the energy consumption and 33 per cent of carbon dioxide emissions in the world. Within building sectors, almost half of the energy use is related to heating, ventilation and air conditioning (HVAC) systems [1]. Reducing the building energy costs has become an urgent task, due to the increasing environmental concerns and energy prices. Despite of this fact, HVAC systems at the existing buildings are not operating in the most efficient ways. Therefore, this study aims to develop a building modelling approach, which is suitable for the design of predictive

control strategies in commercial buildings. The control strategy can be used to reduce the energy consumption and improve thermal comfort in the buildings.

Most current, proportional-integral-derivative (PID) control and on/off control are being widely used for commercial HVAC systems. They use current measured temperatures as the inputs to control local actuators, such as chilled water valves and mechanical dampers. However, since building dynamics have strong thermal inertial, the indoor temperature may delay in response to the control actions. This causes a waste of energy use and poor thermal comfort. In recent years, researchers have shown predictive control strategies can significantly reduce the energy costs associated with HVAC systems, through both simulation [2–6] and experimental studies [7–10]. Predictive control allows one to take advantage of weather forecast and occupancy prediction to reduce energy costs and improve thermal comfort. In general, predictive control can be regarded as an integration of different supervisory control methods, such as optimal start-stop control [6], load shifting control [11] and demand-limiting control [12]. The most crucial step of implementing such a control strategy is to create a thermal dynamic model, able to accurately predict changes in the building temperature. For control purpose, the model should have simple structure and be suitable for a wide operational range. However, building modelling is challenging, for several reasons. The complexities of building dynamics modelling are listed as below:

1. A building's operational environment is a time-varying system with many uncertain variables. For example, a sudden change in the number of occupants or accumulated change in solar gain will cause fluctuation of indoor temperature.

2. Air-conditioned buildings possess several nonlinear variables, such as temperature, relative humidity and outdoor air damper actions, which are difficult to model using the standard methods (such as the simplified physical model).

3. HVAC systems have several coupled control processes that cannot be treated in-

dependently. For example, air handling unit (AHU) processes are affected by the chilled water temperature changes and flow-rate fluctuations.

4. The internal space of buildings is divided into adjacent zones, each controlled by an individual AHU. The temperatures of the individual zones are not uniform, and are coupled, which makes building modelling a multiple-input, multiple-output (MIMO) problem.

A variety of approaches has been proposed for modelling the thermal dynamics of the buildings. Probably the most commonly used one is resistance-capacitance (RC) networks, which is based on the first principle of thermal dynamics. The use of RC models for model predictive control (MPC) has been applied to several building energy studies [11, 13–16]. RC networks use lumped capacitance and resistance in an analogy electric circuit to represent the thermal elements of a building. When heat transfer among zones is considered, RC networks can be used to model multi-zone buildings by linking a series of linear differential equations [17, 18]. For example, Goyal et al. [19] model inter-zone convection of a building with RC networks. They conclude that the temperature predicted by the RC model that includes convection effects are closer to the measured temperature than those by the model that considers conductive heat transfer only. However, applying such an approach to model convective heat transfer among the zones can cause model mismatch, mainly because the uncertain coupling effects between zones can hardly be identified by the simplified models.

Statistical models derived from system identification methods have also been investigated. This includes autoregressive with the exogenous (ARX) model [20], autoregressive moving average model with exogenous inputs (ARMAX) model [21] and subspace model [7]. For example, Morosan et al. [22] presented a distributed model predictive control strategy for a multi-zone building with intermittently operating mode. They found that the distributed MPC which considers the thermal interaction among zones outperforms the MPC which does not consider thermal interaction. However, because the statistical

models are linear, time-invariant, they can easily lose accuracies when strong nonlinearity and uncertainties are presented at the systems. Therefore, growing attention has also been paid to artificial neural network (ANN) models, for building modelling and control [23–26]. ANN models are suitable for building dynamics modelling due to their abilities to deal with nonlinear, multivariable modelling problems. Different from the physical models, the parameters of ANN are the number of neurons and the values of interconnection weights and biases. If a dynamic ANN model is employed, the orders and delay terms should also be considered during the model development.

Several studies have proven ANN models superior to linear models [24, 27] and physical models [25, 28] in modelling the nonlinearity of HVAC systems. Using a feed-forward neural network, Lu and Viljanen [27] constructed a nonlinear autoregressive with external input (NARX) model to predict both indoor temperature and relative humidity. Ruano et al. [25] incorporated a radial basis function neural networks to build an adaptive model to predict indoor temperature of a school building. Ferreira et al. [26] tested an ANN based model predictive control at a campus building, and applied a discrete branch and bound approach to optimise the energy usage. Spindler and Norford [28] built a multi-zone, multi-node ANN model to predict indoor temperature inside a multi-zone residential building. The accuracy of the predictive model is smaller than the one obtained in other similar studies. In Ref. [29], a predictive control method was developed to determine the optimal cooling mode, which results in a reduced fan energy usage while maintaining a comfortable temperature. Garnier et al. [6] built an ANN model-based predictive control strategy to satisfy the thermal comfort index of a non-residential building. The result shows that the predictive controller which considers the heat transfer between the adjacent rooms offers improvement in both energy efficiency and thermal comfort.

In summary, previous studies focusing on neural network modelling have largely considered multi-input, single-output (MISO) structures for single zones. The effects of thermal interactions (for example, convective or conductive heat transfer) have rarely been

addressed. Multi-zone modelling using ANN can be found in [6, 28]. However, the effects of thermal interaction between zones on the modelling accuracies have not been discussed in detail by these studies. It is believed that with enough building data, ANN models are able to model effectively the thermal interaction between the zones, towards the achievement of a MIMO model with better prediction accuracy and generalisation capabilities. Motivated by this, this study proposes a new ANN model-based modelling approach for multi-zone buildings. The model considers factors such as mechanical cooling, ventilation, weather conditions and heat transfer between the adjacent zones. Further, we investigate the significance of convective heat transfer among zones, through comparing predictive accuracies of single-zone models to a multi-zone model. To verify our method, an airport terminal building equipped with a modern HVAC system is employed as the research vehicle. The accuracies of the models are validated and compared using field data measured from the building. Based on the proposed models, a predictive control framework with a simple structure is also proposed, with the objective being to reduce energy consumption while maintaining comfortable temperature at the investigated building. The merits of the multi-zone model based control method as compared to the single-zone model based control method will also be discussed.

This paper is structured as follows: Section 2 describes the building and the HVAC system used in this study. Section 3 addresses the physical analysis of the building dynamics, and the detailed procedures of obtaining an optimal ANN model. The principle of the optimal start-stop control method is introduced in Section 4. Section 5 illustrates the simulation results and compares model performance through error analysis. The use of ANN-based optimal start-stop control at the investigated system is discussed in Section 6. The paper concludes with a description of future work.

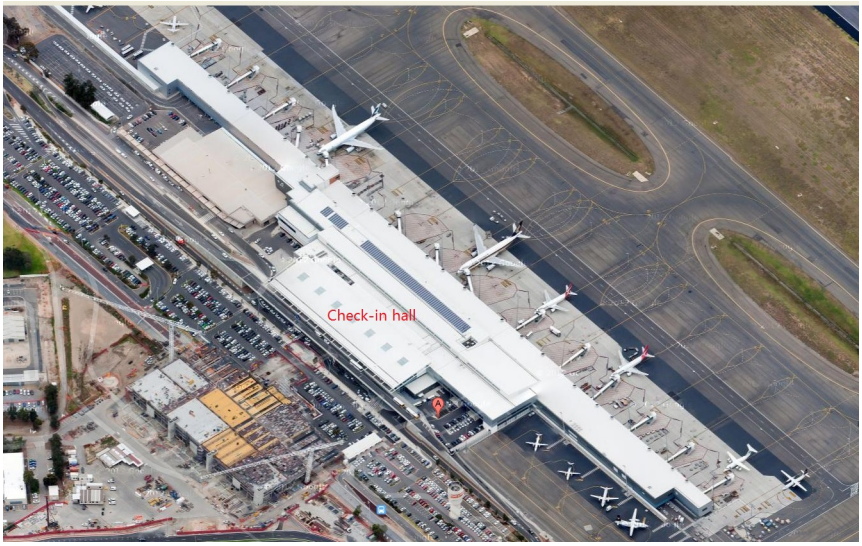


Figure 5.1: The top view of T-1 building, Adelaide Airport.

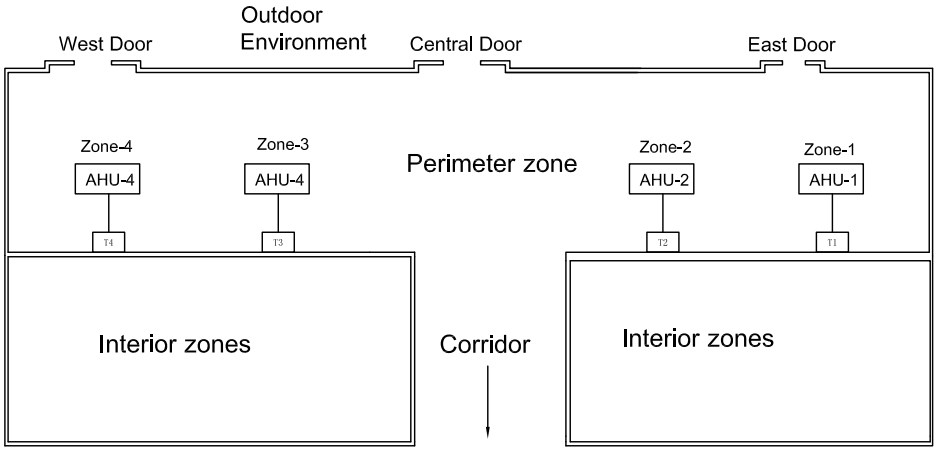


Figure 5.2: Check-in hall located at level-2 of Adelaide airport.

## 5.2 Building Description

The test building, as shown in Fig. 5.1, is the Terminal 1 building of Adelaide Airport, South Australia. The check-in hall consisting of four thermal zones was selected as the experimental area. Each zone is served by an individual AHU, as illustrated in Fig. 5.2. The selected zones are located at the perimeter areas of level-2 of the building, isolated from the outdoor environment by a large glass facade to the north. Two motorised blinds are installed at the north window, which is used to reduce the effects of solar radiation. During the occupied hours, passengers enter the check-in hall through automatic doors. The investigated zones are lightweight in structure, because it has a significant thermal coupling with the outdoor environment and the adjacent space. The uncertainties such as solar radiation, internal gain, leakage and thermal interaction make the modelling work very difficult.

The building is controlled by a Johnson Controls Australia Pty Ltd BMS. At the high level, three chillers provide chilled water to the entire water circle. The chilled water is transmitted from the chiller plants to local AHUs through variable-speed water pumps. At the lower level, AHUs transfer the cooling energy from the chilled water circuit into air-flows, and then supply to the local thermal zones. Fig. 4.2 shows the schematic diagram of the AHU used in this study. During the operation period, the return air is recirculated through the outdoor air damper and then mixed with the return air. The mixed air then passes through the cooling coil and the air temperature decreased after the heat exchange. The chilled water valve is controlled proportionally to the difference between measured zone temperature and set point temperature, in order to maintain the zone temperature at the desired value. The AHUs are installed with an economizer. When the outdoor air temperature is lower than the return air temperature but higher than a minimum value, the mixed air damper will control the return air volume mixed with the outdoor air. Each AHU is mounted with three sensors: a supply air temperature sensor, a return air temperature sensor, and a zone temperature sensor. There are also two sensors installed at the

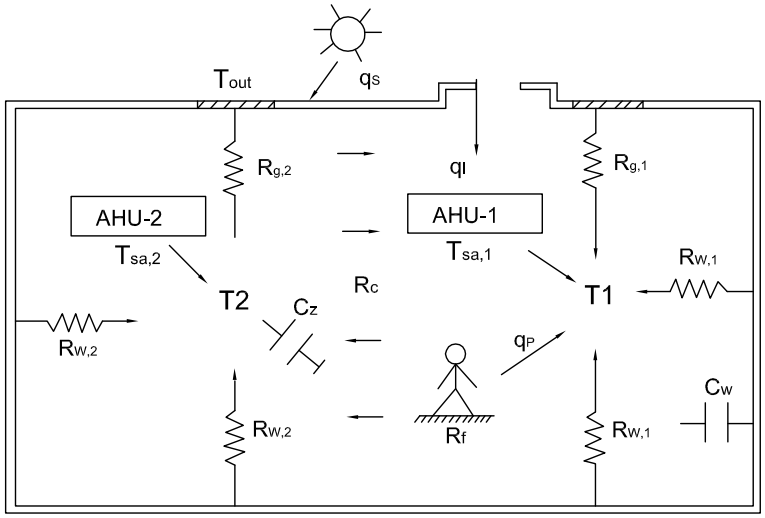


Figure 5.3: Model for calculating zone temperatures.

building's roof to provide information on outdoor air temperature and relative humidity. All information is connected to the BMS, allowing a master PC workstation to monitor and control different zones throughout the building. In this study, we mainly focus on the investigation of the cooling plant. However the proposed method can also be applied to the heating system, which uses boilers as the central plant.

## 5.3 Modelling

### 5.3.1 Analytical Model

This section introduces simplified physical models to illustrate the thermal hehaviour of a multi-zone building. The models are modified based on the zone model introduced in Ref. [30]. Fig. 5.3 shows the energy balance network diagram of a double-zone case. The selected zones are identical to each other and have no wall built in between. Therefore, the convective heat transfer between the two zones becomes an important factor to concern. At first, the following assumptions are made:

1. The air in the zone is fully mixed, so that the temperature distribution in each zone is uniform;

2. The density and flow rate of the air in the zones are constant and not influenced by the temperature change.

3. The walls and ceiling have the same thermal influence on the zone temperature. The effect of ground on the zone temperature is not considered.

Under the assumptions made above, the energy and mass balance-governing equations of the zones can be derived as below:

$$C_z^1 \frac{dT_1}{dt} = \dot{m}C_a(T_{sa,1} - T_1) + \frac{(T_2 - T_1)}{R_f} + \frac{T_{out} - T_1}{R_{g,1}} + \frac{T_{w,1} - T_1}{R_{w,1}} + Q_1, \tag{5.1}$$

$$C_z^2 \frac{dT_2}{dt} = \dot{m}C_a(T_{sa,2} - T_2) + \frac{(T_1 - T_2)}{R_f} + \frac{T_{out} - T_2}{R_{g,2}} + \frac{T_{w,2} - T_2}{R_{w,2}} + Q_2, \tag{5.2}$$

$$C_w^1 \frac{dT_{w,1}}{dt} = \frac{T_1 - T_{w,1}}{R_{w,1}} + \frac{T_{out} - T_{w,1}}{R_{w,1}}, \tag{5.3}$$

$$C_w^2 \frac{dT_{w,2}}{dt} = \frac{T_2 - T_{w,2}}{R_{w,2}} + \frac{T_{out} - T_{w,2}}{R_{w,2}}, \tag{5.4}$$

where $C_z^{i,(i=1,2)}$ denotes thermal capacitance associated with the fast-dynamic masses such as the air around the temperature sensors, $C_w^{i,(i=1,2)}$ represents the thermal capacitance associated with the slow-dynamic masses, such as the internal walls and ceiling, $\dot{m}$ is the mass flow rate of the supply air, $C_a$ is the specific heat of the air, $T_{i,(i=1,2)}$ represents the air temperatures of zones 1 and 2, $T_{out}$ is the outdoor air temperature, $T_{w,i,(i=1,2)}$ denotes the mean wall temperatures in zones 1 and 2, $T_{sa,i,(i=1,2,)}$ is the temperatures of the supply air to zones 1 and 2, $R_{g,i,(i=1,2)}$ represents the thermal resistance related with the elements with little thermal capacitance, such as windows, $R_c$ represents the heat transfer coefficient between the zones, $Q_{i,(i=1,2)}$ represents the heat gains caused by solar radiation ($Q_s$), leakage ($Q_l$) and occupants ($Q_p$).

Eqs. (5.1) to (5.4) illustrate that the coupling strength between the adjacent zones depends on two factors: 1. The temperature difference between two zones, and 2. The heat transfer coefficient ($R_f$). Although the temperature difference can be measured by the temperature sensors mounted in the individual zones, the convective heat transfer coefficient, which is related with the air flow rate between the zones, is hard to estimate. Additionally, the unmeasured disturbances variables $Q_1$ and $Q_2$ also contain uncertainties, which can hardly be directly modelled by traditional mathematical equations.

### 5.3.2 NARX Model for MIMO Modelling

As the building thermal system is nonlinear in nature, and is involved with several stochastic uncertainties, the simplified physical models described above can hardly represent a real building system. Therefore, we employ a nonlinear autoregressive models with exogenous input (NARX) as the model structure [31, 32]. The NARX is a recurrent dynamic network, with feedback connections enclosing several layers of the network. An important feature of the NARX model is that its output depends not only on the current inputs to the network, but also on the current and previous outputs of the network. According to the NARX structure, a MIMO dynamic system in discrete form can be expressed by the following equations:

$$\hat{y}(k+1) = f[\phi(k), w] + e(k), \tag{5.5}$$

$$\phi(t) = [y(k)...y(k-n_y), u(k-n_k), ..., u(k-n_u-n_k)], \tag{5.6}$$

where $u = [u_1, u_2, ..., u_n]^T$ and $y = [y_1, y_2, ..., y_n]^T$ are the system input and output vectors, respectively, k denotes the time step, $\hat{y}(k+1)$ denotes the output predicted by the model, $n_k$ is the delay time of the inputs, $\phi(k)$ is the regression vector, and $n_u$ and $n_y$ are the orders for the input and output variables, respectively. $f$ is the nonlinear neural network function, and $e$ represents the prediction errors. Eq. (5.6) illustrates that the output values of $y_1$ at

time steps $k$, $(k-1)$,...,$(k-n_y)$ are the inputs to $\hat{y_1}(k+1)$. Further, the output $\hat{y}_1(k+1)$ is also affected by the output from its neighbouring system: $[y_2(k), y_2(k-1), ...y_2(k-n_y)]^T$.

For model training, it is necessary to prepare the input-output data in a proper way so that they can be fitted into the NARX structure. The double-zone case (as shown in Fig. 5.3) is used to demonstrate the method of data preparation. The inputs of the NARX model are the outdoor temperature ($T_{out}$) and supply air temperatures of the two zones $T_{sa,1}$ and $T_{sa,2}$. The outputs of the model are the zone temperatures: $T_1$ and $T_2$. The delay time of input is chosen to be $k = 0$, because the time lag from input to output is shorter than the sampling time of the system (10 min). Therefore, the input-output matrix written in Eq. (5.8) can be altered as:

$$U = \begin{pmatrix} T_i(r) & \cdots & T_i(r-n_a+1) & T_{out}(r) & \cdots & T_{out}(r-n_b+1) & T_{sa,i}(r) \\ T_i(r+1) & \cdots & T_i(r-n_a+2) & T_{out}(r+1) & \cdots & T_{out}(r-n_b+2) & T_{sa,i}(r+1) \\ \vdots & \ddots & \vdots & \vdots & \ddots & \vdots & \\ T_i(n) & \cdots & T_i(n-n_a+1) & T_{out}(n) & \cdots & T_{out}(n-n_b+1) & T_{sa,i}(n) \end{pmatrix}, \tag{5.7}$$

$$Y = \begin{pmatrix} \hat{T}_i(r+1) \\ \hat{T}_i(r+2) \\ \vdots \\ \hat{T}_i(r+n) \end{pmatrix}, \tag{5.8}$$

where $T_{i,(i=1,2)}$ is the temperature in zones 1 and 2; $T_{sa,i,(i=1,2)}$ is the supply air temperature in zones 1 and 2; $n_a$ and $n_b$ denote the orders of output and input, respectively; $r$ denotes order of the system, which equals to the maximum order of the inputs.

## 5.4 Model Selection

To retain the accuracy and efficiency of the model, this paper employs a forward selection method to perform model selection [33]. Forward selection selects individual candidate variables one at a time. It increases the input variables linearly, until the optimality criteria is reached. This method searches for the optimal set of input variables, as well as their corresponding orders for the ANN. The detailed procedures of performing forward selection are as described as follows:

1. Select the most relevant input variables according to the physical characteristics of the system. Use an initial order of one, for each input.

2. Use the input-output data set to train the ANN model. Compute the Root Mean Square Error (RMSE) between measured and modelled output on a separate set of validation data, to evaluate the performance of the model.

3. Increase the order of each input, adjust the hidden layer number and repeat Step 2 until the minimum RMSE is reached. The training parameters (such as momentum, learning rate and training algorithm) are kept the same during the process.

4. Compare the performance of the updated model with the previous one. If increasing the ordinal number of the existing inputs improves the model's performance, consider a higher order. Otherwise, incorporate a new input into the model and then repeat Steps 2 and 3.

The above loop is repeated, which makes the dimension of the matrices Eqs. (5.7) and (5.8) varying with different inputs combinations, and selection of orders. The entire searching procedure terminates when the increment of input variables fails to reduce the RMSE. As the forward selection method starts with the simplest models, and trials increasingly larger input variable sets until the optimal set is reached, it will eventually generate the ANN models with a small input variable set.

### 5.4.1 ANN Model Training

The description about the ANN has already been given is Section (4.3.1). This section focuses on the training method.

BMS provides a wide variety of data for building modelling. In the proposed model, we use the same set of variables listed in Table 4.1 for training purpose. To achieve satisfactory performance, the data used for the training neural network should cover a wide operational range, and the coverage of data within this range should be uniform. During the training phase, the data gathered from the days with the maximum and minimum historical records were added to the training data set, to increase the ability for generalisation. However, because the data used for training in this study were selected from the summer season, the performance of the model will deteriorate when the weather conditions change. The sliding window method can be applied to make the ANN model adaptive to the change of weather [25]. With this method, the data used for training are stored in a sliding window, and updated at each time interval. The recently measured data will replace the oldest pair stored in the window. The ANN can be retrained using the newest data so that the model can be updated periodically. Data from January, 2013 (4464 points) were selected as the training data. Among the selected training data, 70 per cent are used for training the network, 15 per cent for the validation set and 15 per cent for the test set. The data are scaled between -1 and 1, before it is fed into the neural network for training to avoid the dominant effects of certain variables. Eq. (4.12) is used to scale the all the variables into [-1,1].

Every time the neural network function is used, the output values of the network should be reversed to obtain the real system output.We employed Bayesian regularisation as the training method, to obtain the ANN parameters. This algorithm has a slower convergence speed, compared with the LM algorithm, but can improve the generalisation of ANN models and prevent overfitting [34]. The ANN was trained in 500 epochs (iterations) and the training process was terminated when the target mean square error (MSE)

was reached.

### 5.4.2 Multi-step-ahead Prediction

To test the prediction accuracy of the obtained ANN model, another set of data, completely different from the training data were employed for validation purpose. The validation data were selected from 1th Feb, 2013 to 6th Feb,2013 (864 points). Due to slow dynamics of the building process, short-term prediction can always achieve very accurate result. However, for predictive control design purposes, long-term prediction is often needed. For example, an optimal start-stop control strategy requires a prediction horizon that is longer than the response time of the cooling (heating) systems [20]. A load shifting strategy which considers time-of-use electricity price may require a prediction horizon of hours to a day [2]. Therefore, the quality of the model can be better evaluated by multi-step-ahead prediction accuracy, rather than one-step-ahead accuracy. In multi-step-ahead prediction, measured outputs are only used for the first step. Starting from the second step, the predicted outputs are used instead of the measured ones to perform the next prediction. The controllable inputs are the ones which need to be optimised, so they still use the measured values during the validation. The trajectory of the future weather inputs, e.g. dry bulb temperature and relative humidity, are obtained from Bureau of Meteorology of Australia. Therefore, the model can be used to perform a real-time prediction, once the weather forecast becomes available. For example, if we consider a system with two inputs: $T_{out}, V_c$ with the input orders of 2 and 1 respectively, and one output $T_1$ with an order of 3, the k-step-ahead validation process can be expressed as such:

$$\hat{T}_1(4) = f(T_1(3), T_1(2), T_1(1), T_{out}(3), T_{out}(2), V_c(3)), \tag{5.9}$$

$$\hat{T}_1(5) = f(\hat{T}_1(4), T_1(3), T_1(2), T_{out}(4), T_{out}(3), V_c(4)), \tag{5.10}$$

$$\hat{T}_1(6) = f(\hat{T}_1(5), \hat{T}_1(4), T_1(3), T_{out}(5), T_{out}(4), V_c(5)), \tag{5.11}$$

$$\vdots \qquad\qquad \vdots$$

$$\hat{T}_1(k) = f(\hat{T}_1(k-1), \hat{T}_1(k-2), \hat{T}_1(k-3), T_{out}(k-1), T_{out}(k-2), V_c(k-1)), \tag{5.12}$$

From Eqs. (5.9) to (5.12), it can be seen that the estimation error from the previous steps return to the validation process, which increases the prediction error for the next step repeatedly. This process is defined as error accumulation [31]. If the step size k is a small number, the measured outputs can be used to replace the predicted ones to correct the error. If k extends to an infinite step, no correction will be made and the k-step-ahead prediction will become a pure simulation [28]. In principle, a model can be regarded as accurate enough if it is capable of overcoming the error accumulation during a pure simulation. When this method is used to validate the multi-zone model, it works in a similar way: at each step, the estimated values of all the outputs (zone temperatures in all the investigated zones) are used as the inputs to predict the temperatures at the next step. In this manner, the coupling effects of the predicted temperature values of a certain zone to its neighbouring zones can be captured.

To test generalisation ability of the proposed model, that is, ability to deal with data never seen before, we selected six successive days, during which the ambient temperature continued to increase for a validation purpose. These data are classified into mild summer days and hot summer days, according to the maximum daytime outdoor temperature. Days in which the maximum temperature reached above 30 °C are defined as hot days, and those in which the maximum outdoor zone temperature was below 30 °C are defined as mild days. As well as RMSE, Normalised Mean Squared Error (NMSE) fitness value and Maximum Absolute Error (MAE) are used to evaluate the models' performance. Using the aforementioned input selection method, both the single-zone and multi-zone models

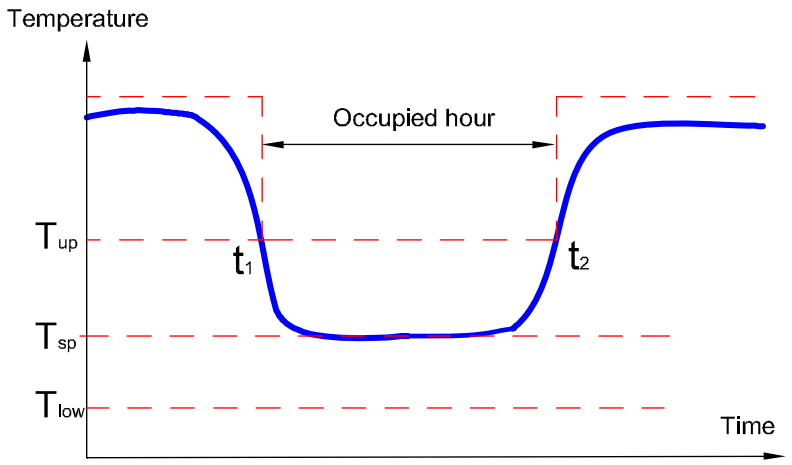


Figure 5.4: Indoor temperature trajectory in an air-conditioned zone.

are obtained, which are illustrated in Fig. 5.6.

$$RMSE = \sqrt{\frac{1}{n}\sum_{n}^{k=1}(y_k - \hat{y}_k)^2}, \tag{5.13}$$

$$NMSE_{fit} = 1 - \left(\frac{\|y_k - \hat{y}_k\|}{\|y_k - mean\,(y_k)\|}\right)^2, \tag{5.14}$$

where $y_k$ and $\hat{y}_k$ denote the actual and predicted outputs, corresponding to a set of test data.

## 5.5 Control Design

### 5.5.1 ANN Model-based Optimal Start-stop Control

The proposed predictive model can be useful in a variety of ways. For example, it can be used for nonlinear MPC design [26], optimal start-stop control [6], and fault detection [35]. In this study, we focus on the use of an ANN based optimal start-stop control strategy to achieve energy savings for the investigated building. The energy saving potential of applying this control approach stems from the fact that most commercial buildings

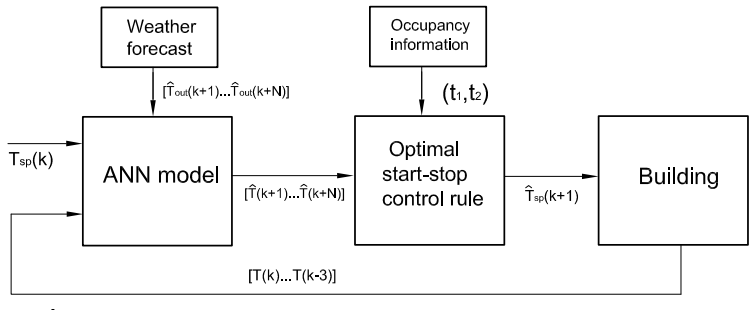


Figure 5.5: Block diagram of the optimal start-stop control strategy.

are not continuously occupied. Therefore, comfortable temperature should only be maintained during occupied hours. Due to the thermal initial of the buildings, the AHUs should be turned on (off) before the start (end) of occupation, so that energy will not be wasted cooling an empty space. Fig. 5.4 illustrates the temperature profile when the optimal control strategy is applied. In this figure, $T_{up}$ and $T_{low}$ represent the upper and lower comfort limits, respectively, and $[t_1, t_2]$ is the scheduled occupied hour. Due to the complexity of the building system, it is difficult to accurately estimate response time of the system. In this study, we employ the proposed ANN model as a basis to achieve the control purpose.

The block diagram of the proposed optimal start-stop control strategy is proposed in Fig. 5.5. The controller uses the identified ANN models to predict the temperature, and optimises the start-stop time of AHUs, taking into account the comfort requirement during the occupied periods. For online implementation, two modules have been created: a weather prediction module, receiving real-time forecast data from the public website, and an occupancy module, used to receive occupancy information from the BMS. The weather forecast module is updated every ten minutes, and imports the predicted outdoor temperature data ($\hat{T}_{out}$) into the ANN model. The occupancy information is set according to actual flight schedules, from 5:00 am until 9:30 pm. If a change occurs in occupancy information (for instance, due to the flight delay), the previous schedule will be updated and sent to the occupancy module. Therefore, the optimal start-stop controller will operate according to a new occupancy schedule.

Instead of conducting a nonlinear optimisation, we apply a rule-based algorithm in this study. The control rule works in the following way: Prior to the start of occupancy $t_{oc}$ at each time stamp, the controller sets the set point temperature $T_{sp}$ to the desired value, and then calculates the output trajectory within the prediction horizon $N_1$:

$$\left(\hat{T}(k+1) \quad \hat{T}(k+2) \quad \cdots \quad \hat{T}(k+N_1)\right), \tag{5.15}$$

It checks whether the following two criterions can be met simultaneously:

$$\hat{T}(k+n-1) \geq T_{uc} \qquad \hat{T}(k+n) < T_{uc}, \tag{5.16}$$

If the conditions of Eq. (5.16) are met, it checks if the following condition can be met:

$$round(0.1(t_{up} - t(k)) = n, \tag{5.17}$$

where $t_{up}$ and $t_k$ denote the clock time at start of occupancy and step k, respectively. If conditions Eqs. (5.16) and (5.17) are both met, $T_{sp}$ will be set into the set point value (22 $^{o}$C), which in turns starts the AHU; otherwise, the same procedure will be repeated when the next sampling time begins. As the time stamps progress, the optimal start point will be ultimately sought. Similarly, before the end of the occupancy, the controller discards the controllable inputs, and repeats the prediction. This operation determines the best stop time for AHU, to ensure a smooth transition from an occupied to an unoccupied hour.

### 5.5.2 Energy Model

To examine the energy saving potential of the proposed control strategy, it is necessary to calculate the energy use of the individual AHUs. As the measurement of the energy consumption for the AHUs is not available, we use the simplified models introduced in [10, 11] to estimate them. The simplified models are built based on two assumptions:

1. The energy consumed by the transfer of latent heat is negligible.

2. The mixed air ratio of return air to outdoor air is proportional to the opening level of the outdoor air damper.

With the above assumptions, the model used to calculate the energy consumption are

$$P_c = \frac{\dot{m} C_a \Delta T_c}{\text{COP}}, \tag{5.18}$$

$$\Delta T_c = (1 - D_{out}) T_r + D_{out} T_{out} - T_{sa}, \tag{5.19}$$

$$P_f = C_o + C_1 \dot{m} + C_2 \dot{m}^2, \tag{5.20}$$

where $P_c$ is the power consumption related to the cooling energy consumed by the cooling coils, $\dot{m}$ is the flow rate of the air passing through the cooling coil, $C_a$ is the specific heat of the supply air, $\Delta T_c$ is the temperature change of the supply air after the heat exchange occurred at the cooling coil, COP is coefficient of performance of the chiller plant, $D_{out}$ is the opening level of the outdoor air damper, $T_r$ is the return air temperature, $\Delta T_c$ is the temperature change of the supply air after the heat exchange occurred at the cooling coil, $P_f$ is the energy consumed by supply fan, and $C_o$ to $C_2$ are parameters related to the fan energy. In Eqs. (5.18) to (5.20), $T_r$, $T_{sa}$ and $D_{out}$ are measured by BMS, $\dot{m}$, COP and $\eta_c$ all use fixed values. The models are employed to compare the energy use when different control strategies are used.

## 5.6 Modelling Results and Discussion

### 5.6.1 Single-zone Results

This section validates the accuracies of the models. The numerical results of the identified model parameters and the corresponding simulation results are shown in Table 5.1, where models 1-5 represent the different ANN models representing zone 1, using different inputs

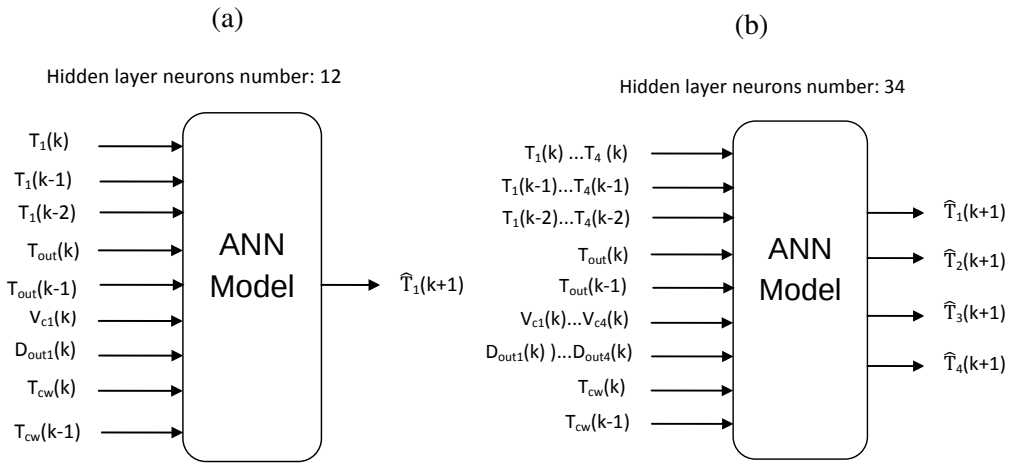


Figure 5.6: Structure of the ANN models used for zone temperature prediction. (a) Single zone model. (b) Multi-zone model.

combinations. The same approach was applied to the other three zones, to obtain the corresponding optimal model structures.

Fig. 5.7 shows the results of performing six-day-ahead temperature prediction, using the single-zone models developed for zones 1 to 4. It can be seen that the models work reasonably well during most investigated days. However, the single zone models sometimes over-predict zone temperatures, especially during the unoccupied hours. For example, the maximum error occurred at 120th hour, when the absolute errors of zone 1, zone 2 and zone 3 are 0.5 °C, 1 °C, and 0.5 °C, respectively.

Table 5.1 shows that in zone 1, the overall model performance on mild days is better than on hot days. Fig. 5.7(a) and 5.7(b) indicate that the largest error occurred during the last two days in zone 1 and 2, when the outdoor temperature was at its maximum value. The reason is that when the outdoor temperature was high, the cooling demand of the investigated area could not be met as expected. Therefore, the desired set point temperature value could not be reached even with 100% opened cooling valves. This model performance was substantially improved after the chilled water temperature was employed as an input (in model 3). It can be observed that, by adding the chilled water

Table 5.1: RMSE, MAE and NMSE in °C for simulation results with different model structures in zone 1.

| Order number of the inputs | **Model-1** | **Model-2** | **Model-3** | **Model-4** | **Model-5** |
|---|---|---|---|---|---|
| $T_1$ | 3 | 3 | 3 | 3 | 3 |
| $T_{out}$ | 2 | 2 | 2 | 2 | 2 |
| $V_c$ | 1 | 1 | 1 | 1 | 1 |
| $D_{out}$ | 0 | 1 | 1 | 1 | 1 |
| $T_c$ | 0 | 0 | 2 | 2 | 2 |
| $H_r$ | 0 | 0 | 0 | 1 | 0 |
| $S_r$ | 0 | 0 | 0 | 0 | 1 |
| Hidden Layer Number | 10 | 12 | 14 | 16 | 16 |
| $T_{out} < 30°C$ | | | | | |
| RMSE (in °C) | 0.28 | 0.17 | 0.17 | 0.22 | 0.20 |
| MAE (in °C) | 0.45 | 0.71 | 0.54 | 0.82 | 0.58 |
| NMSE(fitness in %) | 80% | 92% | 93% | 84% | 89% |
| $T_{out} > 30°C$ | | | | | |
| RMSE (in °C) | 0.52 | 0.58 | 0.43 | 0.64 | 0.48 |
| MAE (in °C) | 1.13 | 1.17 | 0.85 | 1.14 | 0.92 |
| NMSE(fitness in %) | 80% | 79% | 85% | 76% | 84% |

Table 5.2: Simulation results using single-zone and multi-zone models.

| | Zone-1 | Zone-2 | Zone-3 | Zone-4 |
|---|---|---|---|---|
| **Single-zone models** | | | | |
| RMSE (in °C) | 0.35 | 0.47 | 0.30 | 0.40 |
| MAE (in °C) | 1.08 | 1.27 | 0.94 | 1.34 |
| NMSE (fitness in %) | 79% | 74% | 78% | 77% |
| Training time (in s) | 3.6 | 6.7 | 4.3 | 4.8 |
| Simulation time (in s) | 55 | 58 | 60 | 56 |
| **Multi-zone model** | | | | |
| RMSE (in °C) | 0.29 | 0.41 | 0.26 | 0.32 |
| MAE (in °C) | 0.71 | 1.23 | 0.87 | 1.01 |
| NMSE (fitness in %) | 91% | 77% | 85% | 83% |
| Training time (in s) | | 37.6 | | |
| Simulation time (in s) | | 58 | | |

temperature, the RMSE improves from 0.36 °C to 0.19 °C and the NMSE improves from 79 per cent to 85 per cent on hot days. Additionally, it was found that adding relative humidity as a variable in model-4 does not improve the prediction accuracy of the model. This suggests that the effect of relative humidity variables on dry bulb temperatures is small. It was also found that when solar radiation is considered, the resultant model (model 5) could not achieve improved model performance either. This also makes sense, because with the operation of the blinds in this area, the effects of the solar gain on the indoor temperature were significantly reduced.

### 5.6.2 Multi-zone Results

In this section, we extend the single-zone approach to a multi-zone case, by considering the thermal interaction among all the adjacent zones. Compared to the conductive heat transfer between zones through the walls, the convective heat transfer through open space is more significant. Therefore, we ignore the conductive heat transfer for simplicity in this study.

Table. 5.2 presents a comparison of simulation results between the multi-zone and the single-zone models. It shows that the prediction errors for all the investigated zones were decreased after the multi-zone model was used. The RMSE was reduced by about 0.1°C and RMSE of 5% on average. Prediction results from zones 1 to 4, using multi-zone model, are illustrated in Fig. 5.8. It can be observed that the aforementioned over-prediction phenomenon was eliminated. This illustrates that thermal interaction between the adjacent zones exist, and the proposed multi-zone model has revealed the phenomenon. Another important finding is that the convective heat transfer appears to be more significant during night time, when all the AHUs stopped working. This is because when the AHUs were turned off, no cooling energy was supplied to the space, so that the environmental variables become the dominant inputs. As a result, all the room temperatures either increase or decrease along with the outdoor temperature, and will eventually reach the same value. In opposition, zone temperatures are less influenced by the heat transfer when the AHUs are running, because the control command forced the temperature to be maintained at the set point values, making the thermal coupling less significant.

The programs for model training and validation were coded in Matlab, which runs on a PC with Intel Core i7 CPU 2.4GHz. Training a multi-zone model takes more time than training a single-zone model, as expected. For example, it takes 37.6 s to train a multi-zone model while only 3.6 s to train a single-zone model (as shown in Table 5.2). This is because the multi-zone model has a larger size of input variables and hidden layer

neurons than the single-zone models. However, because the process of training a neural network model is performed offline, this process time is not critical. On the other hand, the execution time of conducting the pure simulation using the multi-zone model is closed to the time using the single-zone models. However, by exchanging information among the zones, several multiple-step-ahead prediction problems can be solved simultaneously, using the multi-zone model. It is not necessary to repeatedly run several single-zone models. Therefore, running the multi-zone model for real-time prediction is a more computational efficient approach than the single-zone models. Normally, a predictive control strategy often requires a much shorter prediction horizon than the pure simulation. For example, in this study we consider a prediction horizon of 2 hours (12 steps), which only takes about 0.8s for the multi-zone model to complete.

Six-days' pure simulation have an RMSE of 0.2 °C-0.4 °C for most zones. This result is similar to the results obtained in [28]. Since the prediction horizon used for simulation is much longer than the one required by predictive control, we can conclude that the proposed model is suitable to be used for predictive control design purpose.

## 5.7 Control Results and Discussion

### 5.7.1 Energy Saving with the Predictive Control

To test the aforementioned control strategy, a simulation study is scheduled using historical data on 24th, January, 2013. The selected area is zone 1 located at the east end of the building. An assumption made is that the weather condition can be perfectly predicted. The occupied hour is from 5:00 am to 9:30 pm. The upper comfort limit is set to be 24 °C, and the set point temperature is set to be 22 °C. The prediction horizon is chosen to be 2 hours (12 steps). As a default setting, all the AHUs were running from 4:00 am to 22:00 pm, to offset the time delay caused by thermal inertia. This is defined as the baseline control. During the simulation process, we run the predictive control algorithm

under the simulation environment with the initial temperature equals to the measured zone temperature. After, temperature performance and corresponding energy consumption are compared, when using these two different strategies.

Fig. 5.9(a) shows the performance comparison between baseline control and the proposed predictive control at zone 1. With the baseline control, zone temperature reaches 24 °C, before people started to enter the building. Concurrently, after the AHU was stopped, the temperature started to increase, but did not reach upper comfortable temperature of 24 °C. This control method is not energy efficient, because the controlled space was over-cooled at the start and end of occupation. When the predictive control was applied, the start time was delayed by 20 minutes, with zone temperature reaching the upper comfortable temperature of 24 °C when the first members of staff arrived at the building. Similarly, with the predictive control, the AHUs are set to unoccupied mode several hours earlier than the baseline control method. Due to the thermal storage ability of the building, the zone temperature can be kept within the comfortable range before the end of occupation. The indoor temperature rises slowly after the unoccupied mode was used, because the ambient temperature was decreasing in the afternoon. On the specific day, a daily saving of 28% can be achieved using the proposed control algorithm, as shown in Fig. 5.9(b). By extending the simulation result to a month, an estimation of 10% of energy savings can be achieved by applying the proposed control strategy.

The percentage of energy that optimal start-stop control can save depends on the weather condition. For example, when the outdoor temperature is low enough, the current control logic will open the outdoor air dampers more widely, bringing in more cool outdoor air to assist mechanical cooling. As a result, the cooling energy required to bring the temperature to the set point value, as well as the possible savings due to the use of optimal start-stop control, become less significant compared with those in hot days. When time of use electricity price is considered, it is also possible to apply a load shifting control strategy to reduce the utility costs.

### 5.7.2 Influence of Heat Transfer on Control Performance

As the heat transfer between the zones affects the accuracies of the predictive models, a complementary study is conducted to investigate the influence of the thermal interaction on the performance of the controller. Zone-1 is selected for comparison purpose. Before the start/stop time , the predictive controller is used to perform prediction and make control decision. Fig. 5.10(a) depicts the temperature trajectory generated by the proposed control algorithm. It is evident that the estimated time it takes to drop the temperature to the upper comfortable band (23.5 °C) using the multi-zone model is 30 minutes, while the one estimated by the single-zone model is 40 minutes. The response time estimated by the multi-zone model is closer to the actual one, compared with the one estimated by the single-zone model. Therefore, the multi-zone approach avoids violating thermal comfort at the start of the occupancy. Similarly, Fig. 5.10(b) shows that the rising time estimated by the single-zone model is about 0.5 hours less than the actual one, which results in late stop and a waste of energy at the end of occupancy. The multi-zone approach, on the other hand, predicts the rising time more accurately. It can be concluded that the predictive control method based on the multi-zone model provides improvement in both achieving better thermal comfort and saving more cooling energy.

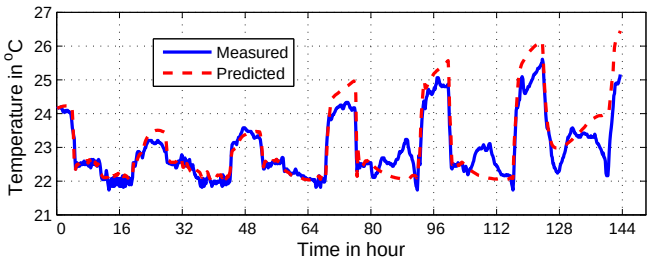


(a) Zone-1

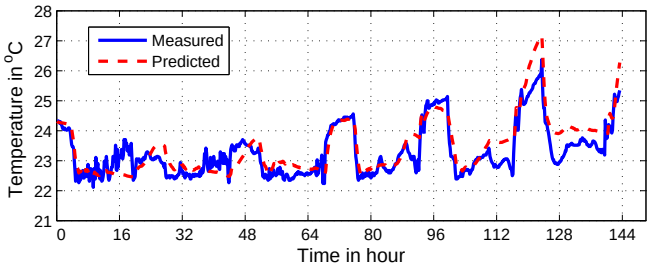


(b) Zone-2

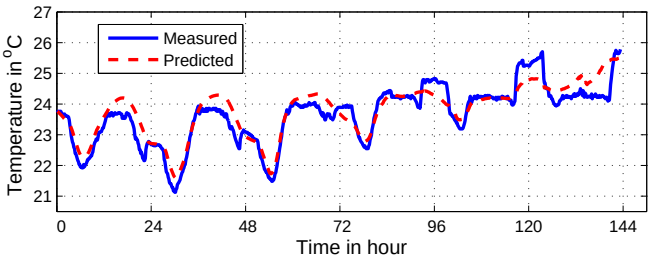


(c) Zone-3

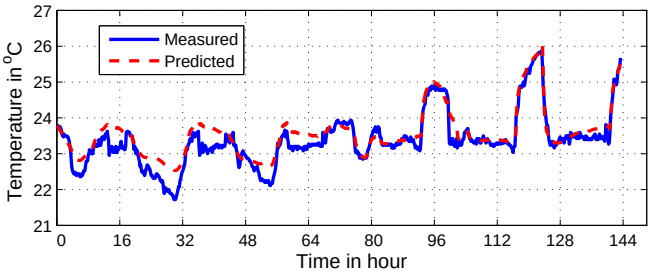


(d) Zone-4

Figure 5.7: Simulation results for zones 1 to 4, when four individual, single-zone models were used. The solid lines represent the measured temperature values from February 1 to February 8, 2013. The dashed lines represent the temperature values predicted by the single-zone ANN models.

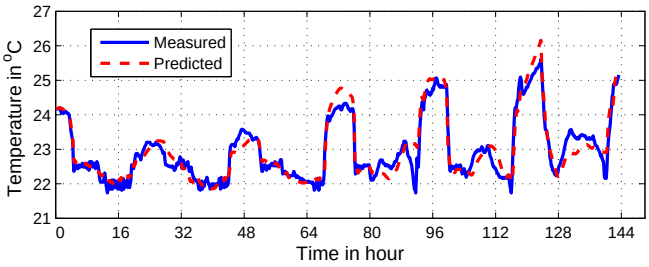


(a) Zone-1

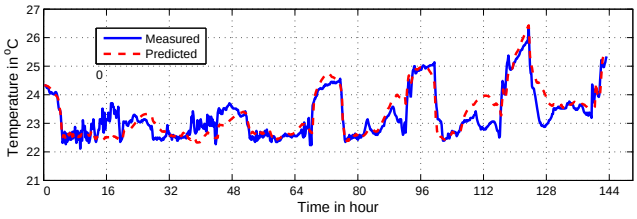


(b) Zone-2

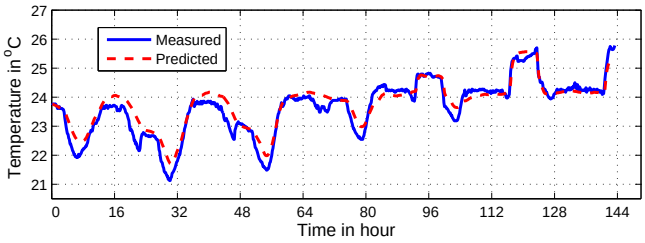


(c) Zone-3

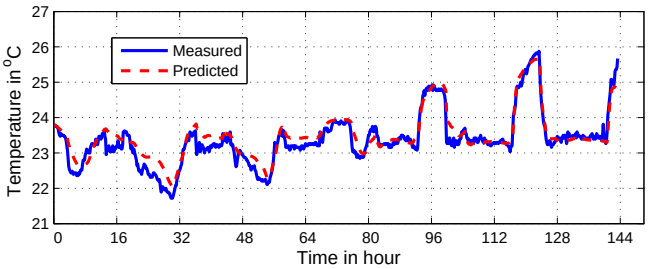


(d) Zone-4

Figure 5.8: Simulation results for zones 1 to 4, when the multi-zone model was used. The solid lines are the measured temperature values from 1st to 8th February, 2013. The dashed lines are the temperature values predicted by the multi-zone ANN model.

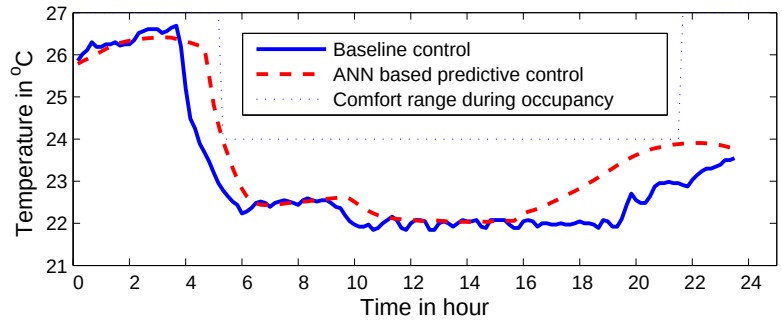


(a)

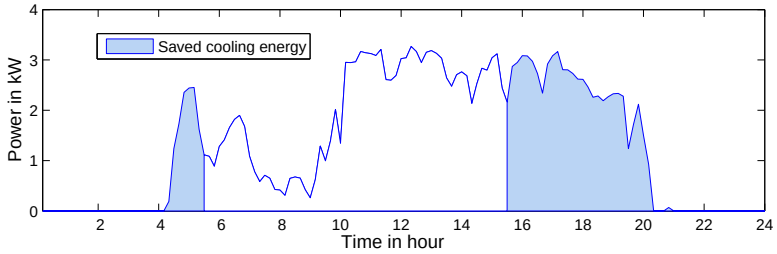


(b)

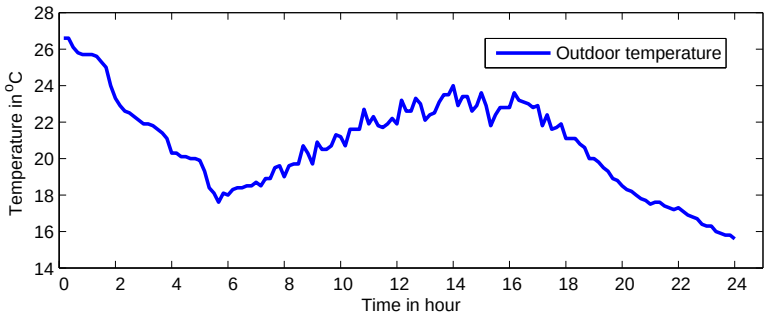


(c)

Figure 5.9: (a) Temperature trajectory when the baseline and optimal start-stop control are used on 24th, January, 2013, (b) Estimated cooling energy consumption during the day, the shaded area represents the saved energy due to the use of the predictive control, (c) Outdoor temperature.

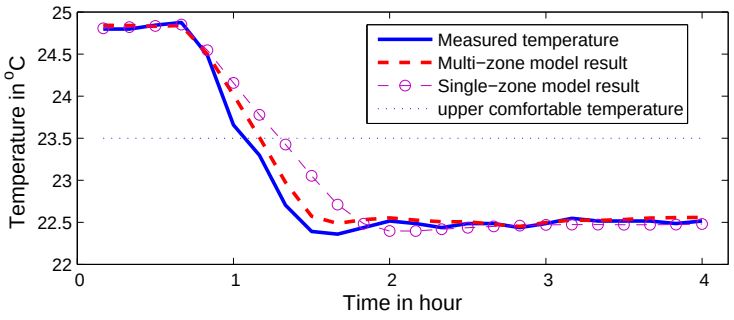


(a)

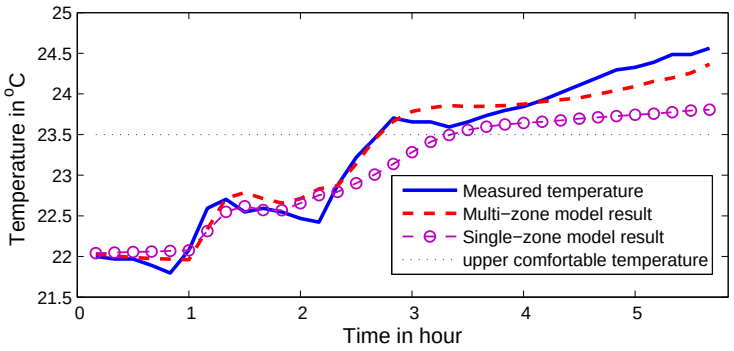


(b)

Figure 5.10: Comparison of measured and predicted response time for the zone temperature to reach upper comfortable temperature after the AHU was: (a) turned on, and (b) turned off.

## 5.8 Conclusions

This paper presents an ANN-based thermal dynamics modelling approach for real-world commercial buildings. While most existing building modelling studies only investigate a single zone, the modelling framework proposed in this study, extends the methodology to a multi-zone case. This provides a practical solution for the temperature modelling in large commercial buildings, especially those with wide open space. During the study, we used a forward inputs selection method to obtain the optimal model structure. Through several cycles of training-validation processes, the most critical input variables which affect the modelling accuracy were searched out. It is found that an accurate ANN model does not necessarily have to be big in size: the best model usually contains an order number no larger than four. Conversely, an oversized network with large input order and hidden layer number will result in large prediction errors with high frequency noises.

The effect of thermal coupling between the adjacent zones through convective heat transfer is hard to model, because the airflow between the zones is an uncertain factor. We consider the ANN as a suitable tool to solve such a problem. The simulation results prove that the method can accommodate the effect quite well: the overall prediction accuracies for all investigated zones were increased to a certain extend after the MIMO model was used. It is also found that the degree of thermal interaction between zones depends on weather conditions and the operational status of AHUs. For example, the errors due to the ignorance of thermal interaction appear to be bigger during the time when the AHUs were not running, and the days with higher ambient temperature. The proposed multi-zone model also has a faster computational speed than single-zone models, which enables the development of a more accurate and effective ANN-based predictive control. Finally, the effectiveness of applying the proposed model to achieve energy savings is demonstrated. It is found that since the multi-zone model predicts zone temperature more accurately than the single-zone models, the predictive control method built upon the multi-zone model can be used to achieve energy savings in a more reliable way. This illustrates that the

proposed methods have the potential to become valuable tools for modelling and control in commercial buildings.

# References

[1] L. Pérez-Lombard, J. Ortiz, and C. Pout, "A review on buildings energy consumption information," *Energy and Buildings*, vol. 40, no. 3, pp. 394–398, 2008.

[2] F. Oldewurtel, A. Parisio, C. N. Jones, D. Gyalistras, M. Gwerder, V. Stauch, B. Lehmann, and M. Morari, "Use of model predictive control and weather forecasts for energy efficient building climate control," *Energy and Buildings*, vol. 45, no. 0, pp. 15 – 27, 2012.

[3] N. Morel, M. Bauer, M. El-Khoury, and J. Krauss, "Neurobat, a predictive and adaptive heating control system using artificial neural networks," *Solar Energy Journal*, vol. 21, pp. 161–201, 2001.

[4] M. Maasoumy, M. Razmara, M. Shahbakhti, and A. S. Vincentelli, "Handling model uncertainty in model predictive control for energy efficient buildings," *Energy and Buildings*, vol. 77, no. 0, pp. 377 – 392, 2014.

[5] M. Avci, M. Erkoc, A. Rahmani, and S. Asfour, "Model predictive HVAC load control in buildings using real-time electricity pricing," *Energy and Buildings*, vol. 60, no. 0, pp. 199 – 209, 2013.

[6] A. Garnier, J. Eynard, M. Caussanel, and S. Grieu, "Low computational cost technique for predictive management of thermal comfort in non-residential buildings," *Journal of Process Control*, vol. 24, no. 6, pp. 750 – 762, 2014.

[7] S. Pívara, J. Široký, L. Ferkl, and J. Cigler, "Model predictive control of a building

heating system: The first experience," *Energy and Buildings*, vol. 43, no. 23, pp. 564 – 572, 2011.

[8] J. Široký, F. Oldewurtel, J. Cigler, and S. Prívara, "Experimental analysis of model predictive control for an energy efficient building heating system," *Applied Energy*, vol. 88, no. 9, pp. 3079 – 3087, 2011.

[9] Y. Ma, F. Borrelli, B. Hencey, B. Coffey, S. Bengea, and P. Haves, "Model predictive control for the operation of building cooling systems," *Control Systems Technology, IEEE Transactions on*, vol. 20, pp. 796–803, May 2012.

[10] H. Huang, L. Chen, and E. Hu, "A new model predictive control scheme for energy and cost savings in commercial buildings: An airport terminal building case study," *Building and Environment*, vol. 89, pp. 203 – 216, 2015.

[11] Y. Ma, A. Kelman, A. Daly, and F. Borrelli, "Predictive control for energy efficient buildings with thermal storage: Modeling, stimulation, and experiments," *Control Systems, IEEE*, vol. 32, pp. 44–64, Feb 2012.

[12] K. Lee and J. E. Braun, "Model-based demand-limiting control of building thermal mass," *Building and Environment*, vol. 43, no. 10, pp. 1633 – 1646, 2008.

[13] J. E. Braun and N. Chaturvedi, "An inverse gray-box model for transient building load prediction," *HVAC Research*, vol. 8, no. 1, pp. 73–99, 2002.

[14] F. Oldewurtel, A. Parisio, C. N. Jones, D. Gyalistras, M. Gwerder, V. Stauch, B. Lehmann, and M. Morari, "Use of model predictive control and weather forecasts for energy efficient building climate control," *Energy and Buildings*, vol. 45, no. 0, pp. 15 – 27, 2012.

[15] I. Hazyuk, C. Ghiaus, and D. Penhouet, "Optimal temperature control of intermit-

tently heated buildings using model predictive control: Part 1building modeling," *Building and Environment*, vol. 51, no. 0, pp. 379 – 387, 2012.

[16] S. F. Fux, A. Ashouri, M. J. Benz, and L. Guzzella, "EKF based self-adaptive thermal model for a passive house," *Energy and Buildings*, vol. 68, Part C, no. 0, pp. 811 – 817, 2014.

[17] S. Bengea, V. Adetola, K. Kang, M. J. Liba, D. Vrabie, R. Bitmead, and S. Narayanan, "Parameter estimation of a building system model and impact of estimation error on closed-loop performance," in *Decision and Control and European Control Conference (CDC-ECC), 2011 50th IEEE Conference on*, pp. 5137–5143, 2011.

[18] S. Goyal and P. Barooah, "A method for model-reduction of non-linear thermal dynamics of multi-zone buildings," *Energy and Buildings*, vol. 47, no. 0, pp. 332 – 340, 2012.

[19] S. Goyal, C. Liao, and P. Barooah, "Identification of multi-zone building thermal interaction model from data," in *Decision and Control and European Control Conference (CDC-ECC), 2011 50th IEEE Conference on*, pp. 181–186, Dec 2011.

[20] P.-D. Moroan, R. Bourdais, D. Dumur, and J. Buisson, "Building temperature regulation using a distributed model predictive control," *Energy and Buildings*, vol. 42, no. 9, pp. 1445 – 1452, 2010.

[21] L. Ferkl and J. Široký, "Ceiling radiant cooling: Comparison of ARMAX and subspace identification modelling methods," *Building and Environment*, vol. 45, no. 1, pp. 205 – 212, 2010.

[22] Y. Ma, G. Anderson, and F. Borrelli, "A distributed predictive control approach to building temperature regulation," in *American Control Conference (ACC), 2011*, pp. 2089–2094, 2011.

[23] S. Karatasou, M. Santamouris, and V. Geros, "Modeling and predicting building's energy use with artificial neural networks: Methods and results," *Energy and Buildings*, vol. 38, no. 8, pp. 949 – 958, 2006.

[24] G. Mustafaraj, G. Lowry, and J. Chen, "Prediction of room temperature and relative humidity by autoregressive linear and nonlinear neural network models for an open office," *Energy and Buildings*, vol. 43, no. 6, pp. 1452 – 1460, 2011.

[25] A. Ruano, E. Crispim, E. ConceiA, and M. LAcio, "Prediction of building's temperature using neural networks models," *Energy and Buildings*, vol. 38, no. 6, pp. 682 – 694, 2006.

[26] P. Ferreira, A. Ruano, S. Silva, and E. Conceiçâo, "Neural networks based predictive control for thermal comfort and energy savings in public buildings," *Energy and Buildings*, vol. 55, no. 0, pp. 238 – 251, 2012.

[27] T. Lu and M. Viljanen, "Prediction of indoor temperature and relative humidity using neural network models: model comparison," *Neural Computing and Applications*, vol. 18, no. 4, pp. 345–357, 2009.

[28] H. C. Spindler and L. K. Norford, "Naturally ventilated and mixed-mode buildings part1: Thermal modeling," *Building and Environment*, vol. 44, no. 4, pp. 736 – 749, 2009.

[29] H. C. Spindler and L. K. Norford, "Naturally ventilated and mixed-mode buildingspart 2: Optimal control," *Building and Environment*, vol. 44, no. 4, pp. 750 – 761, 2009.

[30] B. Tashtoush, M. Molhim, and M. Al-Rousan, "Dynamic model of an hvac system for control analysis," *Energy*, vol. 30, no. 10, pp. 1729 – 1745, 2005.

[31] M. Mohammadzaheri, S. Grainger, and M. Bazghaleh, "Fuzzy modeling of a piezoelectric actuator," *International Journal of Precision Engineering and Manufacturing*, vol. 13, pp. 663–670, 2012.

[32] T. Lu and M. Viljanen, "Prediction of indoor temperature and relative humidity using neural network models: model comparison," *Neural Computing and Applications*, vol. 18, pp. 345–357, 2009.

[33] G. D. Robert May and H. Maier, "Review of input variable selection methods for artificial neural networks artificial neural networks," in *Artificial Neural Networks - Methodological Advances and Biomedical Applications* (K. Suzuki, ed.), 2011.

[34] D. J. MacKay, "Bayesian interpolation," *Neural Computation*, vol. 4, pp. 415–447, 1991.

[35] Z. Du, B. Fan, X. Jin, and J. Chi, "Fault detection and diagnosis for buildings and hvac systems using combined neural networks and subtractive clustering analysis," *Building and Environment*, vol. 73, no. 0, pp. 1 – 11, 2014.

# Chapter 6

# Hybrid Model Predictive Control

This chapter is based on the following paper:

*Full citation*: Huang H., Chen L., Hu E., "A new model predictive control scheme for energy and cost savings in commercial buildings: An airport terminal building case study", In Building and Environment, vol. 89, pp. 203 - 216, 2015.

*Contribution of this chapter*: A hybrid model predictive control is proposed for commercial buildings for optimising energy costs in buildings. Feedback linearisation is used to simplify the optimisation problem, and an inverse neural network model is applied to handle system nonlinearity associated with the AHU process. Experiment shows the proposed MPC reduces the operational costs by 11%, through performing free cooling and shifting cooling load.

# Statement of Authorship

| | |
|---|---|
| Title of Paper | A new model predictive control scheme for energy and cost savings in commercial buildings: An airport terminal building case study |
| Publication Status | ☑ Published ☐ Accepted for Publication<br>☐ Submitted for Publication ☐ Unpublished and Unsubmitted w ork w ritten in manuscript style |
| Publication Details | Huang H., Chen L., and Hu E., (2015), A new model predictive control scheme for energy and cost savings in commercial buildings: An airport terminal building case study, Building and Environment, Vol. 89, 2015, Pages 203-216. doi: 10.1016/j.buildenv.2015.01.037 |

## Principal Author

| | |
|---|---|
| Name of Principal Author (Candidate) | Hao Huang |
| Contribution to the Paper | Developed model and control system, process data, performed experiment work, wrote manuscript and acted as the corresponding author. |
| Overall percentage (%) | 55% |
| Certification: | This paper reports on original research I conducted during the period of my Higher Degree by Research candidature and is not subject to any obligations or contractual agreements with a third party that would constrain its inclusion in this thesis. I am the primary author of this paper. |
| Signature | Date 15/10/15 |

## Co-Author Contributions

By signing the Statement of Authorship, each author certifies that:

i. the candidate's stated contribution to the publication is accurate (as detailed above);
ii. permission is granted for the candidate in include the publication in the thesis; and
iii. the sum of all co-author contributions is equal to 100% less the candidate's stated contribution.

| | |
|---|---|
| Name of Co-Author | Lei Chen |
| Contribution to the Paper | Supervised research, helped with data collection and experiment setup, evaluate and review the manuscript. |
| Signature | Date 15/10/15 |

| | |
|---|---|
| Name of Co-Author | Eric Hu |
| Contribution to the Paper | Supervised research, eveluated and edited manuscript. |
| Signature | Date 15/10/15 |

**Abstract**

Predictive control technology for heating, ventilation and air conditioning (HVAC) systems has been proven to be an effective way to reduce energy consumption and improve thermal comfort within buildings. Such methods rely on models to accurately predict the thermal dynamics of a specific building to achieve the optimal control. Implementing a predictive control at the building level faces several challenges, since buildings thermal dynamics are nonlinear, time-varying, and contain several uncertainties. This paper presents a hybrid model predictive control (HMPC) scheme, which can minimise the energy and cost of running HVAC systems in commercial buildings. The proposed control framework combines a classical MPC with a neural network feedback linearisation method. The control model for the HMPC is developed using a simplified physical model, while the nonlinearity associated with HVAC process is handled independently by an inverse neural network model. To achieve the maximum energy saving, the proposed MPC integrates several advanced air-conditioning control strategies, such as an economizer control, an optimal start-stop control, and a load shifting control. This approach has been tested at the check-in hall of the T-1 building of the Adelaide Airport, through simulations and a field experiment. The merits of the proposed method compared to the existing control method are analysed from both the energy saving and cost saving points of view. The result shows that the proposed HMPC scheme performs reasonably well, and achieves a considerable amount of savings without violating thermal comfort.

## 6.1 Introduction

The building sector is one of the world's largest energy consumers. It has been estimated that buildings consume 40 per cent of the world's energy and generate 33 per cent of the carbon dioxide emissions [1]. Heating, ventilation and air conditioning (HVAC) systems are one of the major building energy consumers, which account for almost one-half of the total building energy use. Despite their significance, HVAC systems in existing buildings

are not operating in the most efficient ways. Therefore, this study develops an advanced control strategy, with the aim of reducing the energy consumption and improving the thermal comfort in large commercial buildings.

Despite great efforts having been dedicated to the research into advanced HVAC control technology, proportional-integral-derivative (PID) control and on/off control are still the most commonly used control methods in commercial buildings. They use the current and previous temperatures as the inputs to control local actuators, such as chilled water valves, pumps, and dampers. As building dynamics are a slow process, subject to the passively changing ambient environment, the HVAC may respond to an indoor temperature change with a significant time delay using the control methods. This causes over-heating (cooling), high on-peak demand and poor thermal comfort in the buildings. In recent years, researchers have demonstrated that the energy costs associated with HVAC can be reduced greatly by implementing predictive control strategies [2–7]. MPC is a control strategy which optimises the control input based on the system dynamics, constraints, and couplings between the local controllers. When MPC is applied to buildings, it uses the prior knowledge from the weather forecast, occupancy prediction, and time-varying electricity prices, to achieve energy savings as well as improve thermal comfort in buildings.

MPC is often employed at the supervisory level to optimise the energy use at the building scale. The idea of using MPC to save building energy stems from the concept of supervisory control [8]. This includes optimal start-stop control [9], pre-cooling control [10], economizer control [11], and demand-limiting control [12]. MPC is a strategy which integrates all these supervisory control methods into a single control scheme. Since commercial buildings are not continuously occupied, the thermal comfort requirement should only be met during the occupied hours. For this reason, the cooling or heating systems are usually turned on (off) before the start (end) of occupation, so that thermal comfort will only be maintained within the occupied hours. By solving an optimisation problem, MPC is able to realise this start-stop control function [9, 13, 14]. Further, under certain condi-

tions, MPC can aslo shift the cooling (heating) load from peak hours to off-peak hours, using passive or active building thermal storages. This strategy is based on the efficient use of the building's thermal mass. Since such an approach uses cheap off-peak electricity and free cooled ambient air, the utility costs of running HVAC systems can be greatly reduced [15]. The pre-cooling strategy has been successfully applied to buildings with both active and passive thermal storage, and has achieved significant savings [4, 10, 16–18].

However, implementing MPC for real-world buildings is not straightforward, for a list of reasons, which can be summarised as follows:

1. Building dynamics have several uncertain disturbances and thermal delays. This requires the prediction of disturbances such as the ambient temperature and occupancy load, which are non-Gaussian distributed, and subject to stochastic errors [7].

2. The simplified building models for control purposes are nonlinear. This is because the cooling and heating energy are computed by a multiplication of the supply air mass flow rate, temperature, and outdoor damper opening level, which results in control inputs in a bilinear form [7, 17].

3. Air-conditioned buildings possess several nonlinear variables, such as the temperature, relative humidity, and outdoor air damper actions, which can hardly be accurately modelled using simplified physical models.

4. The internal space of a building is divided into several adjacent zones, each of which is controlled by an individual air handling unit (AHU). Therefore, the thermal dynamics of a building is a multiple-input, multiple-output (MIMO) system.

To solve the above problems, the first and most important step is to create a transient thermal dynamic model, able to describe the relations between the input variables (such as the outdoor temperature, and the HVAC operating status) and the output variables (such as the indoor temperature). For control purposes, the developed model should have the

ability to predict both short-term unexpected changes and long-term accumulated changes in the building temperature. They should also be simple in structure, so that they can be implemented within the existing building management system.

To build such a model, resistance–capacitance (RC) thermal models [3, 17–20], statistical models [13, 21, 22], and neural network (NN) models [6, 23, 24] have been employed in previous studies. The RC models are preferred by most researchers, because they are physically meaningful and transparent in structure, making them understandable and reliable to use. With some prior knowledge about the system, the principle parameters of the RC models can be identified using grey box identification methods [19]. The resulting model can be transformed into a linear state-space form so that the classical control algorithms can be applied [25]. Several successful examples can be found. For example, Bengea et al. [26] used a performance sensitivity approach to establish an estimation error target for the physical parameters of control models. They found that the most critical parameters are the heat transfer coefficients of the building's ceiling and ground. Hazyuk et al. [14] built a low-order building model using an RC model. They considered solar gain as the major disturbance source and modelled it using mathematical equations. A modified cost function was used to determine the optimal operation for an intermittently heating system [27].

Building statistical models requires less effort than an RC model, as they are purely built on input–output data. These models are also in linear state-space forms, making them able to be used for classical MPC design. Privara et al. [5] developed a multi-zone building using a subspace state-space model. The MPC built on the model was proved to achieve promising results compared with the rule based control. Both the RC model and statistical models are linear and time-invariant, so a model mismatch sometimes occurs, which in turn influences the control performance. To solve this issue, several advanced MPC strategies have been proposed, such as robust MPC [28], stochastic MPC [7, 29], and distributed MPC [13, 30]. Oldewurtel et al. [7] developed a stochastic MPC to handle

the model uncertainty caused by weather forecast errors. Maasoumy et al. [28] employed an unscented Kalman filter technique to estimate the parameters and states online. The adaptive model was used for a robust MPC, which can handle the system uncertainties well.

In recent years, growing attention has also been paid to artificial neural network (ANN) models, for building modelling and control [6, 23, 24]. ANN models are suitable for modelling building dynamics due to their ability to deal with nonlinear, multivariable modelling problems. The parameters of an ANN include the number of neurons and the values of the interconnection weights and biases. If a dynamic ANN model is employed, the orders and delay terms should also be considered during the model development. Past studies have shown that ANN models have better performance than linear models [31, 32] and physical models [24] in modelling a building's thermal dynamics. An ANN can also be directly used for nonlinear model predictive control. Spindler and Norford [33] built a predictive control method to determine the optimal cooling mode, resulting in a reduced fan energy use. Ferreira et al. [33] developed an ANN-based model predictive control for a campus building, and used a discrete branch and bound approach to optimise the energy use. Although neural networks are effective in emulating nonlinear building dynamics systems, two major drawbacks arise when they are used in an MPC structure:

1. A nonlinear optimisation routine must be used to calculate the control sequence using the ANN model. This requires very high computational effort and may result in a merely local minimum.

2. The well established theory of designing and tuning linear controllers cannot be used for tunning nonlinear controllers.

For the above reasons, the implementation of an ANN-based MPC faces challenges, and there is a need to re-think the use of neural networks in building energy control. Besides, although a number of successful cases can be found, some research questions still need to be answered to make a practical MPC. These include:

1. How to effectively handle the nonlinearity and uncertainties of the system dynamics.

2. How to choose the appropriate MPC schemes for different buildings.

Concerning the above problems, this paper aims to develop an MPC strategy, which can be implemented within the building management system (BMS) to optimise the energy use and reduce the cost of HVAC systems.

As the first contribution of this paper, a hybrid MPC (HMPC) for building predictive control is presented. The approach exploits the excellent non-linear approximation ability of the ANN model and the reliability of the simplified physical model, to improve the control performance of the MPC method. The control model uses a linearised RC model, which enables a linear programming optimisation method to minimise energy consumption. A recurrent NN model captures the nonlinearity and uncertainty related to the HVAC system, and provides a 'real' control command to the building system. This method results in a simple linear controller with a wide operating range, without the need for carrying out a computationally intensive non-convex optimisation at each time instant. Although this control structure has been used in process control [34], it has not been used for the building energy control before. Additionally, we introduce a novel simulation platform to evaluate the closed-loop performance of the proposed HMPC. In this platform, a forward neural network is used to approximate the thermal dynamics of the building, which updates the initial status for the HMPC operation. This method allows the parameters of the model and controller to be reliably tuned, before they are tested at the real plant. This represents the second contribution of this paper. Finally, an MPC which integrates the economizer control with other supervisory control methods is introduced. Its energy saving potential is evaluated using a real-time flight schedule and time-of use (TOU) electricity prices, through both a simulation and an experimental study. All the above methodologies are presented based on the BMS data collected from an airport terminal building. The building has several wide open, adjacent zones, which are irregular

Figure 6.1: Outside view of check-in hall of Adelaide airport.

in shape and structure. These factors make the case study different from the ones appearing in the existing literatures. In this study we focus on the cooling plant, but the same approach can be easily extended to heating as well.

The layout of this paper is arranged as follows: Section 2 introduces the simplified physical models used to represent the building dynamics and HVAC process. The design of the linear MPC using a feedback linearisation and an inverse neural network method are introduced in Section 3. Section 4 demonstrates the results of the proposed MPC, including the simulation and experimental results. The energy and cost saving potential of the proposed method is analysed in that section. This paper ends with a conclusion and a description of future research.

## 6.2 Modelling

### 6.2.1 Building Thermal Dynamics Modelling

The test building is the T1 building of Adelaide Airport, South Australia. The check-in hall consisting of four thermal zones was selected as the experimental area. Fig. 6.1 shows the external appearance of the investigated zones. The selected zones are located at the perimeter areas of level 2 of the building, isolated from the outdoor environment by a large

glass wall to the north. Two motorised blinds are installed at the north window, to reduce the effects of solar radiation. The blinds schedule is programmed into the BMS according to the solar angle at different times of year. The AHU is with a constant air volume (CAV), while the angle of the jet nozzle changes according to the measured temperature. Fig. 5.2 shows the general layout of the four-zone case. It can be seen that each zone is served by an individual AHU. All the zones are with open space, and adjacent to each other. In the rest of the paper, zone 1 and zone 2 are used as a benchmark to explain the proposed method.

The thermal dynamics of the zones are modelled by an RC thermal network, which uses resistances and capacitances to represent the heat transfer coefficients of a building. Past study has shown that 3R2C models represent the best compromise between prediction accuracy and model complexity [35]. Therefore, this model structure is employed in this study. The schematic of the RC network for these two zones is shown in Fig. 5.3. This study focuses on a single zone, but the influence of the thermal interaction of its adjacent zone will also be discussed. Before building the RC model, the following assumptions were made:

A1. The temperature distribution in each zone is uniform.

A2. The density and flow rate of the air in the zones are constant and not influenced by the temperature change.

A3. The walls and ceiling have the same effect on zone temperature. The windows have negligible thermal capacitance.

A4. The convective heat transfer between open space is more significant than conductive heat transfer through walls.

Based on the above assumptions, the energy and mass balance governing equations

for zone 1 can be written as

$$C_z^1 \frac{dT_1}{dt} = \dot{m}C_a(T_{sa,1} - T_1) + \frac{T_f - T_1}{R_f} + \frac{T_{out} - T_1}{R_g} + \frac{T_w - T_1}{R_w} + \frac{T_2 - T_1}{R_c} + Q_1, \tag{6.1}$$

$$C_w^1 \frac{dT_w}{dt} = \frac{T_1 - T_w}{R_w} + \frac{T_{out} - T_w}{R_w}, \tag{6.2}$$

where $C_z^1 = C_a \rho V_z$ is the overall thermal capacitance of the zone, $\rho$ is the density of the air, $V_z$ is the volume of the zone, $C_w^1$ is the thermal capacitance of the internal walls and ceiling, which is much larger than $C_z^1$, $\dot{m}$ is the mass flow rate of the supply air, $C_a$ is the specific heat of the air, $T_1$ and $T_2$ are the air temperatures of zones 1 and 2, respectively, $T_{out}$ is the outdoor air temperature, $T_w$ is the mean temperature of the walls and ceiling, $T_f$ is the mean temperature of the floor, $T_{sa,1}$ is the temperature of the supply air to zone 1, $R_w = 1/(h_w A_w)$ is the thermal resistance of the wall and ceiling, $R_f = 1/(h_f A_f)$ is the thermal resistance of the floor, $R_g = 1/(h_g A_g)$ is the thermal resistance of the window facade, $R_c$ is convective heat transfer coefficient between adjacent zones, $h_w$ and $h_f$ are the convective heat transfer coefficients per unit area associated with the walls (including the ceiling) and the floor, respectively, $h_g$ is the conductive and convective heat transfer coefficient per unit area of the windows, $A_w$, $A_f$ and $A_g$ are the areas of the walls, floor and window surfaces, respectively, and $Q_1$ represents the heat gains caused by solar radiation ($Q_s$), leakage ($Q_l$) and occupants ($Q_p$).

The installed motorised blinds in the test zones prevent the sun from irradiating the space, which greatly reduces the effects of solar radiation. Therefore, the solar radiation is not directly modelled by the equations. Instead, it will be modelled as a stochastic variable. The heat gain from the occupants is indicated by the carbon dioxide concentration in the investigated zone [28], which can be directly obtained from the BMS database. The occupancy load is indicated with the following equation:

$$q_p = \alpha CO_2(i) + \nu, \tag{6.3}$$

where $\alpha$ and $v$ are parameters which will be identified together with Eq. (7.1). Other disturbances, such as solar gain, the heat generated by electronic equipment, and the leakage and coupling from other un-controlled spaces, are modelled by a white noise with Kalman gains: this will be discussed later. Eqs. (7.1) and (7.2) are discretized by using the backward Euler method:

$$C_z^1 \frac{T_1(k)-T_1(k-1)}{\Delta t} = \dot{m}C_a(T_{sa,1}(k-1)-T_1(k)) + \frac{T_f(k-1)-T_1(k)}{R_f} + \frac{T_{out}(k-1)-T_1(k)}{R_g} + \frac{T_w(k-1)-T_1(k)}{R_w} + \frac{T_2(k-1)-T_1(k)}{R_c} + q_p(k-1) + k(e), \quad (6.4)$$

$$C_w^1 \frac{T_w(k)-T_w(k-1)}{\Delta t} = \frac{T_1(k-1)-T_w(k)}{R_w} + \frac{T_{out}(k-1)-T_w(k)}{R_w}, \quad (6.5)$$

where $\Delta t$ is the sampling time of the measured data. Eqs. (6.4) and (6.5) can be written in innovation represenation state-space form [36]:

$$x_{k+1} = Ax_k + Bu_k + Ed_k + ke(k), \quad (6.6)$$

where $x = [T_1, T_w]$ is the vector containing the states of zone 1, $u = [T_{sa,1}, \dot{m}]$ is the vector of controllable input variables, and $d = [T_{out}, T_2, CO_2]$ are the measured disturbance variables; $k$ and $e$ are the Kalman gain and Gaussian noise, respectively, which represent the stochastic part of the system. The method used to estimate the Kalman gain is derived from the Algebraic Riccati Equation (ARE) [36]. A grey box identification method is used to identify the unknown parameters in Eq. (7.4). During the identification, the initial states and the boundary conditions of the unknown parameters [$R_w$, $R_g$, $R_f$, $R_c$, $\alpha$, $C_z^1$,$C_w^1$] were configured first, based on the static parameters defined previously. The unknown parameters are identified by a nonlinear least squares algorithm using real-time BMS data with a sampling interval of 10 minutes [36]. The data used for training were collected from between the 1st and 31st of January 2013, and the validation data were selected

from between the 1st and 10th of February, 2013. The output of the model is the indoor temperature. The inputs to the model are the supply air temperature, the supply air mass flow rate, the neighbouring zone temperature, and the carbon dioxide concentration. The outdoor temperature $T_{out}$ is obtained from the Bureau of Meteorology of Australia. The identified parameters for the RC model are listed in Table 6.1.

The performance of the models is evaluated by the normalised relative mean squared error (NRMSE) fitness value:

$$NRMSE = \frac{1}{N-1}\sqrt{\frac{\sum_{k-1}^{n}(y(k)-\hat{y}(k))^2}{\sum_{k-1}^{n}(y(k))^2}}, \tag{6.7}$$

where $y$ is the measured output and $\hat{y}$ is the predicted output. In building predictive control, different prediction horizons are needed for different control purposes. In this study we used a pure simulation as the validation approach: the measured outputs are only used for prediction at the first step, and starting from the second step, the predicted outputs are used instead. This operation allows the performance of the control oriented model to be tested under infinite prediction horizons. The pure simulation uses more strict evaluation criteria than with an one-step-ahead prediction result, and thus can better reflect the 'quality' of the models.

The first set of simulations was performed using a single-zone model. When a single-zone model is used, the impact of the thermal coupling with the adjacent zone is not taken into consideration. This approach is subjetive to errors, as a change in the neighbouring zone temperature may affect the zone investigated. Fig. 6.2(a) shows that the single-zone model has a fitness of 72% when a pure simulation is conducted. The prediction error is mainly caused by the ignorance of unmeasured disturbances, such as the coupling with the neighbouring zones, leakage and the solar radiation. Clearly, the RC model is able to capture the main thermal characteristics of the building with its simple structure. This is because when the system is operating within a small operational range, the building's

Table 6.1: Parameter estimation results for RC model

| Parameter | Value | Parameter | Value |
|---|---|---|---|
| $C_w^1$ | 252,000 kJ/K | $C_z^1$ | 9080 kJ/K |
| $R_g$ | 43 K/kW | $R_w$ | 0.9 K/kW |
| $R_f$ | 2.2 K/kW | $k$ | [0.5,0] |

thermal dynamics can be approximated by a linear, time invariant model. A strategy, such as, a multiple model approach can be adopted to make the building model suitable for a wider operational range [37].

To investigate the effects of the thermal coupling on the investigated zone, another RC model, which takes into consideration the thermal coupling between the zones, was developed. In this model, the neighbouring zone temperature $T_2$ is considered as a disturbance, and assumed to be known in advance. Fig. 6.2(b) shows that the model that considers the neighbouring zone temperature ($T_2$) generates smaller prediction errors than the single-zone model. This proves the fact that the thermal interaction between the adjacent zones influences the accuracy of the models. However, since the value $T_2$ is only known until the current step, it cannot be directly employed for MPC, which requires multiple step prediction. In the subsequence experiment, the same control command will be used for zone 1 and zone 2, based on their average temperatures. This is to simplify the multi-input, multi-output (MIMO) control problem into a multi-input, single-output (MISO) problem.

### 6.2.2 HVAC Process Modelling

#### Chiller Plant

The investigated building is controlled by a Johnson Controls Australia Pty Ltd BMS. At the building level, three chillers provide chilled water to the entire water circle. Each

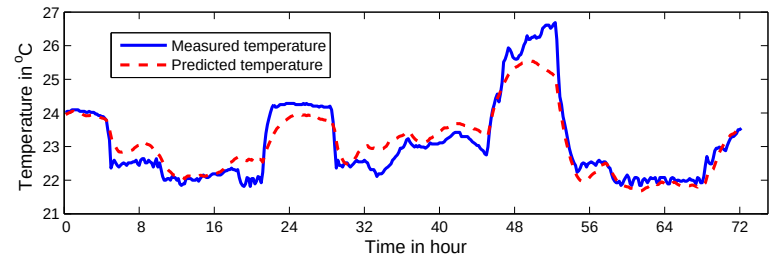


(a)

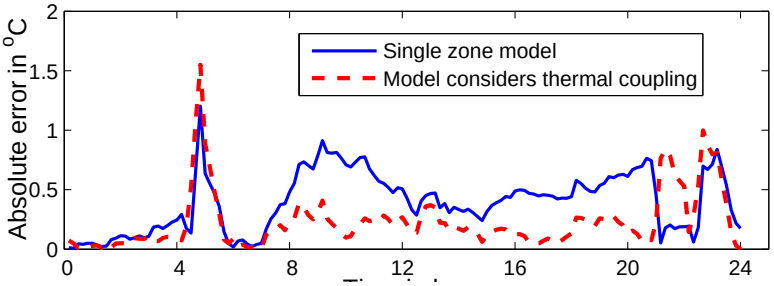


(b)

Figure 6.2: (a): Simulation results of RC model (Model fit = 0.72); (b) Error distribution comparison between single-zone RC model and RC model with thermal coupling

chiller is rated at 1767 kW output and 320 kW electrical inputs at a full load. The chilled water is transmitted from the chiller plants to local AHUs through variable-speed water pumps. There are 200 AHUs running simultaneously to meet the cooling requirement of the entire building. The total cooling load of the building can be expressed by

$$Q_{chil} = C_{pw} m_w (T_{cwr} - T_{cws}), \tag{6.8}$$

where $Q_{chil}$ is the cooling load of the building, $C_{pw}$ is the specific heat capacity of the chilled water, $m_w$ is the mass flow rate of the chilled water, and $T_{cws}$ and $T_{cwr}$ are the chiller water supply and return temperature, respectively. The set point temperature for the supply chilled water temperature has a constant value of 7°C. If the supply chilled water temperature ($T_{cws}$) in the primary loop is above 12°C for more than five minutes, the BMS will automatically start another chiller to meet the cooling load requirement.

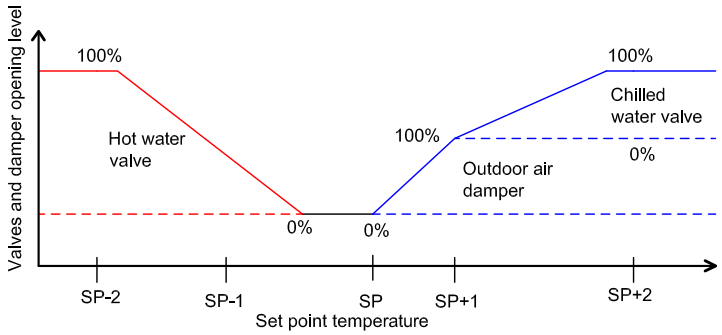


Figure 6.3: Control logic of the economizer.

The cooling load consumed by the chiller plant accounts for the majority of the energy consumption, which is distributed to the local AHUs.

### AHU Process Modelling

At the subsystem level, the AHUs transfer the cooling energy from the chilled water circuit to the airflows, and then supply it to the local thermal zones. Fig. 4.2 shows the schematic diagram of the AHU used in this study. During the operation period, the return air is recirculated through the outdoor air damper and then mixed with the return air. The mixed air then passes through the cooling coil and the air temperature decreases after the heat exchange. The chilled water valve uses the difference between the measured zone temperature and the set point temperature to maintain the zone temperature at the set point value. The actuating signal to the system is the cooling valve position, which regulates the mass flow rate of the chilled water. The AHUs also have $CO_2$ sensors installed in the return air ducts. When the measured $CO_2$ level rises above 500 ppm, the outdoor damper will be modulated to maintain good air quality. In this study, the $CO_2$ sensor is also used to indicate the level of occupancy.

As the measurements of some important variables within the AHU process are not available, a series of simplified physical models are used. The main purposes of building the simplified models are: 1. To estimate the energy consumption of the individual AHUs,

and 2. To build connections between the air-side and water-side dynamics within the AHU process. Before building the model, other assumptions are made:

A5. The air inside the cooling coil is perfectly mixed so that the supply air temperature equals the air temperature inside the cooling coil.

A6. The energy consumed by the transfer of latent heat is negligible.

A7. The mixed air ratio of return air to outdoor air is proportional to the opening level of the outdoor air damper.

With these assumptions, the energy balance equations for the air side can be written as

$$\Delta T_c = (1 - D_{out})T_r + D_{out}T_{out} - T_{sa}, \tag{6.9}$$

$$P_c = \frac{\dot{m}C_a\Delta T_c}{\text{COP}}, \tag{6.10}$$

where $P_c$ is the power consumption related to the cooling energy consumed by the cooling coils, $\dot{m}$ is the flow rate of the air passing through the cooling coil, $\Delta T_c$ is the temperature change of the supply air after the heat exchange has occurred at the cooling coil, COP is the coefficient of performance of the chiller plant, for which we use a fixed value of 3, $D_{out}$ is the opening level of the outdoor air damper, and $T_r$ is the return air temperature. At water side, the following equations introduced in [2] are used:

$$Q_c = UA_w(T_b - T_{cws}) = \alpha f_{cw}^{\beta}(T_{sa} - T_{cws}), \tag{6.11}$$

where $T_b$ is the temperature of the cooling coil, $T_{cws}$ is the supply chilled water temperature, and $UA_w$ is the heat transfer coefficient of the chilled water. This coefficient can be rewritten as a function of the water flow rates $f_{cw}$, with two time-varying constants ($\alpha$ and $\beta$). Eq. (6.11) illustrates how the supply air temperature varies with respect to the change of supply chilled water temperature and the chilled water flow rate in the coil.

The fan power is expressed by a second order polynomial function:

$$P_f = C_o + C_1\dot{m} + C_2\dot{m}^2, \tag{6.12}$$

where $P_f$ is the energy consumed by the supply fan, with $C_o$ to $C_2$ being the parameters related to the fan power. For Eqs. (6.9)–(6.12), the return air temperature ($T_r$), supply air temperature ($T_{sa}$), supply chilled water temperature ($T_{cw}$), and outdoor air damper action ($D_{out}$) are obtained directly from the BMS measurement. Eq. (6.9) is used to estimate the energy consumed by the individual AHUs, while Eq. (6.11) is used to estimate the required chilled water flow rate to generate the required energy. Despite the fact that the models are simple in structure, they are sufficient to be used for making parallel comparisons between different control strategies when the system is operating within a small operational range.

### 6.2.3 Economizer Modelling

The economizer is an important energy saving function used in modern AHUs. When the zone temperature is lower than the return air temperature but higher than $12^o$C, the economizer will be enabled. The control logic of the economizer is illustrated in Fig. 6.3. In summary, the AHUs' operational modes can be divided into the following three different categories:

1. *Normal mode*. This mode uses 80% of return air as the supply air and 20% of outdoor air to meet the minimum ventilation requirement.

2. *Mixed mode*. This mode is activated when the outdoor air temperature is lower than the return air temperature. The outdoor air damper is 100% open but the AHU still runs mechanical cooling to meet the cooling load demand.

3. *Free cooling mode*. The set point temperature is maintained by a pure ventilation. This mode will only be activated when the cooling load and the ambient air temperature are both sufficiently low.

In order to model the economizer, the energy term in Eq. (7.1) is expressed as

$$Q_u = \dot{m}C_a(T_{sa,1} - T_1), \tag{6.13}$$

where $Q_u$ represents the overall cooling energy supplied to the room. This input will later be used as the new input for the MPC design. From Eqs. 6.9 and 6.10, it can be seen that the actual energy consumed by the cooling coil is not equal to $Q_u$ in Eq. (6.13), because when the economizer is activated, cool outside air will be used to contribute fully or partially to the cooling. Therefore, the energy term is rewritten as

$$Q_u = \underbrace{D_{out}\dot{m}C_a(T_{out} - T_r)}_{Q_f} + \underbrace{(1 - D_{out})\dot{m}C_a(T_{sa,1} - T_r)}_{Q_c}, \tag{6.14}$$

where $Q_c$ is the energy consumed by the cooling coil, and $Q_f$ is the supplied energy by free-cooling. Considering three different phases of the economy cycle control described above, Eq. (7.4) can be written with three time invariant linear models:

$$x(k+1) = \begin{cases} Ax(k) + BQ_u(k) + Ed(k) + e(k), & D_{out} = 20\% \quad T_{out} > T_r \\ Ax(k) + B[Q_c(k), Q_f(k)]^T + Ed(k) + e(k), & D_{out} = 1 \quad T_{min} < T_{out} < T_r \\ Ax(k) + BQ_f(k) + Ed(k) + e(k), & 20\% < D_{out} < 1 \quad T_{out} < T_{min} \end{cases} \tag{6.15}$$

where $T_{min}$ is the outdoor temperature threshold which enables free cooling to be performed. Its value can be identified empirically using historical data. For the normal mode, a minimum of outdoor air (20%) is used, and no free-cooling will be used. For the mixed mode, the energy supplied to the zone is a mixture of mechanical cooling and free-cooling. Under the mixed mode, the outdoor air damper is fully open ($D_{out} = 1$) to maximise the free cooling energy. Therefore, the energy consumed by the system is less than the supplied cooling energy. In the free-cooling mode, the outdoor air damper manipulates between 20% and 100% to ensure the temperature does not exceed the lower comfortable band. Under this mode, the energy consumed by the cooling system will be zero. By dividing the model into the above three forms, the complexity of solving an optimisation problem can be greatly reduced.

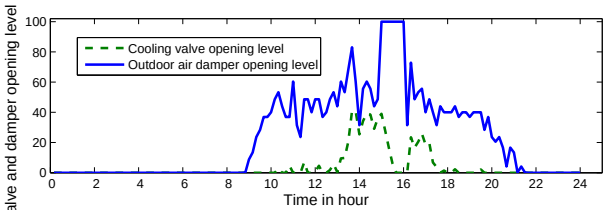


Figure 6.4: The relationship between outdoor air damper operation and cooling valve operation.

In the investigated system, it was found that the outdoor air damper was sometimes not properly settled during the mixed mode: the outdoor air damper is only half open when mechanical cooling is triggered. This has caused an ineffective use of the economizer. To solve the problem, we set a rule in the MPC to force the outdoor air damper to be fully open ($D_{out} = 1$) during the mixed mode. This modification greatly increases the efficiency of the AHUs through employing more free cooling. Another benefit of applying this strategy is that it simplifies the optimisation, because the outdoor air damper can be always operating at the optimal point using this rule. A simple experiment was conducted to illustrate the benefits. During the experimental day the outdoor temperature was low enough to perform free-fooling. Fig. 6.4 shows that from 1:00 pm to 3:00 pm, both cooling valve and outdoor air damper were partially open . After the outdoor damper was forced to be set to fully open, the cooling valve started to be guadually turned off from 3:00 pm to 4:00 pm. This simple experiment demonstrates the effective of this method in achieving energy saving.

The benefit of applying this method will be demonstrated in the discussion section.

## 6.3 Control Design

### 6.3.1 Feedback Linearisation

From Eqs. (6.9) and (6.12), it can be seen that the simplified models associated with both the thermal zone and the HVAC system contain bilinear terms, with the control states ($T_1$) multiplied by the control inputs ($\dot{m}$) and disturbance ($D_{out}$). Additionally, the cooling coil process at the local AHU is affected by both the chilled water temperature and the flow rate fluctuation within the main water loop. This effect is directly related to the working status of the chiller plant. Using these models to conduct optimisation results in a non-convex optimisation problem, which is very hard to solve. Inspired by the universal approximation ability of neural network model, this study uses a neural network based feedback-linearisation method to solve such a problem. The main idea is to cancel the system nonlinearity using a neural network through feedback, so that the problem can be converted from a nonlinear control problem to a linear one. The virtual input is transformed to the real input using a neural network compensator.

The structure of the control framework is shown in Fig. 6.5. Generally speaking, the design of the MPC consists of two steps: the controller design and the approximation of the nonlinear functions. Firstly, a virtual input $v$ is used to replace the original input $u$ by equating $v = \dot{m}C_a(T_{sa,1} - T_1)$. Eq. (6.6) can be written as

$$x(k+1) = Ax(k) + Bv(k) + Ed(k) + ke(k). \tag{6.16}$$

In the next sections, the design of the MPC using a linear programming based on the refined state space model Eq. (6.16) is presented first. Afterwards, the method of converting the linearised input $v$ into a real input $u$ using an inverse NN model is introduced.

### 6.3.2 MPC Design

The basic requirement of HVAC operation is to achieve thermal comfort during the occupied hours. The classic form of cost function for an MPC minimises the set point tracking error and varying rate of the actuator action. This form is useful in terms of providing better set point tracking with a small input varying rate, but is not suitable for supervisory control design. The ASHARE standard 55 [38] defines a comfortable temperature as a range of temperature values instead of a fixed one. Therefore, the cost function should allow the indoor temperature to fluctuate within a specified range during the occupied hour. In this study, the MPC is designed as a linear programming problem with time-varying constraints on thermal comfort and energy costs, which was used in [13, 28]. In particular, the cost function employed in this study should meet the following criteria:

1. It minimises the total energy consumption of an AHU, which includes the energy consumption of the cooling coil and supply fan.

2. The indoor temperature should meet the minimum thermal comfort requirement, which is formulated as a time-varying temperature constraint.

3. The indoor temperature should be maintained at the reference temperature, but can be allowed to deviate to a certain extend.

4. TOU electricity prices should be taken into consideration if the goal is to reduce utility costs. This also requires the peak energy use to be minimised.

Taking into account the above considerations, the following cost function is to be minimised:

$$\begin{aligned} J(k) = a \sum_{k=0}^{N-1} p_e |(v_{k+j|k}) + P_{f(k+j|k)}| + b \sum_{k=1}^{N} |\hat{y}_{k+j|k} - r_{k+j|k}| \\ + c \sum_{k=1}^{N} (|\underline{e}_{k+j|k}| + |\overline{e}_{k+j|k}|) + d \sum_{k=1}^{N} (max|v_{k+j|k}|), \end{aligned} \tag{6.17}$$

subject to:

$$\begin{aligned} x_{k+j+1|k} &= Ax_{k+j|k} + Bv_{k+j|k} + Ed_{k+j|k}, \quad \forall j = 0,...,N-1 \\ y_{k+j|k} &= Cx_{k+j|k}, \quad \forall j = 1,...,N \\ \underline{T}_{k+j|k} - \underline{e}_{k+j|k} \leq y_{k+j|k} &\leq \overline{T}_{k+j|k} + \overline{e}_{k+j|k}, \quad \forall j = 1,...,N \\ U_{k+j|k} \leq v_{k+j|k} &\leq 0, \quad \forall j = 0,...,N-1 \\ \underline{e}_{k+j|k} > 0, \overline{e}_{k+j|k} &> 0, \quad \forall j = 1,...,N \end{aligned} \tag{6.18}$$

where $N$ is the prediction horizon, $k+j|k$ denotes the predicted value of a certain variable at time step $k+j$ starting from time step $k$, $v$ is a vector of the control inputs within the prediction horizon, $\hat{y}_{k+j|k}$ is the predicted output at time $k$, which is obtained by iteratively solving Eq. (6.18) using the control input vector $v$, $P_f$ is the energy consumed by the supply fan, $d$ is the predicted disturbance, and $r$ is the reference temperature. $\underline{e}$ and $\overline{e}$ are the temperature violations from the lower and upper comfortable temperatures, respectively, and $\underline{T}$ and $\overline{T}$ are the lower and upper comfortable temperatures, respectively. $U$ denotes the maximum cooling energy that the system can supply, which is a negative value if a cooling system is considered. $p_e$ is the time-varying electricity price in dollars per kWh. The cost function in Eq. (6.17) minimises a weighted sum of the energy costs, the deviations from the set point temperature, and the deviations from the comfortable bands. These terms are penalised by the weighting coefficients $a$, $b$, $c$ and $d$, respectively. Some constraints should also be met:

1. $T_{oc} \in$ [ 21°C, 24°C] Thermal comfort during occupied hours.

2. $T_{uo} \in$ [ 19.5°C, 26°C] Thermal comfort during unoccupied hours.

3. $Q_u \in$ [ 0, 12Kw] Maximum cooling energy that can be supplied to each zone.

4. $D_{out} \in [20\%, 100\%]$ Outdoor damper should meet the minimum amount of supply air requirement.

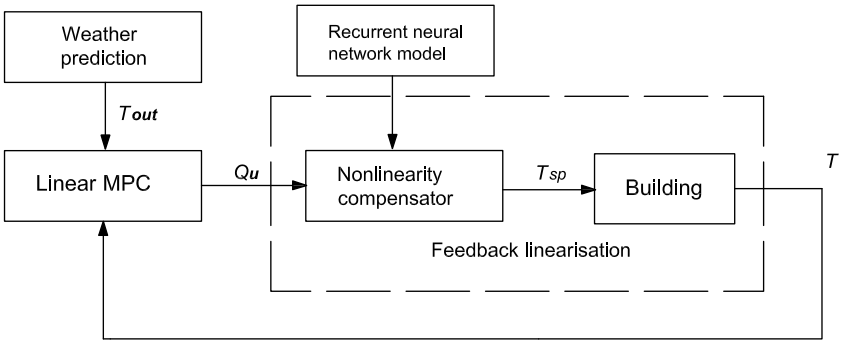


Figure 6.5: Hybrid MPC control scheme based on RNN.

As the time step progresses, the time-varying constraints on thermal comfort shift forward. Meeting the constraints guarantees a smooth transition from an occupied hour to an unoccupied hour, without violating the comfort requirement. The constraint for the refined control inputs $Q_u$ is nonlinear in principle, as it is bilinear and affected by the cooling capacity of the AHUs. This constraint is also time-varying, because it is influenced by the chilled water temperature at the main water loop. For simplicity, this constraint is calculated by Eq. (6.9) using the historical data of the supply air temperature, zone temperature, and outdoor air damper opening level. This enforces that the energy generated by the mechanical cooling should not exceed the maximum energy that the cooling coil can generate. Also, the free cooling energy supplied by ventilation is constrained by the outdoor air temperature. The requirement of a minimum percentage of outdoor air during occupied hours should also be met, to ensure good ventilation.

The linear programming optimisation problem is solved using Yalmip [39], which generates an optimised input variable trajectory. The first control signal $v_{1|k}$ is applied to the building, and the rest are disposed of. When a new time interval starts, the optimisation problem is repeated again with the updated initial condition $x_{k+1}$ and shifted constraints.

### 6.3.3 Inverse Neural Network Modelling

In the aforementioned optimisation problem, the optimised input is the supply energy $Q_u$. However, the real inputs to be optimised are the cooling valve operation and outdoor air damper. To obtain the actual input signal, this section employs an inverse NN model to establish the connection between the virtual input and the actual input. In this study, both a forward neural network model and an inverse model are used in the feedback loop. The forward neural network model is used during the simulation process to provide feedback to the MPC. The inverse model serves as a nonlinear compensator, which supplies the appropriate control action, $u$, to drive the system towards its desired states.

When ANN is used for control purposes, its output is the controllable input to the building. For this consideration, an inverse ANN model representing the inverse of the system dynamics is used [40]. In an inverse ANN, the network is fed with the required future output ($v$) together with the past inputs and the past output variables, with the aim of predicting the current input. The inverse NN model has the following form:

$$u(k) = f[y_r(k+1), y(k), ..., y(k-n_a+1), u(k-1), ..., u(k-n_b+1)], \tag{6.19}$$

where $y_r$ denotes the desired output, which in this case is the optimal input $v$ calculated by solving the linear programming problem.

The training was performed for both the forward and inverse models using the same training data. For the inverse NN model, the inputs to the network are the past and present values of the chilled water temperature, return air temperature, outdoor temperature, air mass flow rate, and the desired output $Q_u$. The output of the neural network model is the opening level of the chilled water valve. The delay time $n_k$ is set to be 0, as the time lag from input to output is shorter than the sampling time of the system (10 minutes). Among the selected training data, 70 per cent is used for training; 15 per cent for the validation set and 15 per cent for the test set. The data are scaled between -1 and 1 using Eq. (4.12). The orders of the inputs and the number of neurons are determined through a trial

and error method. The models which generate the best validation results are maintained. Mathematically, the following models are derived:

The forward neural network model has the following form:

$$\hat{y}(k) = f[T_1(k-1), T_1(k-2), T_1(k-3), T_{out}(k-1), T_{out}(k-2), V_{cw}(k-1), D_{out}(k-1), T_{cws}(k-1)], \tag{6.20}$$

The inverse neural network model has the following form:

$$\hat{u}(k) = f[v(k+1), T_r(k), T_{out}(k-1), T_{out}(k-2), u(k-1), T_{cws}(k)]. \tag{6.21}$$

The simulation results of applying the ANN for temperature prediction are illustrated in Fig. 7.6(a). It can be seen that the forward ANN model has a fitness of 85%, which is better than the previously illustrated RC model. This is because when the system is modelled as a linear RC model, the unmeasured disturbances are assumed to be Gaussian distributed, while in neural network modelling, the uncertainties are directly modelled through learning from the historical data. Fig. 7.6(b) depicts the one-step ahead prediction results from using the inverse model. It can be seen that the desired control input can be predicted accurately. Still, some offsets from the idealised control input can be seen. These errors occurred also due to the presence of the uncertainties within the building system, and are impossible to eliminate completely. Fig. 6.7 illustrates the inverse mappling from energy $Q_u$ to setpoint $T_{sp}$.

## 6.4 Results and Discussions

### 6.4.1 Simulation Setup

Before incorporating the hybrid MPC strategy in an on-line experiments, it was tested under the simulation environment. The objective of the simulation study was to examine the closed-loop performance of the MPC and investigate its stability with regards to

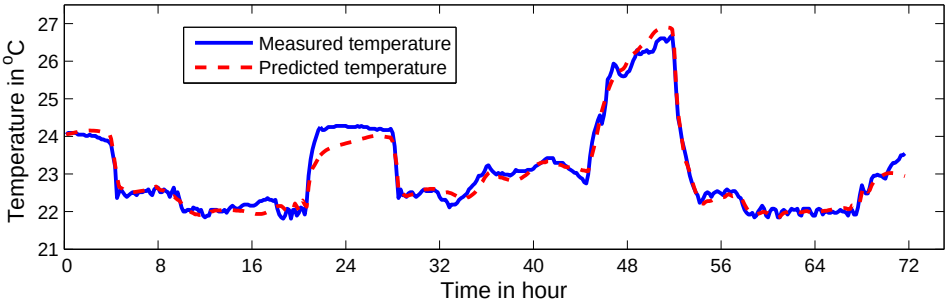


(a)

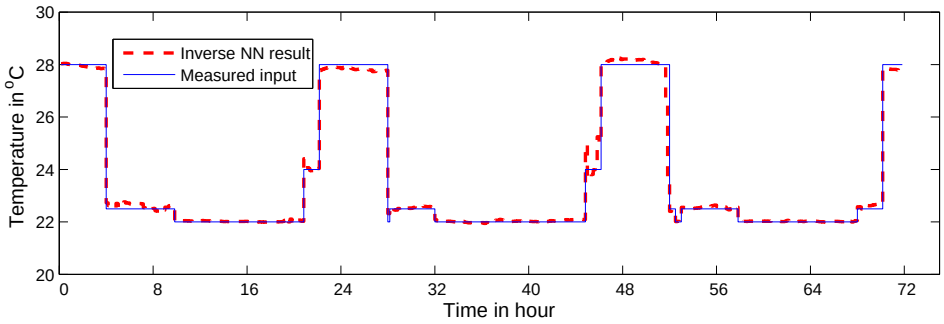


(b)

Figure 6.6: (a): Simulation results of the forward NN model (model fit=0.85), (b) one-step ahead prediction results of the inverse NN model.

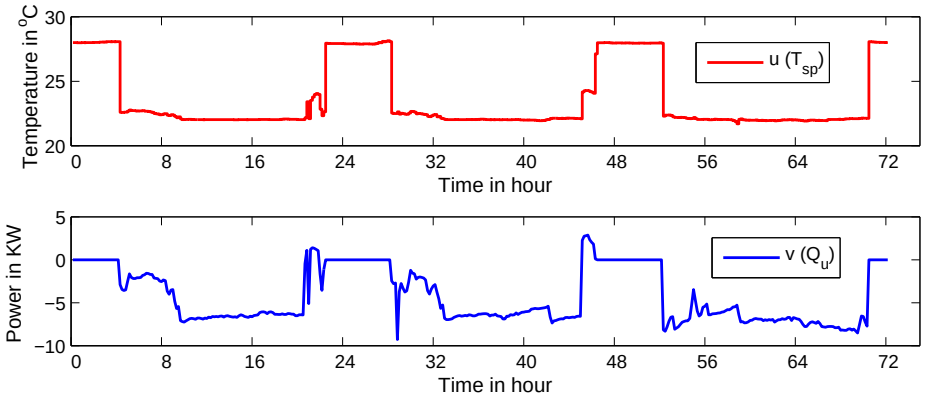


Figure 6.7: Mapping from power input $Q_u$ to actual setpoint $T_{sp}$

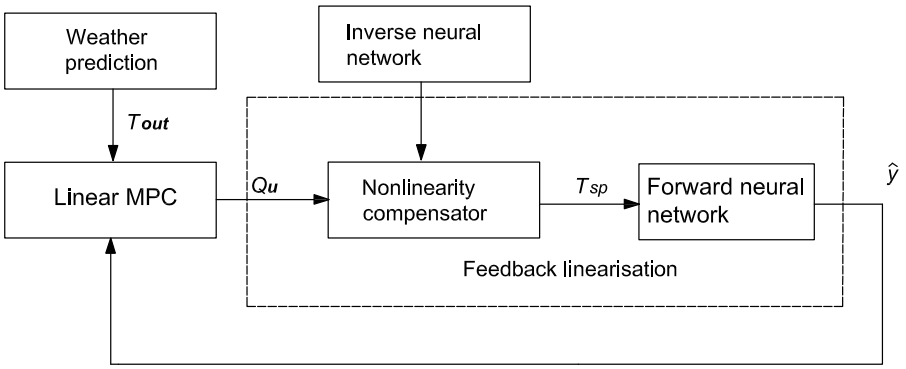


Figure 6.8: Test platform for model predictive control using the forward neural network model.

plant/model mismatch. Usually, when MPC is applied online, the system outputs are measured by the sensors and then fed back to the controller. For simulation purposes, the reference model (which is used to approximate the real building) should be different from the control model, otherwise a model mismatch would result in errors during the simulation. A commonly applied approach is to replace the real building by a detailed physical model [21] to provide system feedback. In this study, the forward neural network model developed previously is used to achieve the same purpose, as shown in Fig. 6.8. The forward neural network works as an observer to provide the feedback to the controller. The benefits of conducting a simulation in such a way is that the model output is very similar to the real output, so that it will not be disturbed by the errors generated by the linear models. This allows the MPC to be tested before it is applied to the real building.

The selected zone for simulation purpose is zone 1 located at the east end of the building. A detailed description of this zone is given in Section 2. The reason for choosing this area is that the space is only adjacent to one neighbouring zone, thus is less affected by thermal interactions. The occupancy hours are set according to the existing flight schedule, which are from 5:00 am to 9:30 pm. The default schedule of AHUs are from 4:00 am to 9:00 pm. The building uses two electricity rates, which are shown in Table

Table 6.2: Electricity rate of a T-1 building

| | Time of day | Energy charge ($/kWh) |
|---|---|---|
| Peak | 7:00 am–9:00 pm | 0.090 $/kWh |
| Off-peak | All other | 0.024 $/kWh |

6.2. The weighting coefficients of the cost function were found empirically as $a = 5$, $b = 1$, $c = 1.5$, and $d = 1.5$. The prediction horizonwas set to be six hours (36 steps). The historical BMS data from the 24th to 25th January, 2013 was chosen for comparison purposes. The outdoor temperature is the forecast temperature provided by the Bureau of Meteorology of Australia.1 In particular, we compare the following two MPC schemes with the baseline control method.

1. Optimal start-stop MPC considers time-varying constraints based on real-time schedule.

2. Pre-cooling MPC (PMPC) considers time-varying constraints and TOU electricity prices.

### 6.4.2 Simulation Results

In the first simulation, the performance of the optimal start-stop MPC was evaluated on 24th January, 2013. To better illustrate the method, a real-time flight schedule is added into the existing schedule: besides the normal operational schedule, 10:00 am to 12:00 pm is also set to be unoccupied as there were no passengers checking in at the investigated area during the time. This is to show the special suitability of this strategy for intermittently occupied buildings, such as an airport terminal building. Fig. 6.9(a) shows the control results of using the optimal start-stop MPC. It illustrates that when the MPC is applied, the zone temperature can be kept within the comfortable bound only during the occupied hours. Fig. 6.9(b) indicates the set point trajectory computed by MPC. Fig.

6.9(c) compares the power consumption when the baseline control and MPC are used. In the morning, the MPC turns on the AHUs later than the default setting, so that the temperature reaches the upper comfortable temperature at the start of occupancy. Similarly, before the end of the occupancy hours, MPC turns off the AHUs earlier, to maintain a comfortable temperature before the end of occupancy. Whenever the building is unoccupied during the day (according to the schedule), the cooling supply of AHUs will also be turned off to save energy. The AHU stops supplying cooling energy between 6:00 am and 12:00 pm. It is shown that this simple optimal start-stop MPC achieves up to 41% of the energy savings compared to the baseline control method.

In the second simulation, a pre-cooling test is conducted on 25th January, 2013. Fig. 6.10(e) shows that, on the investigated day, there is a big difference in temperature between morning and daytime This day belongs to a category of weather pattern when a pre-cooling can achieve a satisfactory result. Fig. 6.10(a) shows that the initial zone temperature during the simulation day was not high (24°C). As a consequence, the baseline control waited until the zone temperature started to increase to run the AHU. On the other hand, the PMPC precools the temperature to $21^{o}$C after the AHU was turned on. This operation was taken because the MPC takes advantage of cheap off-peak electricity prices to precool the building's thermal mass and to store cooling energy. Fig. 6.10(b) shows that the pre-cooling process ended before the peak hour started (7:00 am). After 7:00 am, the AHUs were turned off and the stored cooling energy started to release, so that very little cooling energy was needed to compensate for the increasing heat gains during the daytime. It can also be seen that the MPC reduces the power during the peak period by applying a higher set point value, while still maintaining the temperature within the comfort band. The temperature increases slowly until it reaches the upper comfort band (24°C) at the end of occupancy. Fig. 6.10(c) shows that the process of cooling down the zone temperature from 24°C to 21°C does not require the cooling valve to be fully open. This is because the outdoor door air damper was forced to open 100% under the opera-

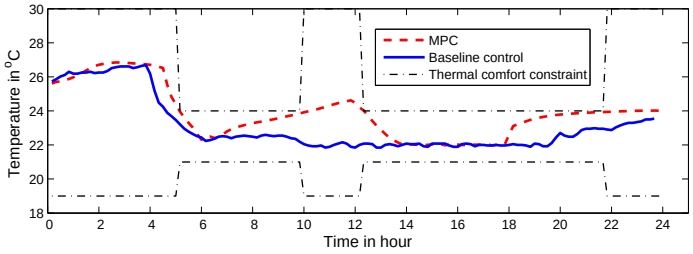


(a) Zone temperature

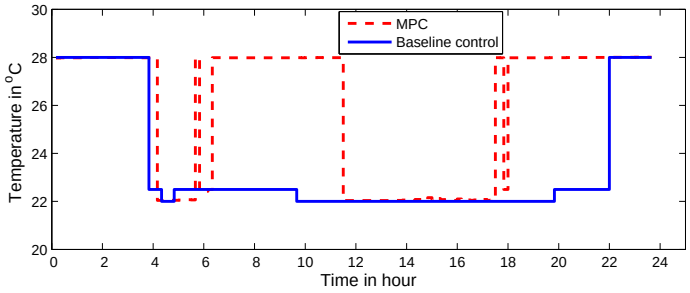


(b) Setpoint trajectory

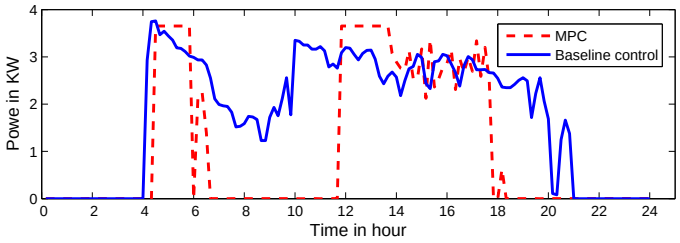


(c) Energy consumption

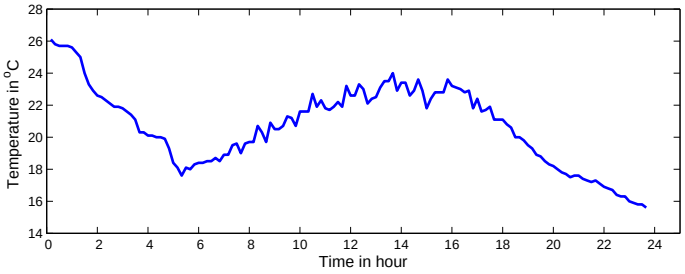


(d) Outdoor temperature

Figure 6.9: Comparison results between baseline control and optimal start-stop MPC.

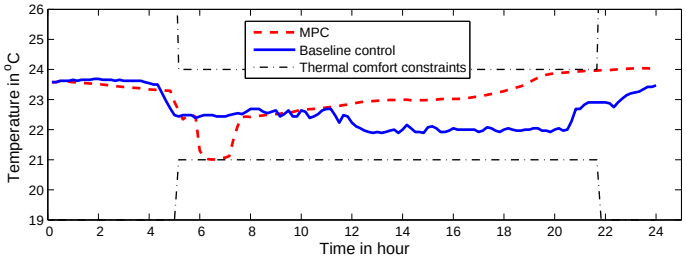


(a) Zone temperature

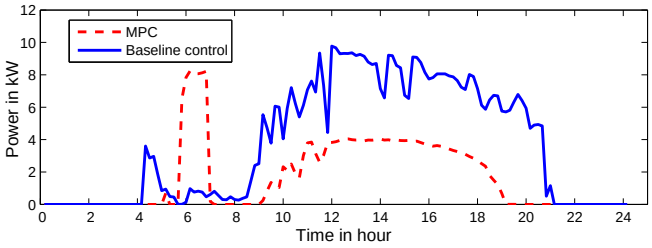


(b) Cooling energy consumption

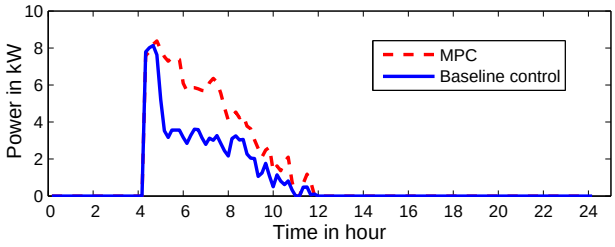


(c) Free cooling energy

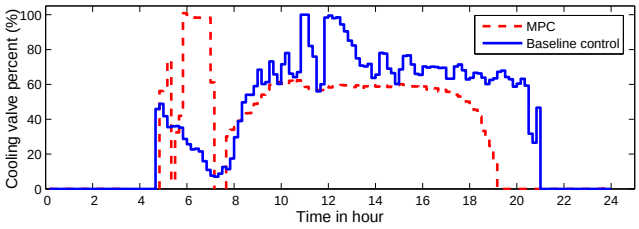


(d) Free cooling energy

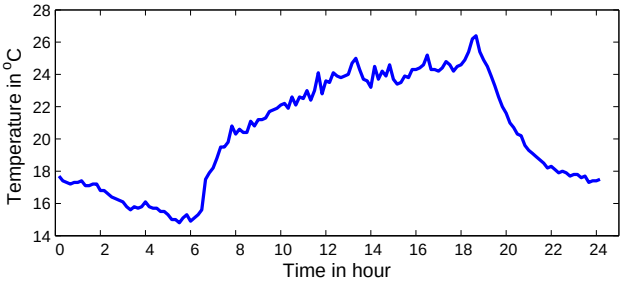


(e) Outdoor air temperature

Figure 6.10: Comparison results between baseline control and PMPC.

tion of the MPC, while with the default setting, the outdoor air damper was only partially open. MPC increases the energy efficiency by employing more cool cooling energy, as illustrated in Fig. 6.10(d).

### 6.4.3 Experiment Results

After simulation, the optimal setting of model parameters and optimisation configurations were determined. The proposed MPC control method was tested at the same area as for the simulation. The experiment was conducted with the following steps:

1. Download the updated building data from the BMS one day ahead of the experiment.

2. Download one-day-ahead weather forecast information from the Australian Bureau of Meteorology.

3. Build both a linear model and a neural network model using the newest building data. Use the aforementioned simulation methods to obtain the optimal control parameters.

4. Calculate the optimal trajectory for the cooling valve operation, and the corresponding zone temperature set point trajectory, for the next day.

5. Send the new set point trajectory to the BMS. Obtain the experimental data and repeat step 1.

The real-time experiment was executed over a period of three successive days: from the 23rd January to the 25th January, 2014. The comfort requirements were set to be the same as during the simulation. Fig. 6.11(a) shows the temperature profile on the investigated days. It can be seen that the AHUs started to pre-cool the space from early morning by setting a low set point value. After 7:00 am, the set point temperature was relaxed to

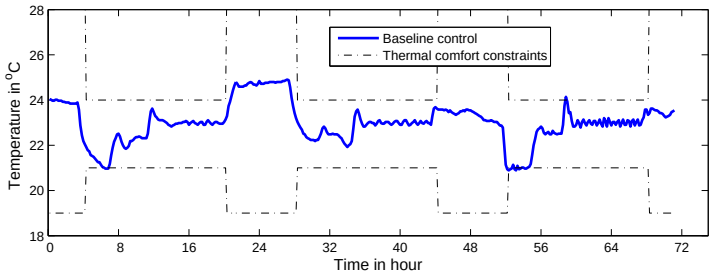


(a) Zone temperature

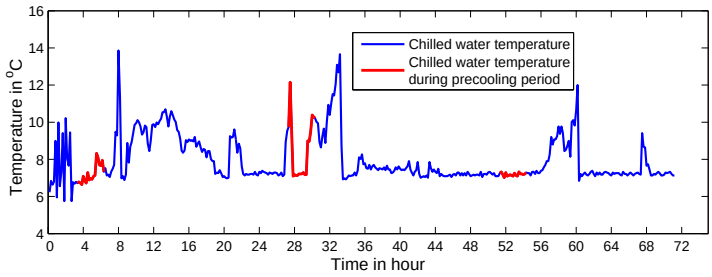


(b) Chilled water temperature

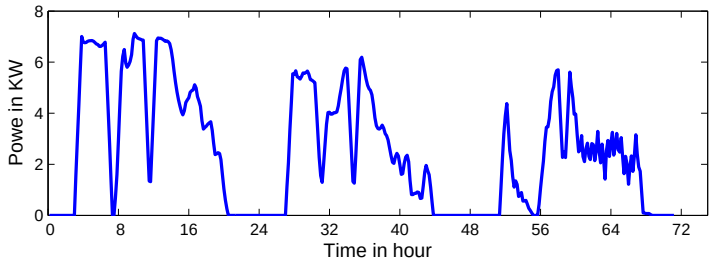


(c) Cooling power consumption

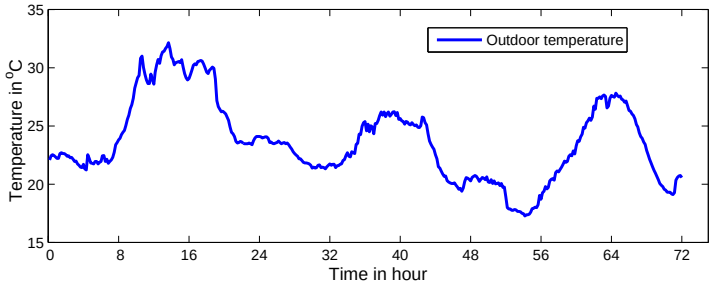


(d) Outdoor temperature

Figure 6.11: Experimental results from 23rd January, 2013 to 25th, January, 2013.

higher values. On day 1 and day 3 the PMPC shifted the cooling load from the peak hour to the off-peak hour. Unexpectedly, the pre-cooling was not able to cool down the temperature to the desired value on day 2, even with a fully opened cooling valve. The reason is that during the pre-cooling process, the instant supply chilled water temperature was not low enough to provide the required cooling demand. The comparison of the chilled water temperature during pre-cooling is highlighted with red in Fig. 6.11(b). Making a comparison between the experimental results with the baseline results over the three successive days is difficult. Therefore, this study employs a comparison method introduced in [41]. This method uses the ratio of peak-hour energy use to overall daily energy use to address the merit of the pre-cooling method. Fig. 6.13 compares the daily percentage of peak hour energy consumption during the normal days with the experimental days. It can be seen that almost all the energy was consumed during peak hours during normal days. After the MPC was applied, the percentages of energy use during peak hours were reduced, compared to those of the normal days.

To better compare the performance of the MPC with the baseline control method, we chose 10th January, 2014 as the reference day. On this day, the outdoor temperature, initial zone temperature, and occupancy level were similar to day 1. For a fair comparison, we only compare the energy use between 3:00 am and 6:00 pm, as there is a big difference in outdoor temperature starting from 6:00 pm; this is shown in Fig. 6.12(c). Fig. 6.12(a) compares the zone temperature trajectory between the baseline control and the predictive control. It is observed that the baseline control simply maintained the temperature at the fixed setpoint, while MPC performed an intensive pre-cooling to bring down the temperature to the lower bound of 21°C before the start of peak hour. As the ambient temperature was not as low as during the simulation, the benefit of applying free cooling was relatively small. However, the cheap off-peak electricity price allows the pre-cooling process to be performed at a very low cost.

When the peak hour started, as the sun irradiated the space and people entered the

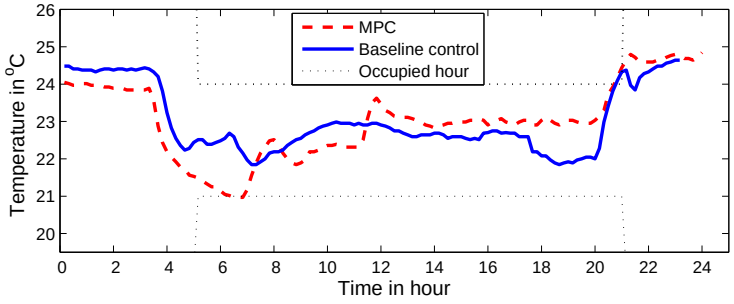


(a) Zone temperature

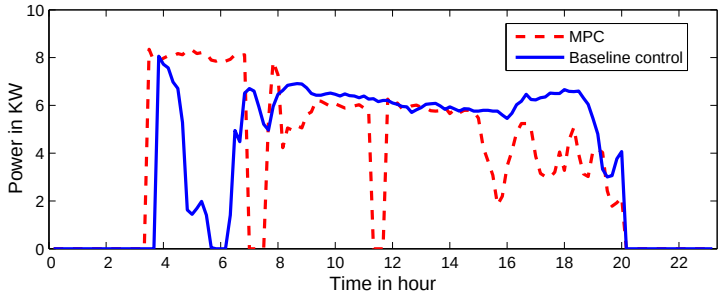


(b) Power consumption

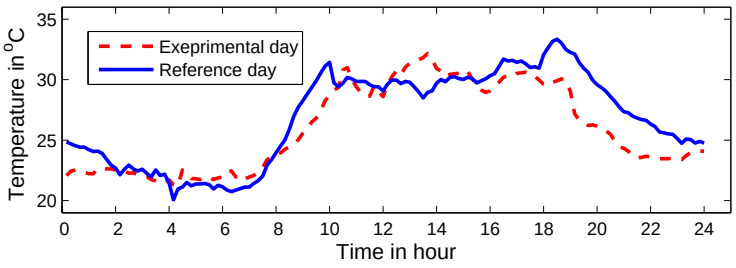


(c) Outdoor air temperature

Figure 6.12: Control performance comparison between two homogeneous days.

Table 6.3: Comparison of performance between baseline control and PMPC from 3:00 am to 6:00 pm

| Controller | Total energy input (kWh) | Off-peak energy input (kWh) | Utility costs (in $) | Cost savings (%) |
|---|---|---|---|---|
| Baseline control(10th Jan.) | 423 | 50.5 | 12.3 | 0 |
| MPC(23rd Jan.) | 447 | 137.1 | 10.7 | 13% |

building, the heat gains of the zone started to increase. Under the operation of the baseline control, the cooling valve opened more widely to compensate for the increasing heat gains. On the other hand, the MPC delayed supplying the cooling energy, by closing down the cooling valve. This is because the cooling energy stored in the thermal mass was being released, which reduced the cooling load during the peak hours. Fig. 6.12 (b) depicts the cooling energy consumed by the AHUs. It can be seen that the MPC has partially shifted the cooling load from an on-peak hours to off-peak hours, at the cost of consuming more off-peak energy (three times that of the reference day). Before the end of the occupancy hour, both the MPC and baseline control closed the cooling valve in advance. By calculation, it is estimated that 13% of cost savings were achieved compared with the baseline control, when the MPC was used during the comparison period (see Table 6.3).

The experimental result matches the simulation result well. However, both the RC thermal network model and the ANN model were trained using historical data when the system was operating under baseline control. The data may not contain enough information that a pre-cooling control requires, which may result in prediction errors. Excitation of the system is needed in order to collect more informative data to improve the quality of the model. In addition, the precooling strategy should be treated carefully because the

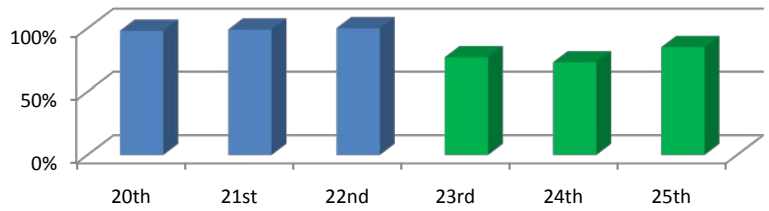


Figure 6.13: Percentage of peak hour energy consumption to overall daily energy consumption. Green: Experimental days, Blue: Baseline days.

process of cooling the thermal resistance may result in extra energy cost. An inaccurate prediction of the indoor temperature may result in wasteful energy consumption.

## 6.5 Conclusion

This study proposes a new type of MPC scheme based on neural network feedback linearisation to achieve energy-savings for a commercial building. In the proposed control framework, the thermal dynamics of the building are modelled by a linearised RC model, while the uncertainties associated with the HVAC process are handled separately by an inverse neural network model. These two models are coupled using a feedback linearisation method. Treating the main characteristics of the building's thermal dynamics as linear, we model it using a simplified RC model and then transformed it into a state-space model. The validation of the model using the field data shows that such a model is able to capture the main characteristics of the building, as the building dynamics has a mild nonlinearity. It is also shown, through simulation and experiment, that satisfying control results can be achieved when applying the proposed method, even though the RC model does not match perfectly the actual building. The results were analysed from both the energy saving and cost saving points of views. To achieve this purpose, two types of MPC schemes are investigated: an optimal start-stop MPC which only optimises the energy use, and a pre-cooling MPC which optimises utility costs. By conducting exper-

iments and simulations, it is shown that when TOU electricity pricewas not considered, the MPC starts the AHU later and stops the AHU earlier to avoid over-cooling, due to the use of time-varying constraints on the thermal comfort. The energy savings become more promising when a detailed occupancy pattern, e.g., the flight schedule within a day, is available. However, when the morning temperature is low, the potential for achieving energy savings by optimal start becomes not very obvious. On the other hand, when the TOU electricity price was taken into consideration, the utility costs can be reduced using the PMPC, despite more off-peak energy being required. The savings come from the use of cheap off-peak electricity, more free cooling, and reduced on-peak electricity demand. The pre-cooling is able to achieve a more significant amount of savings when the ambient temperature is low enough. Additionally, we have also developed a simple strategy, incorporated into the existing MPC, which increases the efficiency of the economizer.

It is found that the performance of the local AHUs is also related to the performance of the chiller plant. For example, during the experiment, the required cooling demand could not always be met. This is because when the instant cooling load of the entire building system is high, a new chiller needs to be run. This causes a change in the input constraints, thereby affecting the performance of the MPC. Therefore, how to handle the input constraints in a more effective way should be investigated in the future. It is also found that the energy storage capability of the building is not very strong, as compared to the ones in the existing literature. The main reason is that the investigated zones have a large window area, unfurnished and wide open areas, making them lightweighted. It is expected that a more significant amount of savings can be achieved if a heavy weight building is treated. Future research will be focusing on the use of the proposed control strategy for building sectors with a sufficient thermal mass. Additionally, how to make the model adaptive to changes in the environment will be another area of research interest. This should be able to improve the robustness of the proposed control method.

# References

[1] L. Pérez-Lombard, J. Ortiz, and C. Pout, "A review on buildings energy consumption information," *Energy and Buildings*, vol. 40, no. 3, pp. 394–398, 2008.

[2] S. Wang and X. Jin, "Model-based optimal control of VAV air-conditioning system using genetic algorithm," *Building and Environment*, vol. 35, no. 6, pp. 471 – 487, 2000.

[3] J. Široký, F. Oldewurtel, J. Cigler, and S. Prívara, "Experimental analysis of model predictive control for an energy efficient building heating system," *Applied Energy*, vol. 88, no. 9, pp. 3079 – 3087, 2011.

[4] Y. Ma, F. Borrelli, B. Hencey, B. Coffey, S. Bengea, and P. Haves, "Model predictive control for the operation of building cooling systems," *Control Systems Technology, IEEE Transactions on*, vol. 20, no. 3, pp. 796 –803, may 2012.

[5] S. Prívara, J. Široký, L. Ferkl, and J. Cigler, "Model predictive control of a building heating system: The first experience," *Energy and Buildings*, vol. 43, no. 23, pp. 564 – 572, 2011.

[6] P. Ferreira, A. Ruano, S. Silva, and E. Conceiçâo, "Neural networks based predictive control for thermal comfort and energy savings in public buildings," *Energy and Buildings*, vol. 55, no. 0, pp. 238 – 251, 2012.

[7] F. Oldewurtel, A. Parisio, C. N. Jones, D. Gyalistras, M. Gwerder, V. Stauch, B. Lehmann, and M. Morari, "Use of model predictive control and weather forecasts for energy efficient building climate control," *Energy and Buildings*, vol. 45, no. 0, pp. 15 – 27, 2012.

[8] A. Afram and F. Janabi-Sharifi, "Theory and applications of HVAC control systems

a review of model predictive control (MPC)," *Building and Environment*, vol. 72, no. 0, pp. 343 – 355, 2014.

[9] A. Garnier, J. Eynard, M. Caussanel, and S. Grieu, "Low computational cost technique for predictive management of thermal comfort in non-residential buildings," *Journal of Process Control*, vol. 24, no. 6, pp. 750 – 762, 2014.

[10] G. P. Henze, D. E. Kalz, S. Liu, and C. Felsmann, "Experimental analysis of model-based predictive optimal control for active and passive building thermal storage inventory," *HVAC R Research*, vol. 11, no. 2, pp. 189–213, 2005.

[11] J. Seem and J. House, "Development and evaluation of optimization-based air economizer strategies," *Applied Energy*, vol. 87, no. 3, pp. 910 – 924, 2010.

[12] K. Lee and J. E. Braun, "Model-based demand-limiting control of building thermal mass," *Building and Environment*, vol. 43, no. 10, pp. 1633 – 1646, 2008.

[13] Y. Ma, G. Anderson, and F. Borrelli, "A distributed predictive control approach to building temperature regulation," in *American Control Conference (ACC), 2011*, 2011, pp. 2089–2094.

[14] I. Hazyuk, C. Ghiaus, and D. Penhouet, "Optimal temperature control of intermittently heated buildings using model predictive control: Part 1 building modeling," *Building and Environment*, vol. 51, no. 0, pp. 379 – 387, 2012.

[15] J. E. Braun, "Reducing energy costs and peak electrical demand through optimal control of building thermal mass," *ASHRAE Transactions*, pp. 264–273, 1990.

[16] C. D. Corbin, G. P. Henze, and P. May-Ostendorp, "A model predictive control optimization environment for real-time commercial building application," *Journal of Building Performance Simulation*, vol. 6, no. 3, pp. 159–174, 2013.

[17] Y. Ma, A. Kelman, A. Daly, and F. Borrelli, "Predictive control for energy efficient buildings with thermal storage: Modeling, stimulation, and experiments," *Control Systems, IEEE*, vol. 32, no. 1, pp. 44–64, Feb 2012.

[18] P. May-Ostendorp, G. P. Henze, C. D. Corbin, B. Rajagopalan, and C. Felsmann, "Model-predictive control of mixed-mode buildings with rule extraction," *Building and Environment*, vol. 46, no. 2, pp. 428 – 437, 2011.

[19] J. E. Braun and N. Chaturvedi, "An inverse gray-box model for transient building load prediction," *HVAC Research*, vol. 8, no. 1, pp. 73–99, 2002.

[20] M. Sourbron, C. Verhelst, and L. Helsen, "Building models for model predictive control of office buildings with concrete core activation," *Journal of Building Performance Simulation*, vol. 6, no. 3, pp. 175–198, 2013.

[21] S. Prívara, J. Cigler, Z. Váňa, F. Oldewurtel, C. Sagerschnig, and k. . Eva Žáčeková, "Building modeling as a crucial part for building predictive control," *Energy and Buildings*, vol. 56, no. 0, pp. 8 – 22, 2013.

[22] M. Avci, M. Erkoc, A. Rahmani, and S. Asfour, "Model predictive HVAC load control in buildings using real-time electricity pricing," *Energy and Buildings*, vol. 60, no. 0, pp. 199 – 209, 2013.

[23] N. Morel, M. Bauer, M. El-Khoury, and J. Krauss, "Neurobat, a Predictive and Adaptive Heating Control System Using Artificial Neural Networks," *Solar Energy Journal*, vol. 21, pp. 161–201, 2001.

[24] A. Ruano, E. Crispim, E. ConceiA, and M. LAcio, "Prediction of building's temperature using neural networks models," *Energy and Buildings*, vol. 38, no. 6, pp. 682 – 694, 2006.

[25] M. Jimnez, H. Madsen, and K. Andersen, "Identification of the main thermal characteristics of building components using MATLAB," *Building and Environment*, vol. 43, no. 2, pp. 170 – 180, 2008.

[26] S. Bengea, V. Adetola, K. Kang, M. J. Liba, D. Vrabie, R. Bitmead, and S. Narayanan, "Parameter estimation of a building system model and impact of estimation error on closed-loop performance," in *Decision and Control and European Control Conference (CDC-ECC), 2011 50th IEEE Conference on*, 2011, pp. 5137–5143.

[27] I. Hazyuk, C. Ghiaus, and D. Penhouet, "Optimal temperature control of intermittently heated buildings using model predictive control: Part II- control algorithm," *Building and Environment*, vol. 51, no. 0, pp. 388 – 394, 2012.

[28] M. Maasoumy, M. Razmara, M. Shahbakhti, and A. S. Vincentelli, "Handling model uncertainty in model predictive control for energy efficient buildings," *Energy and Buildings*, vol. 77, no. 0, pp. 377 – 392, 2014.

[29] Y. Ma, J. Matusko, and F. Borrelli, "Stochastic model predictive control for building hvac systems: Complexity and conservatism," *Control Systems Technology, IEEE Transactions on*, vol. PP, no. 99, 2014.

[30] P.-D. Moroan, R. Bourdais, D. Dumur, and J. Buisson, "Building temperature regulation using a distributed model predictive control," *Energy and Buildings*, vol. 42, no. 9, pp. 1445 – 1452, 2010.

[31] T. Lu and M. Viljanen, "Prediction of indoor temperature and relative humidity using neural network models: model comparison," *Neural Computing and Applications*, vol. 18, no. 4, pp. 345–357, 2009.

[32] G. Mustafaraj, G. Lowry, and J. Chen, "Prediction of room temperature and relative

humidity by autoregressive linear and nonlinear neural network models for an open office," *Energy and Buildings*, vol. 43, no. 6, pp. 1452 – 1460, 2011.

[33] H. C. Spindler and L. K. Norford, "Naturally ventilated and mixed-mode buildingspart 2: Optimal control," *Building and Environment*, vol. 44, no. 4, pp. 750 – 761, 2009.

[34] M. A. Botto, T. J. J. Van Den Boom, A. Krijgsman, and J. S. Da Costa, "Predictive control based on neural network models with I/O feedback linearization," *International Journal of Control*, vol. 72, no. 17, pp. 1538–1554, 1999.

[35] S. Goyal and P. Barooah, "A method for model-reduction of nonlinear building thermal dynamics," in *American Control Conference (ACC), 2011*, June 2011, pp. 2077–2082.

[36] L. Ljung, Ed., *System Identification (2Nd Ed.): Theory for the User*. Upper Saddle River, NJ, USA: Prentice Hall PTR, 1999.

[37] S. H. Kim, "Building demand-side control using thermal energy storage under uncertainty: An adaptive multiple model-based predictive control (MMPC) approach," *Building and Environment*, vol. 67, no. 0, pp. 111 – 128, 2013.

[38] ASHRAE, *Thermal Environmental Conditions for Human Occupancy.* American Society of Heating, Refrigerating, and Air-Conditioning Engineers, 2013.

[39] J. Löfberg, "Yalmip : A toolbox for modeling and optimization in MATLAB," in *Proceedings of the CACSD Conference*, 2004.

[40] K. Hunt, D. Sbarbaro, R. bikowski, and P. Gawthrop, "Neural networks for control systemsa survey," *Automatica*, vol. 28, no. 6, pp. 1083 – 1112, 1992.

[41] J. Ma, S. J. Qin, and T. Salsbury, "Application of economic MPC to the energy and demand minimization of a commercial building," *Journal of Process Control*, vol. 24, no. 8, pp. 1282 – 1291, 2014, economic nonlinear model predictive control.

# Chapter 7

# Robust MPC with Adaptive Bound Estimator

This chapter is based on the following paper:

*Full citation*: Huang H., Chen L., Hu E., "Reducing energy consumption for buildings under system uncertainty through robust MPC with adaptive bound estimator", *Submitted to Building and Environment*, 2015.

*Contribution of this chapter*: This paper presents a robust MPC with a new type of adaptive bound estimator for building temperature regulation. The estimator learns the uncertainty distribution from the historical data to provide a more tightened uncertainty bound for the RMPC. By performing intensive simulations, the advantages of the proposed RMPC over the conventional one for the investigated building are demonstrated.

# Statement of Authorship

| | |
|---|---|
| Title of Paper | Reducing energy consumption in buildings with system uncertainty through robust MPC with adaptive bound estimator |
| Publication Status | ☐ Published ☐ Accepted for Publication<br>☑ Submitted for Publication ☐ Unpublished and Unsubmitted w ork w ritten in manuscript style |
| Publication Details | Huang H., Chen L., and Hu E., (2015), Reducing energy consumption in buildings with system uncertainty through robust MPC with adaptive bound estimator, submitted to Building and Environment. |

## Principal Author

| | |
|---|---|
| Name of Principal Author (Candidate) | Hao Huang |
| Contribution to the Paper | Developed model and control system, analysed data and wrote the manuscript. |
| Overall percentage (%) | 60% |
| Certification: | This paper reports on original research I conducted during the period of my Higher Degree by Research candidature and is not subject to any obligations or contractual agreements with a third party that would constrain its inclusion in this thesis. I am the primary author of this paper. |
| Signature | Date 15/10/15 |

## Co-Author Contributions

By signing the Statement of Authorship, each author certifies that:

i. the candidate's stated contribution to the publication is accurate (as detailed above);
ii. permission is granted for the candidate in include the publication in the thesis; and
iii. the sum of all co-author contributions is equal to 100% less the candidate's stated contribution.

| | |
|---|---|
| Name of Co-Author | Lei Chen |
| Contribution to the Paper | Supervised research, reviewed manuscript. |
| Signature | Date 15/10/15 |

| | |
|---|---|
| Name of Co-Author | Eric Hu |
| Contribution to the Paper | Supervised research, reviewed manuscript. |
| Signature | Date 15/10/15 |

**Abstract**

The use of model predictive control (MPC) for building-energy management system has been widely discussed in the literature. Since physical buildings are influenced by a number of uncertainties, the models cannot always perform indoor temperature prediction precisely. This may cause both thermal comfort violation and energy waste. Robust MPC (RMPC), which requires knowledge of the bounds on the system uncertainty, has been applied to enhance the stability of the MPC. However, the RMPC presented in the previous studies usually assume that the uncertainty bounds are fixed and known *a priori*. This makes the RMPC not suitable for dealing with real-world buildings, which are affected by time-varying and non-Gaussian distributed uncertainty. This paper presents a novel adaptive RMPC scheme for temperature regulation in commercial buildings. The novelty comes from the development of an adaptive uncertainty bound estimator for the RMPC. The estimator depends on a recursive neural network model built using the historical measurement. The proposed RMPC method is tested on a simulation model developed from building data collected from a light-weighted commercial building. By conducting simulation using different MPCs, it is found that the proposed RMPC method is able to behaviour robustly against uncertainty with the least performance loss. This means the maximum energy saving and the least thermal comfort violation.

## 7.1 Introduction

A considerable building-energy savings can be achieved by incorporating supervisory control at the HVAC systems. The supervisory controller determines the set-point temperature for the local controllers that respond to changing weather and building conditions, so that operating costs can be minimised [1]. Improving energy efficiency through developing supervisory controllers is attractive to building managers because it does not involve re-design processes and requires low investment. Recently, the application of model predictive control (MPC) as a supervisory controller for optimising building-energy usage

has received increasing attention. The advantage of MPC over the traditional control strategy is that the former one is able to handle systematically and effectively constraints on control inputs and states, by taking advantage of weather forecast to perform disturbance prediction. In the last decades, researchers have demonstrated that MPC can achieve 10 to 40% of energy saving potential [2–6]. MPCs have also been implemented in real-world buildings and achieved promising savings [2, 7, 8].

The performance of an MPC is largely dependent on how accurately the specific model describes the real building process. While different model types are available for building modelling, the mainstream is to use resistance-capacitance (RC) models as the control-oriented model [8–10].This is because the RC models can be accurately identified using experimental data while maintaining physical significance.

However, generating highly accurate RC models by using experimental data is theoretically not possible, mainly for two reasons. The first reason is the existence of persistent disturbances. For example, the behaviour of the occupants, such as temporary opening of windows, doors and blinds may bring extra heat flux to the building; the second reason is the parametric uncertainty of the thermal dynamic models. When constructing an RC model, many factors have been simplified, which lead to an estimation error of the heat transfer coefficients and system states [11]. The above two factors cause an inaccurate prediction of indoor temperature to happen. Because the MPC saves energy by maintaining the indoor temperature close to the upper (in summer) or lower (in winter) comfort limits, an over-prediction or under-prediction can result in thermal comfort violations or energy waste. For the above reasons, the explicit consideration of the uncertainties becomes especially crucial [12].

Conventionally, the MPC employs linear, time-invariant (LTI) models to predict future dynamics of the system, despite the fact that controlled systems (thermal zones) are non-linear and non-deterministic. This type of MPC is referred to as deterministic MPC (DMPC). Because a receding horizon provides feedback to the control system [13], a

DMPC can achieve a certain degree of robustness under a low level of uncertainty. But as the level of uncertainty increases, the linear MPC will eventually become unstable.

The necessity for developing a more stable MPC for building-energy systems motivates the need for the development of a robust MPC (RMPC). We call the MPC *robust*, if closed-loop performance of the MPC satisfies the constraints for all the known and unknown disturbance sequences. The main idea of RMPC is to consider the model–plant mismatch as an uncertainty and address it explicitly in the control algorithm. One common formulation of RMPC is min–max RMPC, which minimises the 'worst-case' cost that could result from a future disturbance sequence [14–17].

The RMPC has been recently investigated and applied to building-energy systems [18–21]. For example, Kim [18] designed an RMPC to improve the stability of traditional MPCs under uncertainty conditions. He found that robust MPC outperforms DMPC when uncertainty is dominant and the model mismatch is significant. Maasoumy et al. [19] compared the performance of a closed-loop robust MPC with rule-based control and nominal MPC under different levels of uncertainties. They suggest that robust MPC should only be chosen within a certain range of uncertainties. In Ref. [20], a least-restrictive robust MPC law is designed for indoor temperature regulation. The proposed method eliminates the conservativeness of traditional min–max open-loop prediction MPC while guaranteeing reasonable computational complexity. Past studies show that correctly choosing the uncertainty bound is crucial for the design of RMPC: a too narrow bound would cause thermal comfort violation while a too wide uncertainty bound cause performance lose.

An alternative solusion is to use stochastic MPC (SMPC) to obtain a better trade-off between performance and constraint satisfaction. Oldewurtel et al. [22] implemented an SMPC for a building climate control to increase energy efficiency while respecting constraints resulting from desired occupant comfort. In this study, the uncertainty is modelled as an autoregressive model driven by Gaussian noise. Based on this work, an adaptive SMPC is proposed in [23], in which the constraints are adapted according to the histori-

cal thermal violation frequency. By considering a non-Gaussian probability function and chance constraints, Ma et al. [24] proposed an SMPC scheme to deal with the disturbance caused by the occupants. Zhang et al. [25] built a probabilistic disturbance model is built that enables the RMPC to sample directly from the uncertainty set, which removes the assumption that the uncertainty has a Gaussian distribution.

An unsolved issue in the previous studies [18, 19] on RMPC is how to design the uncertain bound properly to reduce conservatism and guarantee robustness. For the convenience of research, the uncertainty bounds in these studies are usually assumed to be fixed and known a priori. This does not work for real-world buildings, as the occurrence of some activities, such as door opening and change of occupants number are actually time-varying and non-Gaussian distributed. The RMPC, based on fixed uncertainty bounds, will inevitably lead to conservative solutions, because it has to work conservatively at all times to guarantee that the thermal comfort is always satisfied. In this paper, we continue with our previous work [5] and presents an adaptive uncertainty bound estimator for the RMPC. The bound estimator is built upon a recursive neural-network model (RNN). The idea is to use the recursive nature of RNN model to capture the uncertainty dynamics and nonlinear properties of the buildings. The uncertainty bounds on the control model can be computed and updated, based on the difference between the output predicted by control model and the RNN model. This algorithm allows one to estimate the error bound in an adaptive fashion over the given prediction horizon. Once the uncertainty bounds are obtained, the optimisation problem is solved as a closed-loop min–max RMPC problem, based on nominal model predictions and tightened constraint sets. We intend to show that by using the proposed adaptive robust MPC (ARMPC), it is possible to deal with both high- and low-uncertainty building plant, in the least restrictive manner. The proposed method is demonstrated at the terminal building of Adelaide Airport, South Australia. The investigated zone is uncertain due to frequent variation of passenger flow, as well as unknown coupling from both controlled and uncontrolled neighbouring space. The

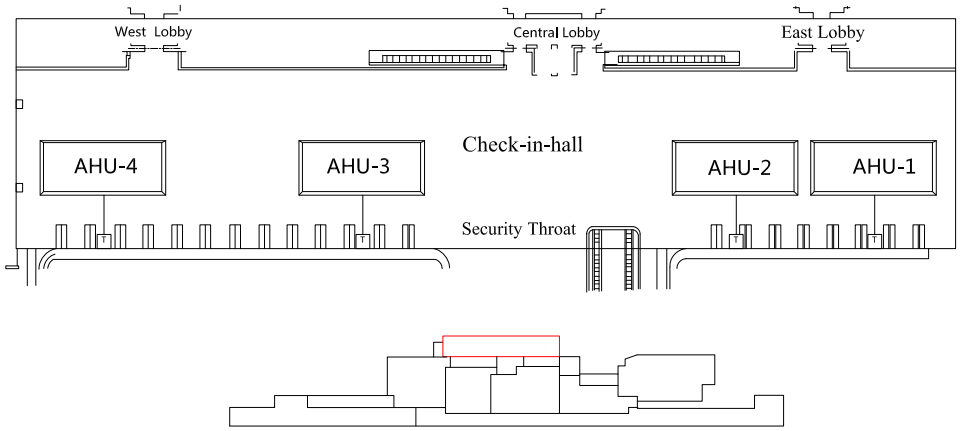


Figure 7.1: The layout of the check-in hall at level-2 of T-1, Adelaide Airport.

complexity and uncertainty of the investigated building make the case study suitable for testing proposed control methods. To summarise, the following contributions are made in this paper:

- Investigate the long-term prediction ability of two types of building models: RC model and RNN model.
- Compare the performance of DMPC with RMPC in presence of model uncertainty.
- Develop an adaptive bound estimator for the RMPC to provide a good compromise between thermal comfort satisfaction and control performance.

The remainder of this paper will proceed as follows: Section 2 introduces grey-box and RNN modelling methods for building thermal dynamics modelling. The design of DMPC, RMPC and the novel RMPC are introduced in Section 3. Section 4 discusses the results of using the proposed controllers, including the control performance comparison between different configurations of DMPC and RMPC. The paper ends with a conclusion and a description of future work.

## 7.2 System Modelling

### 7.2.1 Case Study Building

The test building is the Terminal-1 (T1) building of Adelaide Airport, South Australia. The perimeter zones of the second floor were selected as the test site for the experiment. The layout of the test area is shown in Fig. 7.1. This area serves as the check-in hall from where most passengers enter or leave the building. A large glass facade is installed to the north to ensure good lighting conditions, while two motorised blinds are installed to reduce the effects of solar gain. The position of the blinds is programmed into BMS and controlled with a fixed schedule. The hall is divided into four adjacent zones. Each zone has an associated CAV (Constant Air Volume) box to condition the space and a sensor to measure the zone temperature. Different from other airport terminals, T1 has no flights during the night, so the HVAC system is scheduled to be switched off during the night. The occupied period for the testing area is 7:00 am to 10:00 pm.

### 7.2.2 RC Modelling

Past research has compared different structures of RC models in modelling the thermal dynamics of buildings [11, 26, 27]. A common conclusion that can be drawn from the above studies is that an RC model does not have to be high order to achieve good accuracy. In fact, it has been found that only a few model types are needed to represent both heavy and light mass buildings [27]. For control purposes, this study employs a second order RC model to represent the thermal dynamics of the building.

Before modelling work was begun, we make the following assumptions:

- The air in each zone is evenly distributed.
- Only dry bulb temperature is considered.

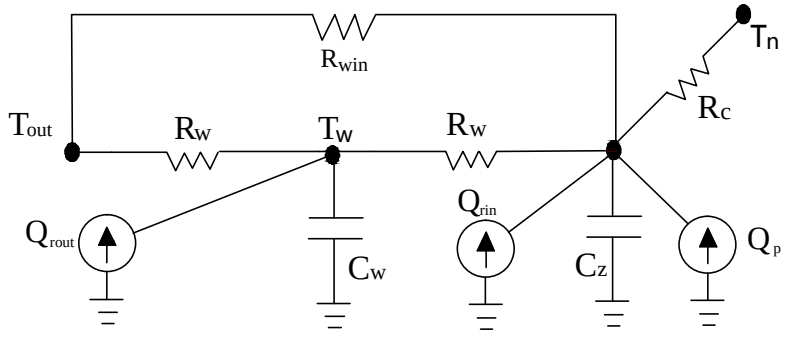


Figure 7.2: RC modelling of the building thermal model.

- The convective resistances between the building envelope and the outdoor and indoor air is the same.
- The influence of the floor temperature on the zone temperature is ignored.

The modelling work is a typical multi-input (thermal energy supplied to individual zones) and multi-output (zone temperatures) problem. The parameters that are of concern are the heat transfer coefficients between the air handling units (AHUs) , adjacent zones, internal walls and uncontrolled spaces. Zones 1 and 2 located at the east end of the building were selected as the experimental area in this study. Zones 3 and 4 are not considered in this study because they have similar dynamics with zones 1 and 2.

The structure of the RC model is depicted in Fig. 7.2. The corresponding energy and mass balance governing equations for a single zone can be written as:

$$C_z\frac{dT_z}{dt} = \dot{m}C_a(T_{sa}-T_z)+\frac{T_{out}-T_z}{R_{win}}+\frac{T_w-T_z}{R_w}+\frac{T_n-T_z}{R_c}+Q_{rin}+Q_p+Q_{inf}, \tag{7.1}$$

$$C_w\frac{dT_w}{dt} = \frac{T_z-T_w}{R_w}+\frac{T_{out}-T_w}{R_w}+Q_{rout}, \tag{7.2}$$

where $C_z$ is the overall thermal capacitance of the air and other fast-response elements, $C_w$ is the thermal capacitance of the interior walls and ceiling, $C_a$ is the specific heat of the air,

$T_z$ is the temperature of the investigated zone, $T_n$ is the temperature of the neighbouring zone(s), $T_{out}$ is the outdoor air temperature, $T_w$ is the mean surface temperature of the interior walls and ceiling, $R_{win}$ is the thermal resistance of the windows, $R_w$ represents the convective resistances between the building envelope and the outdoor and indoor air, $R_c$ is the convective heat transfer coefficient between adjacent zones, $Q_{rin}$ and $Q_{rout}$ denote the inside and outside surface solar radiation heat flux, respectively, $Q_p$ is the internal heat gain generated by the presence of occupants and their behaviours, and $Q_{inf}$ is the internal heat gain from leakage and door openings.

Observing Eq. (7.1), we found that the only non-linear component in the simplified model is the bilinear term $\dot{m}C_a(T_{sa}-T_z)$. Using feedback linearisation, the control input is redefined as $Q_u = \dot{m}C_a(T_{sa}-T_z)$. The new control input $Q_u$ represents the thermal energy supplied to the individual zones.

Eqs. (7.1) and (7.2) are discretised using the Euler forward method:

$$\dot{T} = \frac{T(k+1)-T(k)}{\Delta t}, \tag{7.3}$$

where k is the time step, and $\Delta t$ is the sampling time. By substituting Eq. (7.3) into Eqs. (7.1) and (7.2), the following state space model is obtained:

$$\begin{pmatrix} T_z(k+1) \\ T_w(k+1) \end{pmatrix} = \begin{pmatrix} 1-\frac{\Delta t}{C_z R_{win}}-\frac{\Delta t}{C_z R_w} & \frac{\Delta t}{C_z R_w} \\ \frac{\Delta t}{C_w R_w} & 1-\frac{2\Delta t}{C_w R_w}, \end{pmatrix} \begin{pmatrix} T_z(k) \\ T_w(k) \end{pmatrix} + \\ \begin{pmatrix} \frac{\Delta t}{C_z} \\ 0 \end{pmatrix} \Big( Q_u(k) \Big) + \begin{pmatrix} \frac{\Delta t}{C_z R_{win}} & \frac{\Delta t}{C_z R_c} & \frac{\Delta t}{C_z} & 0 & \frac{\Delta t}{C_z} & \frac{\Delta t}{C_z} \\ \frac{\Delta t}{C_w R_w} & 0 & 0 & \frac{\Delta t}{C_w} & 0 & 0 \end{pmatrix} \begin{pmatrix} T_{out}(k) \\ T_z(k) \\ Q_{rin}(k) \\ Q_{rout}(k) \\ Q_p(k) \\ Q_{inf}(k) \end{pmatrix}, \tag{7.4}$$

There are three disturbance inputs in Eq. (7.4). The first input is the incident solar radiation on the inside and outside of the building envelope. The data used for calculating

the solar radiation heat flux is global horizontal irradiation ($w/m^2$). Therefore, the solar radiation heat flux can be obtained by multiplying $I_r$ by the corresponding surface area. We use $Q_{rin} = \alpha I_r$ and $Q_{rout} = \beta I_r$ for calculating the solar radiation heat flux. $\alpha$ and $\beta$ denote the coefficients associated with the area of the inside and outside building envelop. The second input to the system is the internal gain generated by the occupants. The internal gain is proportional to the number of occupants in the hall, so it can be indicated by the carbon dioxide concentration (ppm). Therefore, it is presented by $Q_p = \gamma CO_2$. Here $\gamma$ denotes the coefficient associated with the number of occupants. The two variables are identified together with Eq. (7.4). The third input $Q_{inf}$ is not measurable so they are regarded as unmeasured uncertainty. Taking into account the uncertainty and measurement noise, Eq. (7.4) can be re-written as state-space form [28]:

$$x(k+1) = Ax(k) + Bu(k) + Ed(k) + Fe(k), \tag{7.5}$$

where A, B, E, and F are the corresponding matrices, $x$ is state vector, $u$ is input vector, $d$ denotes measurable disturbance, and $e$ denotes the uncertainty and measurement noise that is assumed to be Gaussian distributed. The unknown parameters in Eq. (7.5) are identified using measured building data. The data used for model identification were collected from between the 1st and 20th of January, 2013. The input is the supplied cooling energy $Q_u$, the meteorological data of the Bureau of Meteorology of Australia provide disturbance forecast ($Q_r$ and $T_{out}$) to the thermal zones, the output is indoor temperature.

A source of uncertainty in building control comes from the errors in forecasting. The outside ambient temperature forecast uncertainty increases with longer prediction horizon. However, this study does not specifically investigate the effects of weather forecast error on the modelling results. Instead, we use measured outside air temperature instead of the predicted value to perform analyse. All the other uncertainties are lumped into the error terms.

Due to the existence of the uncertain variables in matrix A, the resulting dynamic system is nonlinear. Thus, a nonlinear least-squares problem is solved with respect to $\theta$

as follows:

$$\begin{aligned} &\min[y - f_1(x_1, ...x_m; \theta)]^T [y - f_1(x_1, ...x_m; \theta)] \\ &= \min \sum_{k=1}^{m} [y_k - f(x_k; \theta)]^2, \end{aligned} \tag{7.6}$$

where $f_1$ is a nonlinear function, $x$ is a vector of states variables, $y$ is a vector of output variables, $m$ is number of measured states and outputs variables, $\theta = [R_w, R_g, R_f, R_c, \alpha, \beta, \gamma, C_z^1, C_w^1]$ is a vector of parameters to be identified, the lower and upper bounds of $\theta$ are estimated and initiated, based on the material properties and geometry of the investigated zone. Our objective is to find vector of $\theta$ so that the function $f$ best fits the input-output data $[x_k, y_k]$, The nonlinear least squares problem is solved using a Trust-Region reflective algorithm [29].

In this work, we focus on minimising the supplied thermal energy $Q_u$ at the AHUs level and will not model the efficiency of the AHU system. However, $Q_u$ is not the actual control input to the system. The actual control input might be the set-point command for zone temperature, supply air temperature or the chilled water temperature, depending on the types of HVAC system being considered. The low-level controllers work accordingly to track the designated set-point value. If a variable air volume (VAV) system is considered, the control objective will be both the air flow rate and supply air temperature, then the optimisation problem becomes a non convex one. In this study, a CAV is considered, so the only variable to be optimised is the supply air temperature. One could obtain the optimal set-point temperature once the virtual input $Q_u$ is obtained.

### 7.2.3 Recursive Neural Network Modelling

In this section, the thermal dynamics of the same zone will be modelled by an RNN model. Nonlinear autoregressive with exogenous inputs (NARX) model is used to express

the RNN structure:

$$y(k) = f_2(y(k-1),...y(k-n_y),u(k-1),...u(k-n_u)+e(k), \tag{7.7}$$

where $y(k) = [y_1(k),...y_p(k)]^T$, $u(k) = [u_1(k),...u_m(k)]^T$, and $e(k) = [e_1(k),...e_m(k)]^T$ are the system output, input and noise, respectively; $p$ and $m$ are the number of outputs and inputs, respectively; $n_y$ and $n_u$ are the maximum lags in the outputs and inputs, respectively; $k$ is the process dead time; and $f_2$ is a vector-valued non-linear function. Model order selection is an important step of system identification, but it will not be elaborated this paper. For detailed procedures see [30].

A neural network with three layers of neurons was employed. The network function is expressed with the following equation:

$$\hat{y}(t) = F\sum_{i=1}^{n_h} W_{j,u} f_3(\sum_{i=1}^{n_u} w_{u,i}\varphi_i(k) + b_{u,0}) + B_{j,0}, \tag{7.8}$$

$$f_3(x) = \frac{1}{1+\exp(-x)}, \tag{7.9}$$

where $W_{j,u}$ and $w_{u,j}$ are weights vector to the hidden layer and output layer respectively. $b_{j,0}$ and $B_{u,0}$ are the bias of the hidden units and the output layer, respectively, $\varphi_i(k)$ indicates the vector that contains the regression of the Eq. (7.7) at time step $k$, $f_3$ is sigmoid function expressed by Eq. (7.9), and $F$ uses a linear function and $j = 1$ as only one output is considered. The weight vector $w$ and bias vector $b$ at the hidden layer were initialised using the Nguyen-Widrow method to keep the trained model more consistent. Levenberg-Marquardt algorithm was employed to train the neural networks, which minimises mean square error (MSE). For training the RNN, the input-output data cannot be directly fed into the network but should be arranged to follow the structure of the NARX model.

### 7.2.4 Model Validation and Comparison

The data used for validation purposes were a completely different set of data, obtained from 21st January 2013 to 24th January 2013. Because the primary purpose of building the models is to achieve predictive control, the multi-step-ahead prediction is needed. However, both of the aforementioned training algorithms only minimise the error over a single step ahead. A more reasonable way to validate our model is to consider multi-step-ahead prediction by taking into consideration the recursive feature of the model [5]. To evaluate the performance of predictive models, RMSE (relative mean squared error, NMSE (normalised mean squared error) and MAE (maximum absolute error) are used in this study:

$$\text{RMSE} = \sqrt{\frac{1}{n}\sum_{k=0}^{n-N}\sum_{j=1}^{N}(y_{k+j} - \hat{y}_{k+j|k})^2}, \tag{7.10}$$

$$\text{NMSE}_{fit} = 1 - \left(\frac{\left\|y_{k+j} - \hat{y}_{k+j|k}\right\|}{\left\|y_{k+j} - mean\left(y_{k+j}\right)\right\|}\right)^2, \tag{7.11}$$

$$\text{MAE} = max(|y_1 - \hat{y}_1|, |y_1 - \hat{y}_1|, ..., |y_n - \hat{y}_n|), \tag{7.12}$$

where $y_k$ and $\hat{y}_k$ denote the actual and predicted outputs, corresponding to a set of test data.

The selected inputs for RC model are also used as the inputs for RNN model. Fig. 7.3 plots the simulation results using the RC model and RNN model. Obviously, the RNN model achieves a better prediction accuracy compared with the RC model. It is believed that the RNN model has captured some stochastic uncertainties of the investigated system, using its recurrent property. In other words, the uncertainty information has been included in the temperature regression terms. The RC model generates a larger modelling error, especially during the time from 21:00 to 22:00 pm, which is due to the simplification that has been made (see Fig. 7.4). Fig. 7.5 and 7.6 illustrate one month's simulation result by using the two models. The histogram of the residuals generated by the two models is

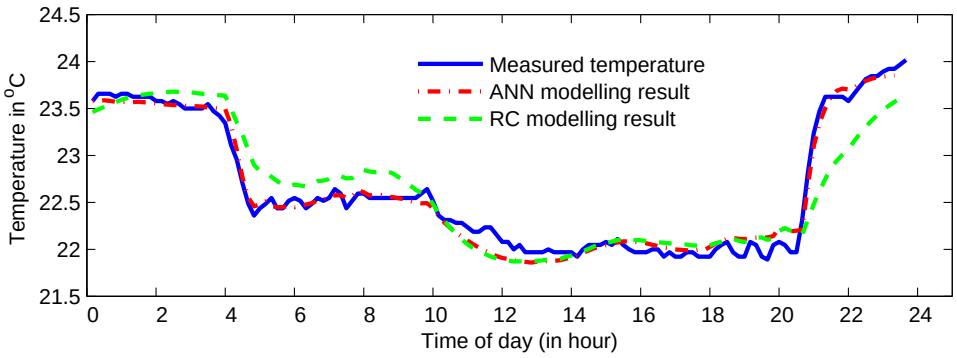


Figure 7.3: Indoor temperature prediction results by conducting multi-step-ahead prediction.

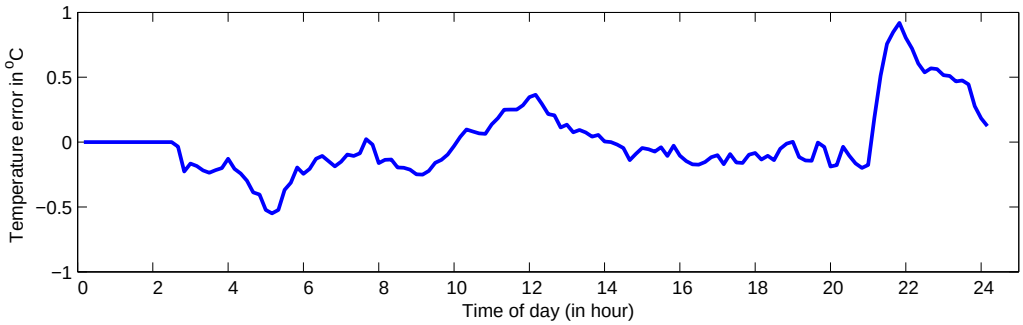


Figure 7.4: Model–plant mismatch generated by RC model.

plotted in Fig. 7.7. Obviously, compared with the RC model, the residuals generated by the RNN model are smaller and closer to a normal distribution.

However, the prediction errors are inevitable even by using the most accurate models. The reasons are summarised below:

- The temperature readings from sensors mounted on the walls are used to approximate the average room temperature. This leads to slightly wrong parameter estimation values.

- Because the investigated zones are wide open, infiltration through the opening door, and coupling from the adjacent space could influence the

- Some heat flows cannot be estimated precisely, e.g. the solar radiation is affected by the tilt angle of the sun and cloud level.
- The internal load, such as heat gain generated by occupancy and their behaviour, is not measurable and also hard to evaluate.
- Weather forecast of solar radiation and outside temperature can introduce some errors.
- Faulty sensor readings and wrong actuator operations could introduce some errors.

The modelling error caused by the above reasons is collectively called uncertainty in the rest of this paper. By analysing the pros and cons of the RC model and the RNN model, we have drawn the following conclusions: First, because RC models are differentiable and physically meaningful, they are suitable for use as control-oriented models. However, as a full-state feedback is always lacking, a large model–plant mismatch always occurs when using low-order RC models. On the other hand, the recurrent nature of RNN model enables the model to capture some stochastic, uncertain features of the building system. Therefore, they generally have better long-term prediction accuracy compared with the RC model. Direct use of RNN models as the control model would result in a non convex optimisation problem, which is computationally intractable. For this reason, the RNN model mainly plays two roles in this study: 1) performs as a comparison model for uncertainty bounds estimation, and 2) works as the reference model during the closed-loop simulation.

## 7.3 Control Design

### 7.3.1 Baseline Control and MPC

Thermal comfort is a complicated parameter and indicated by predicted mean vote (PMV). In this study , for simplicity we employ the dry bulb temperature as the parameter to in-

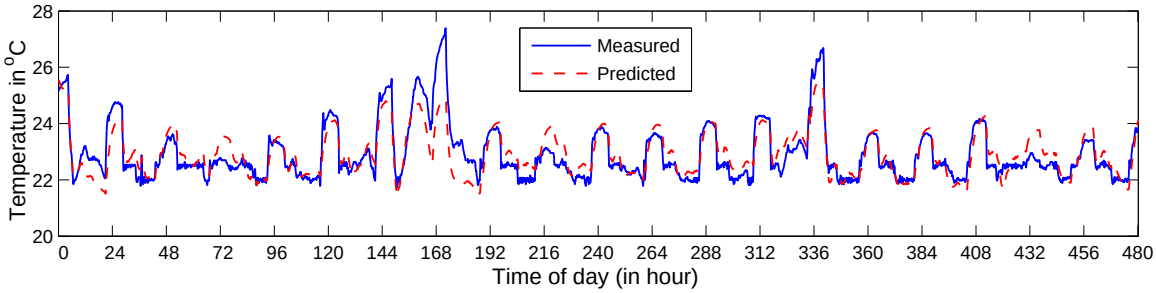


Figure 7.5: 31 days'prediction results generated by RC model.

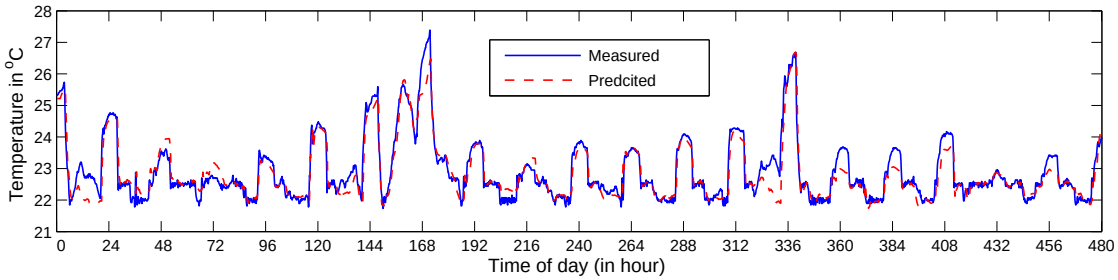


Figure 7.6: 31 days'prediction results generated by RNN model.

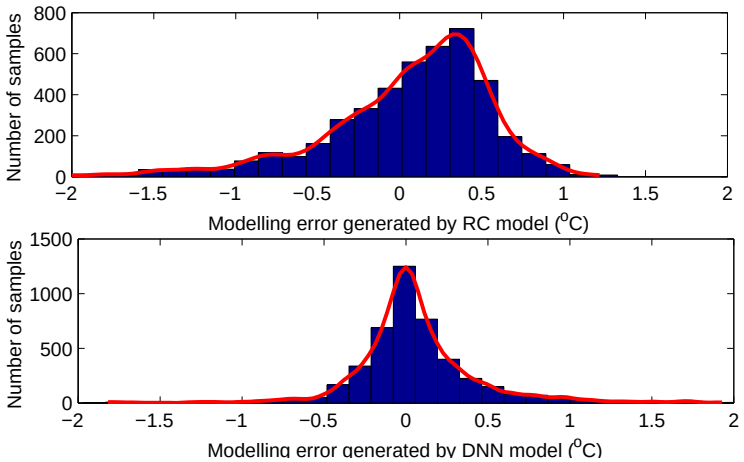


Figure 7.7: Histogram of residuals (31 days) generated by the two models.

dicate the level of thermal comfort. According to ASHRAE Standard 55, indoor temperatures should be maintained within the range 20–23°C in the winter and 22.5-26 °C in the summer [1]. In commercial buildings, the actual comfort requirement would be different from one building to another, which is usually formalised in the lease between building managers and tenant. For the case at hand, the building manager attempts to maintain the indoor temperature at 22 ±0.5 °C in summer and 21.5 ±0.5 °C in winter. These two set-point temperatures are controlled by a simple proportional control at the fixed values during occupancy. Typically, a night setback control with fixed schedules is programmed by the BMS to achieve some basic energy savings. This simple configuration cannot always satisfy the real demands of the occupants, because the conditions in the real building differ greatly from one day to another. In the following sections, we first use a simple example to describe how DMPC saves energy as compared with the baseline night setback control method. Afterwards the use of a closed-loop min–max RMPC for dealing with uncertainty and its drawbacks will be demonstrated. Finally, the use of an adaptive uncertainty bound estimator for improving the RMPC's performance will be presented.

### 7.3.2 Deterministic MPC

We first consider the DMPC formulation as a basis for the discussion of the robust MPC. In particular, the following optimisation problem is considered:

$$\min_{u} \sum_{j=0}^{N-1} p_e|(u_{k+j|k})| + Q(|\hat{y}_{k+j|k} - r_{k+j|k}|) + R\sum_{k=1}^{N}(|\underline{e}_{k+j|k}| + |\overline{e}_{k+j|k}|), \tag{7.13}$$

subject to:

$$\begin{aligned} x_{k+j+1|k} &= Ax_{k+j|k} + Bu_{q,k+j|k} + Ed_{k+j|k} + Fw_{k+j|k}, \quad \forall j = 0,...,N-1 \\ y_{k+j|k} &= Cx_{k+j|k}, \quad \forall j = 1,...,N \\ T_{min,k+j|k} - \underline{e}_{k+j|k} &\leq y_{k+j|k} \leq T_{max,k+j|k} + \overline{e}_{k+j|k}, \quad \forall j = 1,...,N \\ \underline{e}_{k+j|k} &> 0, \overline{e}_{k+j|k} > 0, \quad \forall j = 1,...,N \\ U_{max,k+j|k} &\leq v_{k+j|k} \leq U_{min,k+j|k}, \quad \forall j = 0,...,N-1, \end{aligned} \tag{7.14}$$

The constraints that should be met are:

1. $T_{oc} \in$ [ 21°C , 24°C] Thermal comfort during occupied hours.

2. $T_{uo} \in$ [ 19.5°C, 26°C] Thermal comfort during unoccupied hours.

3. $u_q \in$ [ -10 kW, 12 kW] Maximum cooling energy that can be supplied to each zone.

where the double indices $k+j|k$ denote the prediction value at time $k+j$ made at time $k$, $U = [u_{k|k}, u_{k+1|k}, ..., u_{k+N-1|k}]$ is a vector of the control inputs (supplied energy) applied to the model, $\hat{y}_{k+j|k}$ is the predicted output at time $k$, which is obtained by iteratively solving Eq. (7.14) using the control input sequence $U$, $T_{max} = [T_{max,k|k}, T_{max,k+1|k}, \cdots,$ $T_{max,k+N-1|k}]$ is a vector of the upper comfort temperature band within the horizon, $T_{min}$ is a vector of the lower comfort temperature band, variants $\underline{e}$ and $\overline{e}$ denote the temperature violation from the upper and lower bounds, respectively, $N$ is the prediction horizon, $d$ is the measured disturbance, $r$ is the set-point temperature, $U_{min}$ and $U_{max}$ denote the maximum cooling and heating energy that the system can supply, respectively, $p_e$ denotes time of use (TOU) electricity price in dollars per kWh, $Q$ is the penalty on the comfort constraint violation and $R$ is the penalty on the set-point temperature deviation.

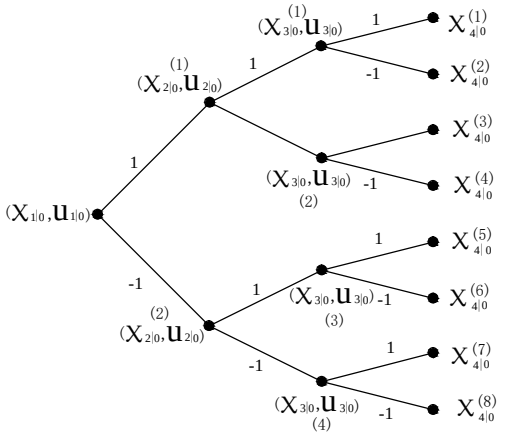


Figure 7.8: Scheme of uncertainty evolution for closed-loop minmax RMPC with a horizon of 3.

### 7.3.3 Closed-loop min–max Robust MPC

In designing the DMPC, it is assumed that the model can predict the real-world building plant perfectly. In the context of RMPC, which is designed to address model mismatch explicitly, the effects of model mismatch on state estimations should be addressed. Therefore, Eq. (7.5) is rewritten as:

$$x(k+1) = Ax(k) + Bu(k) + Ed(k) + Fw(k), \tag{7.15}$$

where $w_k \in \mathbb{W}^2$ denotes the model uncertainty. $w_k$ is bounded but its exact value is not known. In the previously illustrated DMPC, the predicted states are updated by solving iteratively the equality constraints. This does not make any sense for the robust control scheme because it is impossible to make a prediction in the presence of the uncertainty variable $w$. Therefore, we use an explicit representation of the predictions, which is written as:

$$X = Ax_{j|k} + BU + ED + GW \tag{7.16}$$

where $X = (x_{k+1|k}^T, x_{k+2|k}^T, ..., x_{k+N-1|k}^T)^T$ is the vector of predicted states, $D = (d_{k+1|k}^T, d_{k+2|k}^T, ..., d_{k+N-1|k}^T)^T$ is the vector of predicted disturbances and $W = (w_{k+1|k}^T, w_{k+2|k}^T, ..., w_{k+N-1|k}^T)^T$

is the vector of uncertainties.

The basic idea of min–max RMPC is to determine all possible evolutions of the disturbance sequence over the control horizon, and to minimise worst-case cost. Min–max RMPC can be either in the form of open-loop predictions [31] or closed-loop predictions [15, 31]. The open loop approach fails to take into account that feedback is presented in the receding-horizon implementation of the control, therefore leads to conservative solutions and could even make the optimisation problem infeasible [15, 16].

In this study, we focus on the application of a closed-loop RMPC to building-energy control. Different from the open-loop approach, the closed-loop RMPC considers the feedback over the prediction horizon and incorporates it into the prediction. In particular, at each step, the closed-loop RMPC considers the future value X under different disturbance trajectories. The controller generates a family of control sequences, each one corresponds to a different measured state. The maximum costs can be calculated along with some of the worst-case predictions. To consider the feedback term in the optimisation problem, a standard way is to parameterise $U$ as an affine function of X:

$$U = LX + V, \tag{7.17}$$

which can be rewritten as:

$$U = (1 - BL)^{-1}(Ax_{k|k} + BV + GW) + V, \tag{7.18}$$

From Eq. (7.18) it can be seen that the mapping from L and V to X and U is non-linear, hence optimisation over both L and V cannot be solved by a standard convex optimisation method. Therefore, an alternative parameterisation method presented by Lofberg [15] is applied in this study.

$$U = LW + V, \tag{7.19}$$

$$L = \begin{pmatrix} 0 & 0 & \cdots & 0 \\ L_{10} & 0 & \cdots & 0 \\ L_{20} & L_{21} & \cdots & 0 \\ \vdots & \vdots & \ddots & \vdots \\ L_{(N-1)0} & L_{(N-1)1} & L_{(N-1)(n-2)} & 0 \end{pmatrix}, V = \begin{pmatrix} v_{k|k} \\ v_{k+1|k} \\ \vdots \\ v_{k+N-1|k}, \end{pmatrix} \tag{7.20}$$

Instead of parameterising the control trajectory in the future states $x_k$, the control sequence is parameterised directly in the uncertainty. This avoids solving a non convex optimisation problem by considering $U = LX + V$. In considering the trajectory of uncertainty, only extreme disturbances $[\underline{w}, \overline{w}]$ are considered. For example, if one assumes $\overline{w}$=1, $\underline{w}$=-1, for a prediction horizon of 3, there could be $2^3$ disturbance realisations. This is shown in Fig. 7.8. It can be seen that the optimisation problem grows exponentially with the increase of prediction horizon. A prediction horizon that is too long may cause the curse of dimensionality [15]. For this reason, a long prediction horizon should be avoided by using the closed-loop RMPC.

Considering the same control-oriented model and constraints in Eq. (7.14), the following min–max optimisation problem is formulated:

$$\min_{u} \max_{w} \sum_{j=0}^{N-1} p_e |(v_{k+j|k})| + Q(y_{k+j|k} - r_{k+j|k}) + R \sum_{k=1}^{N} (|\underline{e}_{k+j|k}| + |\overline{e}_{k+j|k}|), \tag{7.21}$$

subject to:

$$\begin{aligned} x_{k+j+1|k} &= Ax_{k+j|k} + Bu_{q,k+j|k} + Ed_{k+j|k} + Fw_{k+j|k}, \quad \forall j = 0,...,N-1 \\ y_{k+j|k} &= Cx_{k+j|k}, \quad \forall j = 1,...,N \\ T_{min,k+j|k} - \underline{e}_{k+j|k} &\leq y_{k+j|k} \leq T_{max,k+j|k} + \overline{e}_{k+j|k}, \quad \forall j = 1,...,N \\ \underline{e}_{k+j|k} &> 0, \overline{e}_{k+j|k} > 0, \quad \forall j = 1,...,N \\ \overline{w}_{k+j|k} &\leqslant w_{k+j|k} \leqslant \underline{w}_{k+j|k}, \quad \forall j = 0,...,N-1, \\ U_{max,k+j|k} &\leq v_{k+j|k} \leq U_{min,k+j|k}, \quad \forall j = 0,...,N-1, \end{aligned} \tag{7.22}$$

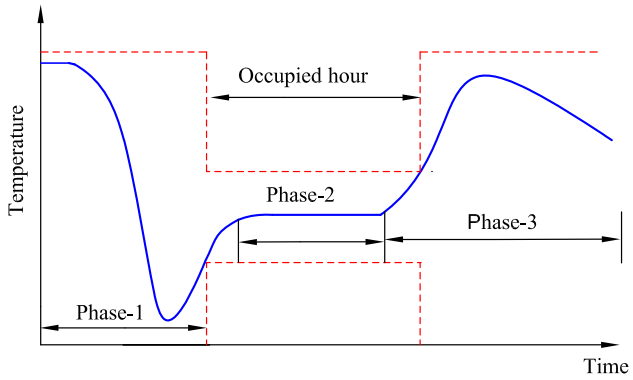


Figure 7.9: Three phases of zone temperature trajectory when the MPC is applied.

where $\underline{w}_{k+j|k}$ and $\overline{w}_{k+j|k}$ denote the lower and upper uncertainty bounds, respectively. By comparing Eq. (7.14) with Eq. (7.22), it can be seen that the difference between RMPC and DMPC is explicit consideration of the uncertainty $w$. All possible trajectories are included in bands that depend on $\underline{w}_{k+j|k}$ and $\overline{w}_{k+j|k}$. The value of $[\overline{w};\underline{w}]$ depends on the future state of the real system, which is not known. Obviously, if all errors lie within the error bound $[\overline{w};\underline{w}]$, the robustness of the MPC can be guaranteed. On the other hand, the optimisation does not necessarily lose robustness if only a single error exceeds the bound [32]. A possible way of estimating the error bounds is to obtain them directly from the historical residuals, e.g. determine the numerical range where a certain probability of the modelling errors happens. However, this method still relies on the choice of the probability density. If the uncertainty set is chosen to be too large, the controller becomes very conservative and control performance will be lost. The conservatism will be demonstrated with an example in a later section.

## 7.4 RMPC with Adaptive Uncertainty Bound

The above-mentioned bounding method can result in conservative solutions, because it is purely based on the historical data but fails to take into account that the errors are also

related to the occurrence of future disturbances. The uncertainty can be predicted using a comparison model [33] or mismatch function [34]. For example, Fukushima and Bitmead [33] used a comparison model to transform the given robust MPC problem into a nominal MPC without uncertain terms. Illustrated by this idea, we propose a novel uncertainty bound estimator in this study, constructed based on the RNN model presented in the previous sections. The idea is to use the recurrent nature of the RNN model to capture the uncertainties that exist in the building system. The RNN model can then make use of the disturbance prediction to conduct long-term prediction. The unknown model mismatch between the RC model and the actual building plant can therefore be approximated by the difference between the RC model and the RNN model. The positive uncertainty can be calculated as

$$\bar{z} = \max_{k \in 1 \ldots n} (\hat{y}_{nn}(k) - \hat{y}_{rc}(k)), \tag{7.23}$$

where $\hat{y}_{rc}$ and $\hat{y}_{nn}$ are open-loop prediction results generated by RC and RNN models, respectively. $\bar{z}$ denotes the maximum error within $n$ steps, $n \leqslant N$ is the number of steps considered.

When solving a building control problem, different uncertainty levels should be considered at different stages. This is explained with a simple example here. Fig. 7.9 illustrates the temperature trajectory generated by an MPC. When temperature is maintained during the occupancy (stage-2), the only goal of MPC is to track the set point temperature, and the uncertainty in the far future becomes less important. So we consider $\bar{z}$ over a small number of steps $(n < N)$ for this stage. During the transitional period (stage-1 and 3), because the MPC needs to foresee the change of occupancy status, the information in the far future becomes more important. Therefore we can choose $n$ the same as $N$ so that a wider uncertainty is allowed to happen during the transitional period.

Because the bounds are estimated based on the RNN models, which are also subject to errors, there is a probability that the actual bound is wider than the estimated bound, and the robustness could not be guaranteed. Therefore, it is also necessary to take the

residuals of the RNN model into consideration. Recall that the error generated by the RNN is close to a normal distribution (see Fig. 7.3), so that a statistical regression analysis can be applied. The confidence region forms uncertainty bands around the response of the calculated error bound:

$$\overline{w} = \bar{z} + r(k) + Z_{\alpha/2}\frac{\sigma}{\sqrt{n}}, \tag{7.24}$$

where $r(k)$ denotes the residuals generated by the RNN model against real plant, $Z_\sigma = 2$ is the confidence coefficient, $\alpha$ is the confidence level, which is chosen to be 95%, $\sigma$ is the standard deviation of $\hat{r}(k)$ calculated over the selected data. $\hat{r}(k)$ is the centre of the residuals. This bounding algorithm allows the designer to choose the probability of this occurrence as a parameter in an adaptive control scheme. For example, applying a higher value of percentage allows the constraints to be tightened more effectively, but this may also result in over-conservative results. On the other hand, a lower percentage value can improve the RMPC but could lead to constraints violations. The choice on the probability should always be based on the accuracy of the designed model. Fig. 7.10 shows the adaptive RMPC (ARMPC) procedure and the adaptive RMPC algorithm is summarised as follows:

**Algorithm: Adaptive Robust MPC**

1. Choose the initial bounds using sampling method introduced in the previous section.

2. DMPC computes the open loop input trajectory $U = [u_1, u_2 ... u_n]$.

3. The RNN performs $n$-steps ahead prediction using input vector U and disturbance vector D to obtain a comparison set of output trajectory $Y = [y_1, y_2 ... y_{1+N}]$.

4. Calculate the error bounds based on Eq. (7.23) and Eq. (7.24) .

5. During occupation period, if $z$ is positive (underestimation), then update uncertainty bounds to $[-\overline{w}, \overline{w}]$ by setting $n = 3$. Else the uncertainty bound is set to the minimum range.

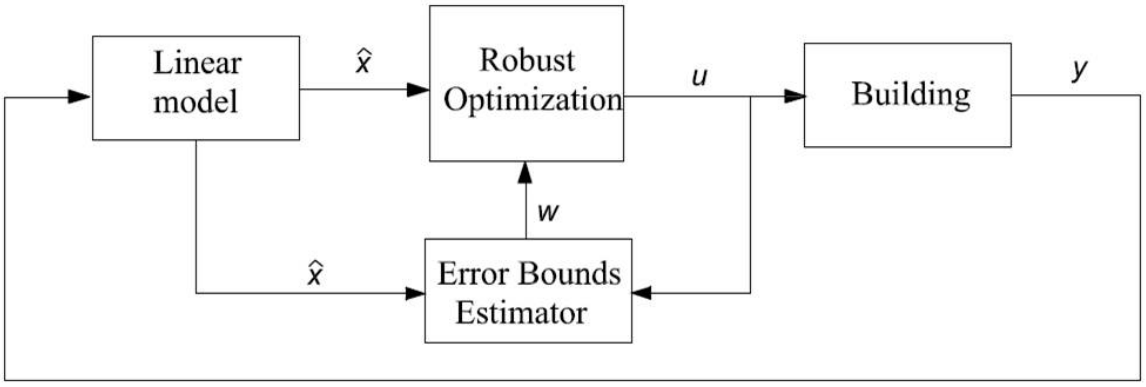


Figure 7.10: Control structure of the ARMPC scheme.

6. During transitional period, if $z$ is positive (underestimation), then update uncertainty bounds by setting $n = N$. Else the uncertainty bound is set to the minimum range.

7. Increment $k$. Go to Step 2.

## 7.5 Results and Discussion

### 7.5.1 Deterministic MPC

In this section, the DMPC is studied as a basis for the discussion of RMPC. The programs for model training, validation and control optimisation were coded in Matlab, which runs on a PC with Intel Core i7 CPU 2.4 GHz. The optimisation problem associated with both DMPC and RMPC are solved using Yalmip [35]. First, we select a day on which the LTI model can achieve a satisfactory result (fitness = 80%). We then use the RNN model as the sub-system models to conduct a closed-loop simulation. During the simulation, while a sequence of $N$ control values is computed, only the first value is applied to the RNN sub-system. Similarly, the RNN only conducts one-step ahead prediction and this is used as the feedback to the DMPC. The coefficients of the DMPC cost function are tuned until

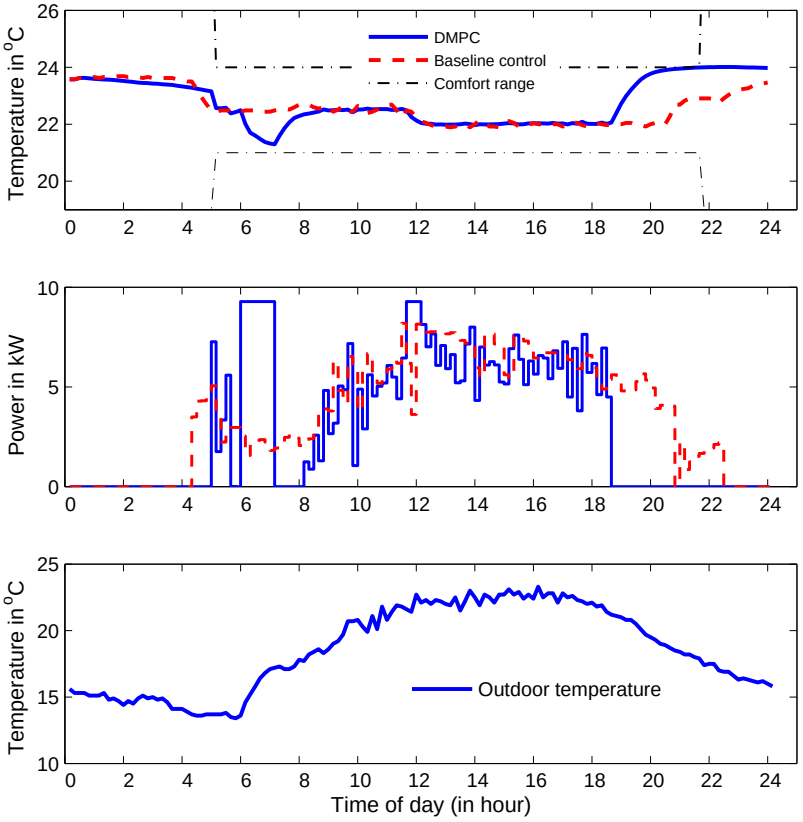


Figure 7.11: Comparison between baseline control and DMPC.

Table 7.1: Parameters of the DMPC.

| DMPC parameters | |
|---|---|
| Sampling interval | 10 min |
| Prediction horizon, N | 30 |
| Control horizon, P | 30 |
| Weight for energy input Q (when TOU is not considered) | 0.8 |
| Weight for energy input Q (when TOU is considered) | 40 |
| Penalty on soft-constraint violation in R | 1 |
| Weight for set-point temperature deviation W | 1 |
| Occupancy hour | 5:00 am to 9:30 pm |
| off-peak hour | 7:00 am to 9:30 pm |
| Peak hour electricity price | 0.090 $ /kWh |
| Off-peak hour electricity price | 0.024 $ /kWh |

the best performance is achieved. The optimised control parameter is shown in Table 7.1.

Fig. 7.11 compares the DMPC with the baseline control strategy. Clearly, the baseline night setback control (red, dashed line) turned on the cooling system too early and off too late, leading to unnecessary energy costs. The blue, solid line illustrates the solution of the DMPC scheme with a prediction horizon of 30 (five hours). It shows that the controller starts to precool the space starting from 5:30 am, with the aim to store the cooling energy using passive building thermal mass. This action saves utility costs because it takes advantage of cheap off-peak electricity and cooler ambient air in the early morning. During the occupied hours, the set-point temperature is maintained at the designated value to ensure maximum thermal comfort. Before the end of occupancy, the DMPC stops the cooling system so that the temperature reaches the upper comfort limit exactly at the end of the occupancy. For the given example, the cost saving of DMPC over baseline control is 26%.

Table 7.2: Parameters of the RMPC.

| RMPC parameters | |
|---|---|
| Prediction horizon, $N$ | 15 |
| Weight for uncertainty term | 0.1 |
| Fixed uncertainty bound | $[-0.2, 0.25]$ |
| Number of look-ahead steps | 10 |

### 7.5.2 DMPC vs RMPC vs ARMPC on Energy Saving

In this section, we present a comparison study on three different MPC approaches, which are DMPC, RMPC and ARMPC, in the presence of model uncertainty. Our goal is to compare the performance of these three controllers in terms of conservatism, stability and computational speed. As illustrated in the previous section, MPC can save energy by keeping the zone temperature close to its upper or lower comfort limit. Because cooling is considered in this study, only underestimation $\hat{T} > T$ will cause thermal comfort violation on the upper comfort bound. We do not consider TOU electricity price during the simulation to speed up the simulation process. The parameters of the RMPC are listed in Table 7.2.

First, we choose a day on which the LTI control model suffers from a considerable amount of uncertainty to conduct the comparison. The uncertainty is illustrated in Fig. 7.12. Remind that the reference model is the RNN model, so the uncertainty is calculated as the difference between the predicted outputs by the LTI model and the RNN model. The uncertainty bound for RMPC is set to be [-0.2, 0.25], based on the simple sampling methods and the histogram of residuals. The set-point value is chosen to be close to the upper comfort temperature (23 °C). Fig. 7.12 compares the performance of RMPC and DMPC when a uncertainty is presented. The red, dashed line indicates the output of DMPC. It can be seen that, although the uncertainty happened during the steady state, it does not impose an unstable influence on the performance of the DMPC. This is because

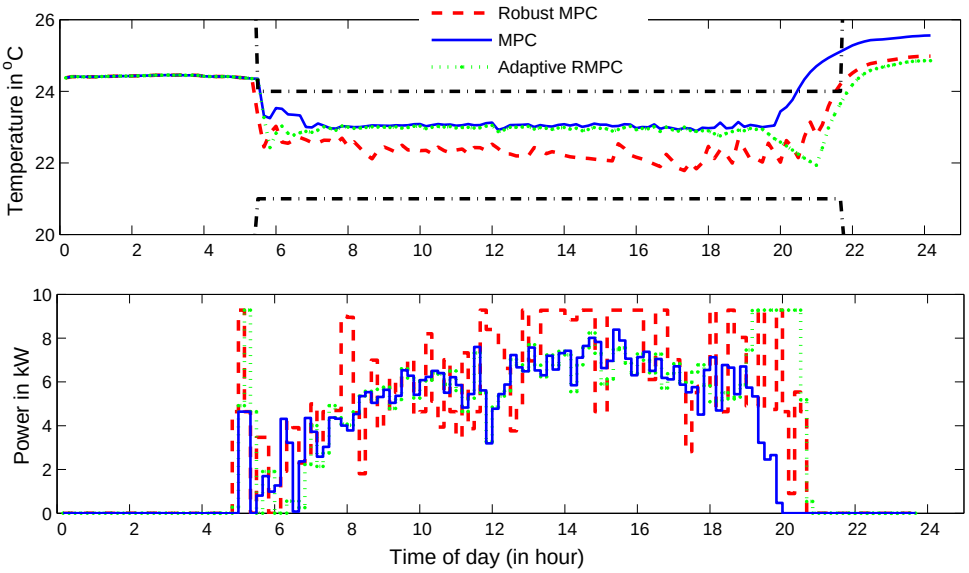


Figure 7.12: Performance of DMPC, RMPC and ARMPC under model uncertainty.

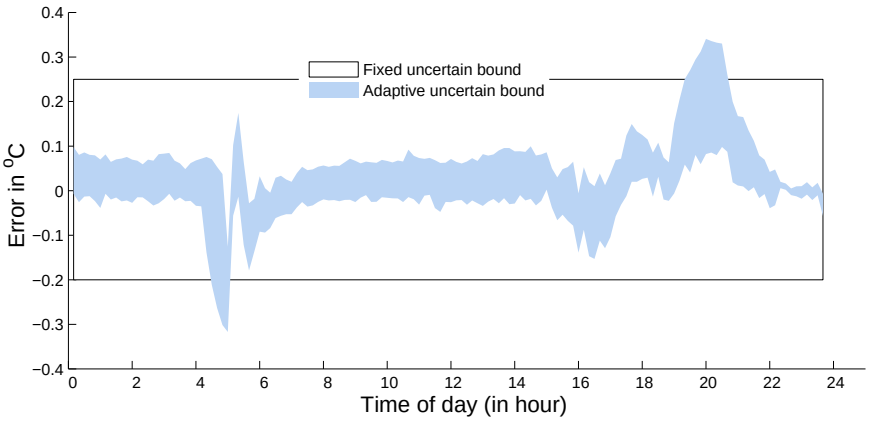


Figure 7.13: Comparison of fixed bound and the adaptive bound.

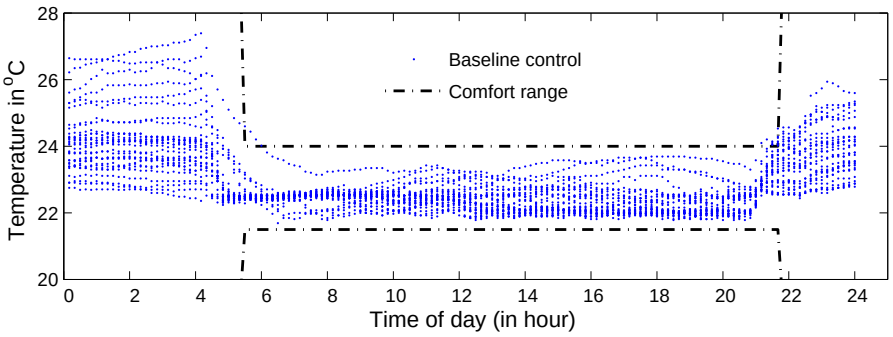


Figure 7.14: Two weeks' control performance of baseline control.

the closed-loop nature of the DMPC makes it robust to some degree of uncertainty. However, when the temperature is moved towards the upper bound, the comfort constraint is violated by the DMPC, which is due to the large error happens before the end of the occupancy. The blue, solid line shows the performance of the RMPC. The thermal comfort is satisfied by the RMPC all the time, as the modelled uncertainty is located within the designated uncertainty bound for most of the time. However, the RMPC consumes more energy (32% with respect to DMPC), by maintaining the temperature below the set-point value during steady states. This is expected because the RMPC performs conservatively by lowering the indoor temperature to make sure that constraints are safely satisfied at all times. The RMPC works in such a way to prevent a potential comfort violation due to the positive uncertainty. The green, dotted line shows the performance of the ARMPC. It can be seen that the ARMPC tracks the set-point temperature well during the steady states, without wasting too much energy. This is because of the use of a smaller uncertainty bound, as shown in Fig. 7.13. This proves the effectiveness of the proposed method, because a smaller, adaptive uncertainty bound indicates a lower degree of conservatism without violating thermal comfort for RMPC. The ARMPC also satisfies the thermal comfort requirement before the end of occupancy, when the uncertainty bound is expanded to allow a larger uncertainty to happen. Similarly, this is because the ARMPC expand the uncertainty bound during the transitional period to ensure a better robustness.

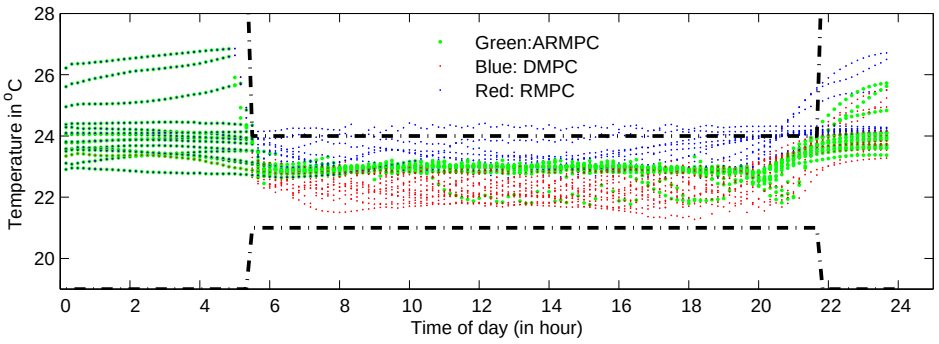


Figure 7.15: Two weeks' control performance of DMPC, RMPC and ARMPC.

The simulation period was then extended to two weeks, from 4th to 28th Feb, 2015. The result is compared with the baseline control, which is shown in Fig. 7.14. One can observe that the temperature trajectory generated by baseline control were away from the upper comfort limit for most of the time, which is the main reason for energy waste.

Fig. 7.15 shows the simulation results using the three above-mentioned control methods. First, it can be seen that the DMPC (blue dotted) tries to save energy by controlling the indoor temperature close to the upper comfort constraint. However, it also causes temperature violations on a number of days, due to underestimated indoor temperatures. The underestimation mainly comes from the use of the LTI model and the presence of unknown uncertainty. Second, from Fig. 7.15, it can be seen that the use of RMPC (red dotted) leads to a significant improvement in thermal comfort, with respect to the situation obtained with the DMPC. However, it also moves the indoor temperature from the steady state towards the lower comfort bound, which causes more energy usage. This is due to the use of a fixed and conservative approximation of the error bound. Third, the temperature profile generated by the ARMPC (green, dotted) is mostly distributed in between the previous two cases. This indicates that the proposed method consumes less energy than the RMPC, and also achieves fewer thermal violations than the DMPC approach. The improvements made in terms of energy saving and thermal comfort come from the use of the adaptive uncertainty bound estimator.

Table 7.3: Performance comparison between DMPC, RMPC and ARMPC.

| | Baseline | DMPC | RMPC | ARMPC |
|---|---|---|---|---|
| Total energy (kWh) | 3580 | 2440 | 3052 | 2656 |
| Number of infeasible days | 3 | 9 | 0 | 0 |
| Simulation time per step | n/a | 0.4 s | 4.4 s | 7.1 s |

A summary of the performance of each controller for the investigated days is reported in Table 7.3. It can be seen that the baseline control consumes the most energy and violated the thermal comfort on 3 days. DMPC consumes the least energy which leads to the greatest energy savings. However, the zone temperature regulated by DMPC violates the comfort constraints in 9 days. This is because the DMPC does not take into account the occurrence of positive uncertainty. The RMPC does not violate any comfort constraints, but consumes 25% more energy than does the DMPC. The ARMPC does not violate the thermal constraints on an days and at the same time consumes 12% less energy than the RMPC. This is because the ARMPC controls the zone temperature much closer to the set-point value. In terms of computational speed, DMPC is the most efficient one. Both RMPC and ARMPC have slower computational speed, because the exponential increased complexity with the increase of prediction horizon. The ARMPC is slower than RMPC because estimating the uncertainty bounds using RNN estimator requires extra computational efforts. The computational speed of ARMPC is reasonable and can be solved , because the RNN model can be trained offline and does not always need to be re-trained.

## 7.6 Conclusions

Studies on the use of MPC for reducing energy consumption in commercial buildings have been studies intensively in the recent years. One of the biggest obstacle of implementing MPC at real buildings is that predictive models may lose accuracy with the presence of

uncertainty, which could lead to thermal comfort violation and performance deteriorate. Using a commercial building as a case study, this study develops a new RMPC framework which can satisfies thermal comfort requirement, while still achieve considerable amount of energy saving under modelling uncertainty. As the major contribution of this paper, we have presented an adaptive bounds estimator, which allows the uncertainty bound of RMPC to vary according to the dynamic changes of the system. It is shown that the proposed method results in a smaller uncertainty bound when the actual uncertainty is low, which greatly reduces the conservatism of the RMPC. This makes the implementation of the MPC at real buildings more feasible. Besides this major finding, we have also made the following findings:

1. We have presented and compared two types of thermal dynamic models for the investigated building. Simulation result shows that the RNN model achieves more accurate long-term prediction result, whose generated error is closer to normal distribution, as compared with the linear RC model. We believe the former approach captures the uncertainty and nonlinearity of the system using its recursive property. The uncertainty causing the modelling error might be the heat gain generated by the occupants and the infiltration due to the opening the doors. This will be experimentally validated in the future study.

2. The closed-loop nature of the DMPC guarantees a certain degree of robustness. The modelling error does not always result in poor control performance, but also depends on the types of uncertainty and the time when this might happen. For example, the DMPC usually performs more robustly during the steady states as compared with the transitional period.

3. The selection of uncertainty bounds has a big impact on the performance of RMPC. An improper choice of the bounds can easily generate over-conservative control results, and waste energy.

Conclusively, the proposed control method has reasonably combined intelligent modelling technology with the classical control method. This opens up a new path for solving complicated real-world building energy control problem. As a future study, the proposed control method will be tested experimentally at the investigated building.

# References

[1] ASHRAE, *ASHRAE Handbook HVAC Applications.* Atlanta: American Society of Heating, Refrigerating, and Air-Conditioning Engineers,Inc., 2003.

[2] Y. Ma, A. Kelman, A. Daly, and F. Borrelli, "Predictive control for energy efficient buildings with thermal storage: Modeling, stimulation, and experiments," *Control Systems, IEEE*, vol. 32, pp. 44–64, Feb 2012.

[3] "Study of the optimal control problem formulation for modulating air-to-water heat pumps connected to a residential floor heating system," *Energy and Buildings*, vol. 45.

[4] D. Gyalistras and M. Gwerder, "Use of weather and occupancy forecasts for optimal building climate control (OptiControl): Two Years Progress Report Main Report," tech. rep., Terrestrial Systems Ecology ETH Zurich R&D HVAC Products, Building Technologies Division, Siemens Switzerland Ltd., Zug, Switzerland, 2010.

[5] H. Huang, L. Chen, and E. Hu, "A new model predictive control scheme for energy and cost savings in commercial buildings: An airport terminal building case study," *Building and Environment*, vol. 89, no. 0, pp. 203 – 216, 2015.

[6] P.-D. Moroan, R. Bourdais, D. Dumur, and J. Buisson, "Building temperature regulation using a distributed model predictive control," *Energy and Buildings*, vol. 42, no. 9, pp. 1445 – 1452, 2010.

[7] M. Gruber, A. Trschel, and J.-O. D. b, "Energy efficient climate control in office buildings without giving up implementability," *Applied Energy*, vol. 154, pp. 934 – 943, 2015.

[8] S. C. Bengea, A. D. Kelman, F. Borrelli, R. Taylor, and S. Narayanan, "Implementation of model predictive control for an HVAC system in a mid-size commercial building," *HVAC&R Research*, vol. 20, no. 1, pp. 121–135, 2014.

[9] J. Cai and J. E. Braun, "A generalized control heuristic and simplified model predictive control strategy for direct-expansion air-conditioning systems," *Science and Technology for the Built Environment*, vol. 21, no. 6, pp. 773–788, 2015.

[10] M. Razmara, M. Maasoumy, M. Shahbakhti, and R. R. III, "Optimal exergy control of building HVAC system," *Applied Energy*, vol. 156, pp. 555 – 565, 2015.

[11] S. F. Fux, A. Ashouri, M. J. Benz, and L. Guzzella, "EKF based self-adaptive thermal model for a passive house," *Energy and Buildings*, vol. 68, Part C, no. 0, pp. 811 – 817, 2014.

[12] S. Goyal, H. Ingley, and P. Barooah, "Effect of various uncertainties on the performance of occupancy-based optimal control of HVAC zones," in *Decision and Control (CDC), 2012 IEEE 51st Annual Conference on*, pp. 7565–7570, Dec 2012.

[13] M. M. F. Borrelli, A. Bemporad, *Predictive control for linear and hybrid systems*. June 2015.

[14] P. J. Goulart, E. C. Kerrigan, and J. M. Maciejowski, "Optimization over state feedback policies for robust control with constraints," *Automatica*, vol. 42, no. 4, pp. 523 – 533, 2006.

[15] J. Löfberg, *Minimax Approaches to Robust Model Predictive Control*. No. 812 in Linkping Studies in Science and Technology. Dissertations, 2003.

[16] S. Lucia, J. A. Andersson, H. Brandt, M. Diehl, and S. Engell, "Handling uncertainty in economic nonlinear model predictive control: A comparative case study," *Journal of Process Control*, vol. 24, no. 8, pp. 1247 – 1259, 2014.

[17] X. Li and T. E. Marlin, "Model predictive control with robust feasibility," *Journal of Process Control*, vol. 21, no. 3, pp. 415 – 435, 2011.

[18] S. H. Kim, "An evaluation of robust controls for passive building thermal mass and mechanical thermal energy storage under uncertainty," *Applied Energy*, vol. 111, no. 0, pp. 602 – 623, 2013.

[19] M. Maasoumy, M. Razmara, M. Shahbakhti, and A. S. Vincentelli, "Handling model uncertainty in model predictive control for energy efficient buildings," *Energy and Buildings*, vol. 77, no. 0, pp. 377 – 392, 2014.

[20] R. Gondhalekar, F. Oldewurtel, and C. N. Jones, "Least-restrictive robust periodic model predictive control applied to room temperature regulation," *Automatica*, vol. 49, no. 9, pp. 2760 – 2766, 2013.

[21] F. Oldewurtel, C. Jones, and M. Morari, "A tractable approximation of chance constrained stochastic mpc based on affine disturbance feedback," in *Decision and Control, 2008. CDC 2008. 47th IEEE Conference on*, pp. 4731–4736, Dec 2008.

[22] F. Oldewurtel, A. Parisio, C. N. Jones, D. Gyalistras, M. Gwerder, V. Stauch, B. Lehmann, and M. Morari, "Use of model predictive control and weather forecasts for energy efficient building climate control," *Energy and Buildings*, vol. 45, no. 0, pp. 15 – 27, 2012.

[23] F. Oldewurtel, D. Sturzenegger, P. Esfahani, G. Andersson, M. Morari, and J. Lygeros, "Adaptively constrained stochastic model predictive control for closed-loop constraint satisfaction," in *American Control Conference (ACC), 2013*, pp. 4674–4681, June 2013.

[24] Y. Ma, J. Matusko, and F. Borrelli, "Stochastic model predictive control for building HVAC systems: Complexity and conservatism," *Control Systems Technology, IEEE Transactions on*, vol. PP, no. 99, 2014.

[25] X. Zhang, G. Schildbach, D. Sturzenegger, and M. Morari, "Scenario-based mpc for energy-efficient building climate control under weather and occupancy uncertainty," in *Control Conference (ECC), 2013 European*, pp. 1029–1034, July 2013.

[26] M. Sourbron, C. Verhelst, and L. Helsen, "Building models for model predictive control of office buildings with concrete core activation," *Journal of Building Performance Simulation*, vol. 6, no. 3, pp. 175–198, 2013.

[27] M. Gouda, S. Danaher, and C. Underwood, "Building thermal model reduction using nonlinear constrained optimization," *Building and Environment*, vol. 37, no. 12, pp. 1255 – 1265, 2002.

[28] L. Ljung, ed., *System Identification (2Nd Ed.): Theory for the User*. Upper Saddle River, NJ, USA: Prentice Hall PTR, 1999.

[29] J. J. Mor and D. C. Sorensen, "Computing a trust region step," *SIAM Journal on Scientific and Statistical Computing*, vol. 4, no. 3, pp. 553–572, 1983.

[30] H. Huang, L. Chen, and E. Hu, "A neural network-based multi-zone modelling approach for predictive control system design in commercial buildings," *Energy and Buildings*, vol. 97, no. 0, pp. 86 – 97, 2015.

[31] J. Lee, "Model predictive control: Review of the three decades of development," *International Journal of Control, Automation and Systems*, vol. 9, no. 3, pp. 415–424, 2011.

[32] A. Richards and J. How, "Robust model predictive control with imperfect informa-

tion," in *American Control Conference, 2005. Proceedings of the 2005*, pp. 268–273, June 2005.

[33] H. Fukushima and R. R. Bitmead, "Robust constrained predictive control using comparison model," *Automatica*, vol. 41, no. 1, pp. 97 – 106, 2005.

[34] K. Hariprasad and S. Bhartiya, "Adaptive robust model predictive control of nonlinear systems using tubes based on interval inclusions," in *Decision and Control (CDC), 2014 IEEE 53rd Annual Conference on*, pp. 2032–2037, Dec 2014.

[35] Löfberg, "Yalmip : A toolbox for modeling and optimization in MATLAB," in *Proceedings of the CACSD Conference*, 2004.

# Chapter 8

# Discussion and Conclusion

## 8.1 Contributions

The focus of this thesis was to develop an MPC framework used for achieving energy and cost savings in a large commercial building equipped with an HVAC system. A summary of the main contributions of this dissertation is provided below:

- *We proposed a cascade NN modelling framework that uses neighbouring zone temperature as an input to conduct indoor temperature prediction*. It shows that the thermal coupling between zones could be significant, which should not be ignored during the control design process. This result could be used to achieve some application purposes. For example, the proposed cascade NN can be used as a tool to test the degree of thermal interaction between zones. For the zones that are not strongly coupled, considering the thermal coupling may not result in any improvement in the modelling accuracy, then it is possible to treat the two zones separately. On the other hand, if the coupling is significant, it is then possible to make use of the neighbouring zone temperature as a disturbance observer to improve the control performance of the investigated zone model. Another interesting application is to use the model structure for sensor-free control: once the thermal connection be-

tween a certain zone and its neighbouring zone is identified, the sensor for this zone can be replaced by an artificial sensor. It is then possible to use the neighbouring zone temperature to monitor or control the temperature in the investigated zone.

- *We proposed a MIMO model that considers the convective heat transfer between zones to model multi-zone buildings*. The MIMO model considers the feedback prediction for several zones, and perform long-term indoor prediction for the investigated zones simultaneously. The result shows that the MIMO model can learn the convective heat transfer phenomenon within the building system, which also results in more accurate long-term prediction results and better control performance as compared to the single zone models. The MIMO model can be used for the purpose of predictive control design.

- *We presented a model based optimal start-stop control method to reduce energy consumption in buildings*. By carefully analysing the historical data, we conclude that one of the main causes for energy waste in the investigated building is that the zone temperature trajectory does not follow the actual occupancy schedules. Therefore, based on the previously developed NN models, we presented an optimal start-stop control method, which generates the optimal operational schedules for the local AHUs. The most attractive feature of this method is that the control algorithm can be built quickly and accurately, once data are available, which directly results in energy savings. The computational burden of this method is also low as the algorithm only need be applied at the start and end of occupancy.

- *We have made a comparison between the two most popular building models: the RC model and the NN model*. It is found that, for the investigated zones, the RNN model in general achieves more accurate long-term prediction result as compared with the low-order RC model. Additionally, the errors generated by the RNN model were closer to a normal distribution. These facts indicate that the RNN models are able

to capture the uncertain property of the investigated building, which is missed by the RC model. Similarly, we have proven that due to their nonlinearity, the AHUs' dynamics cannot be modelled accurately by linear models but the RNN model.

- *We presented an HMPC that combines the merits of classical MPC and intelligent model for achieving energy and cost savings in buildings.* A major advantage of the HMPC is its computational efficiency, since the optimisation problem can be solved using a fast linear programming method. The inverse NN model handles system nonlinearity associated with the AHUs process and provide more accurate control input. Simulation results show that without considering TOU electricity tariffs, the HMPC behaves similarly to the NN based optimal start-stop control method proposed in *Paper-2*. With the TOU electricity tariff considered, the HMPC triggers pre-cooling to store cooling energy and to shift the cooling load.

- *Through an experimental study, we have proven that the pre-cooling technology could also be applied to large commercial buildings to achieve cost savings*. However, because this strategy saves electricity bill at the cost of consuming more off-peak energy, it does not always suit any type of buildings. Factors such as weather conditions, TOU electricity price and the degree of thermal mass contained in the physical body, should be evaluated before applying this strategy to a specific building.

- *We have developed an uncertainty bound estimator for the closed-loop RMPC to reduce its conservatism for building energy control*. By conducting robust analyses in *Paper-4*, it has been found that the probability of thermal comfort violation is higher during the transitional period than during the steady state period. Based on the previously demonstrated RNN model, we have developed an adaptive bounds estimator, which allows the uncertainty bound of RMPC to vary according to the dynamic changes of the system. This method also offers a good compromise be-

tween conservatism and robustness.

## 8.2 Directions for Future Research

The work presented in this thesis has successfully contributed to the knowledge of the application of MPC to building energy systems. The methodology developed in this thesis is not limited to the similar building type but could be extended to a number of other building types, such as rooftop unit systems and compact air conditioners in the residential buildings. Recently, we have applied the optimal start-stop method introduced in Chapter 5 to an educational building, which achieved 30% energy savings. Despite this, some improvements could still be made to improve the existing technology. Some possible directions for future research are outlined below:

- We have shown in *Paper-1* that the thermal interaction plays an important role in controlling multi-zone buildings. However, another raised issue is that the size of the control problem grows rapidly as the number of AHUs and controlled zones increases. This makes the implementation of the designed control method difficult. When the number of considered rooms is large, a distributed MPC may be necessary. Considering the delay in the communication of input trajectories among subsystems may cause problems, future research can be focused on designing more computationally efficient algorithms for handling possible disruptions and delays.

- By conducting field work, it has been found that incorrect operation and faulty components can cause a significant amount of energy waste in the HVAC systems. A typical example is the faults detected in the operation of economizer in *Paper-3*. Considering the complexity of the HVAC systems, the models developed in this thesis can be used for the development of model-based fault detection and diagnosis techniques. These techniques can be used to detect possible faults/failures that may occur in the sensors and actuators of the HVAC systems to achieve energy savings

and guarantee smooth operation of the new control strategy.

- In *Paper-3* the TOU electricity rate has been considered in the cost function. It will be interesting to investigate the performance of the MPC by incorporating both demand charge and time-varying electricity tariff based on the spot market price level into the cost function. This may provide solutions that flavour the electricity grid.

- Considering thermal comfort can further improve the energy efficiency of the building control. Identifying a thermal comfort model adds some difficulties because the estimation problem has a higher dimension when a moisture model is included. The coupling effect makes both the thermal and moisture models nonlinear and their identification becomes computationally demanding when using iterative methods. This is worth investigating and will be considered in our future study.

# Appendix A

# Conference Papers

## A.1 Conference-1

*Full citation*: Huang H., Chen L., M. Mohammadzaheri., Hu E., Chen ML., "Multi-zone temperature prediction in a commercial building using artificial neural network model", In Control and Automation (ICCA), 2013 10th IEEE International Conference on, pp. 1896-1901, 2013.

This paper is an extension of *Paper-1*. This paper uses forecasted outdoor temperature instead of measured one to perform long-term prediction. The influence of weather forecast error on the modelling accuracy is analysed.

2013 10th IEEE International Conference on Control and Automation (ICCA)
Hangzhou, China, June 12-14, 2013

# Multi-zone temperature prediction in a commercial building using artificial neural network model

Hao Huang, Lei Chen, *Member, IEEE*, Morteza Mohammadzaheri, *Member, IEEE*, Eric Hu, and Minlei Chen

***Abstract*— Predicting temperature in buildings equiped with Heating, ventilation and air-conditioning (HVAC) systems is a crucial step to take when implementing a model predictive control (MPC). This prediction is also challenging because the buildings themselves are nonlinear, have many uncertainties and strongly coupled. Artificial neural networks (ANNs) have been used in previous studies to solve such a modeling problem. Unlike most of the studies that have only considered small-scale, single zone modeling task, this paper presents a novel ANN modeling method for the modeling inside a real world multi-zone building. By comparing ANN models with different input variables, it was found that the prediction accuracies can be greatly improved when the thermal interactions were considered. The proposed models were used to perform both single-zone and multi-zone temperature prediction and achieved very good accuracies.**

**Keywords:** ***HVAC; Model predictive control; Artificial neural network; Multi-zone*.**

## I. INTRODUCTION

Heating, ventilation and air-conditioning (HVAC) systems contribute the largest proportion of energy consumption in buildings. A small increase of efficiency in the performance of the HVAC system can result in significant amount of energy savings. For this reason, building energy control has become a very active topic in the recent years [1], [2].

An important reason for the low efficiency of the HVAC systems in commercial buildings is that their control parameters are not adaptable to the changing weather conditions, occupancy level and human activities. This inevitably leads to thermal discomfort, inefficient use of energy, and high maintenance costs [3]. To solve these issues, many researchers have dedicated their efforts on the model predictive control (MPC) for building energy control in the past ten years. [2], [4]–[6]. When the MPC is used for building control, the temperature inside the building is predicted several hours to days in advance, so that the control variables of the HVAC system can be optimized to meet thermal demands and to achieve minimum energy cost. Obviously, a well-designed predictive model which describes the relationships between inputs (ambient temperature, HVAC operating status, etc.) and the output (indoor temperature) is essentially important.

Predicting temperature inside commercial buildings is a complicated task. First, a building's operational environment is time-varying system with several unknown delays and uncertainties. For example, a sudden change of outdoor temperature or occupants number will cause the change of indoor temperature. Furthermore, HVAC systems have complicated nonlinear relationships including temperature, humidity and damper actions. Finally, the internal space of large commercial buildings is always divided into several adjacent zones, each of which is controlled by a standalone air handling units (AHU). The temperatures inside these zones are not uniform and strongly coupled, which makes the accurate prediction of zone temperature very difficult.

To solve such a modeling problem, three approaches have been reported in the literature. The first one is to build thermal models based on energy-and-mass balance equations [2], [7]. A second approach uses lumped capacitance in an analogue electric to represent thermal elements of a building and uses genetic algorithms (GA) to optimize the parameters of the models [1], [8]. The third approach is based on machine learning, in which artificial neural networks (ANNs) were used to model non-linear processes by learning the historical data [3], [9]–[12]. When a large amount of historical data are available from the building management systems (BMS), the ANN becomes the most efficient modeling method because it only requires information on the input-output data.

The use of artificial intelligence in building modeling and control have been extensively studied in the past ten years. For example, an online ANN controller was developed and used in [4] to control a commercial ice storage of an HVAC system. The controller determined the hourly set-points for the chiller plant in order to minimize the total cost over a 24-hour period. In another study, a backpropagation-based ANN model was developed to determine the rising time for a heating system in a building [13]. The similar model structure was later used in [14] to increase the thermal comfort level of occupants and reduce energy consumption by reducing temperature overshoot and undershoot phenomena in an air conditioning system. To make the best of ANN model, Ruano et al. [11] incorporated a multiple objective genetic algorithm with radial basis function neural networks to build an adaptive model to predict indoor temperature of a school building. This model was used to determine ON/OFF time for an air conditioning system, and shows good energy savings result. A feed-forward neural network was used by Lu and Viljanen [12] to construct a nonlinear autoregressive with external input (NNARX) model to predict both indoor temperature and relative humidity. Using as many as ten different input variables, Mustafaraj et al. [5] developed an ANN model using BMS data to predict the thermal behavior of an open office. The ANN model was also shown better compared with the linear model.

[1]Research supported by Adelaide Airport Limited.

[2]All authors are with the Faculty of Mechanical Engineering, University of Adelaide, SA 5005, Australia (email: h.huang@adelaide.edu.au)

A general concern of the above modeling work is that a building process is nonlinear, time-varying and weather dependant. However, they were all focused on single-zone modeling, or made assumption that the zone temperature distribution is unifrom [1]. The coupling affects among adjacent zones were not considered. In real-life buildings, thermal characteristics of the zones are very different from one to another, and are correlated with each other. It is therefore necessary to develop a method suitable for multi-zone modeling, so that they can be used to predict zone temperature at any locations of a building.

The objective of this paper is to present an ANN based modeling method which can be used to predict multi-zone temperature. To achieve the goal, data obtained from different zones of a real building was used for experiment purposes. The proposed model considers neighboring zone temperature as a variable to build relationships among zones. The importance of this variable was evaluated under the guidance of a feed-forward input variables selection criterion. The results show the prediction accuracy of the model was greatly improved when the neighboring zone temperature was taken into account.

The rest of the paper is organized as follows: Section 2 describes the building process using analytical models. Section 3 introduced the employed ANN model, data preparation method and multi-zone modeling method. In section 4, the proposed models will be tested on two separated zones first and then two adjacent zones. The prediction results when the neighboring zone temperature is used as an input or not are compared to shown the importance of thermal interaction in zone temperature prediction.

## II. SYSTEM DESCRIPTIONL

### A. Zone process

To identify the most relevant input variables used for ANN modeling and investigate the thermal interactions affects between zones, some detailed information on the zone process should be investigated. For this reason, analytical models for a double-zone case were built. Fig. 1 shows the energy (balance) network diagram of a double-zone case. These two zones are adjacent to each other with no wall between them. Before building the models, three assumptions were made: 1. Temperature distribution in each zone is uniform; 2. The density of the air and air-flow rates are constant; 3. Two zones have the same heat transfer area of the wall. Energy and mass balance governing equation of the zone can therefore be written as:

$$C_{z1}\frac{dT_1}{dt} = C_{air}f_1\rho_{air}(T_{sa}-T_1)+ C_{air}f_2\rho_{air}(T_2-T_1)+\sum_{s=1}^{n}h_sA_s(T_s-T_1)+q_c, \quad (1)$$

$$C_{z2}\frac{dT_2}{dt} = C_{air}f_1\rho_{air}(T_{sa}-T_2)+ C_{air}f_3\rho_{air}(T_1-T_2)+\sum_{s=1}^{n}h_sA_s(T_s-T_2)+q_c, \quad (2)$$

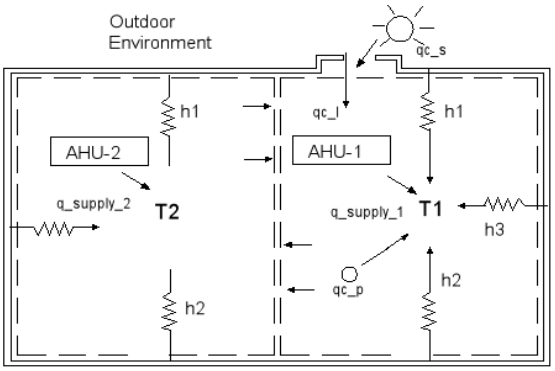


Fig. 1. Model for calculating zone temperatures

where $C_{z1}$ and $C_{z2}$ are the overall thermal capacities (kJ/C) of zone-1 and zone-2 respectively, $T_1$ and $T_2$ are Zone-A and Zone-B temperature, respectively, $T_{out}$ is the outdoor temperature, $T_{sa}$ is the supply air temperature, $T_s$ is the temperature of inside surface of the wall, $\rho_{air}$ is the air density ($kg/s^3$), $f_1$ is volume flow rate of the supply air ($m^3/s$), $f_2$ and $f_3$ are volume flow rates of two zones due to convection respectively ($m^3/s$), $h_s(W/m^{2\circ}\text{C})$ the heat transfer coefficient for surface of the wall, $A_w$ area of the wall $m^2$. $q_c$ stands for heat gain from the solar radiation (qc_l), occupants (qc_p), and leakage of wall (qc_l), etc. Eq. (1) and Eq. (2) illustrate that the rates of temperature change in a zone is related to the air flow rates, temperature difference between zone temperature and outdoor temperature, supply air temperature and neighboring zone temperature. It can be seen that the influence of the neighboring zone on the objective zone is significant only when the temperature difference is big.

The HVAC system used for the case study has 3 chillers for cooling and 3 boilers for heating. Fig. 2 shows the schematic diagram of a chiller plant: chilled water is transmitted from the chiller plants to the cooling coils at individual AHUs through control of variable speed water pumps. The cooling load $Q$ can be calculated by:

$$Q = \dot{m}C_p(T_{chwr}-T_{chws}), \quad (3)$$

where $\dot{m}$ is mass flow rate of chilled water ($kgs^{-1}$), $C_p$ is the specific heat of chilled water ($Jkg^{-1}K^{-1}$), $T_{chws}$ is the temperature of supply chilled water; $T_{chwr}$ is chilled water return temperature (°C). Eq. (3) shows the cooling (heating) capacity of a HVAC system is closely related to the temperature and mass flow rates of the chilled (hot) water. The change of this capacity will cause the change of supply temperature $T_s$), in turn cause the temperature change at individual zones.

At the subsystem level, 177 AHUs are running in parallel to serve different zones. Fig. 3 shows the schematic diagram of a constant air volume (CAV) air-handling unit, which consists of a cooling coil, a heating coil, water valves, fans and air dampers. The return air is recirculated through the

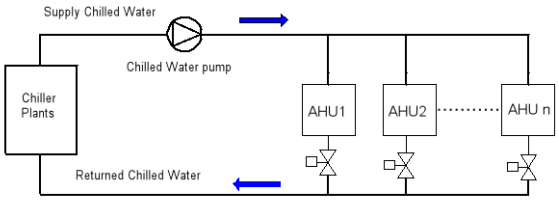


Fig. 2. Schematic of a chiller plant

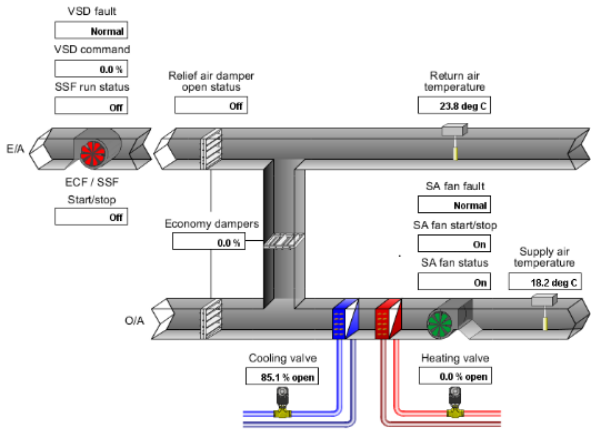


Fig. 3. Schematic of an AHU

mixed air damper or exhausted through the exhaust damper, depending on the position of these two dampers. The fresh air enters the circuit through the outdoor air damper and then mixed with the return air. The mixed air then passes through the cooling coil and the air temperature decreases after the heat exchange. The chilled (hot) water valve is controlled proportionally to the difference between measured zone temperature and setpoint temperature to maintain the zone temperature. The AHUs have fixed-speed fans thus the airflow is a constant value.

After analyzing the main features of zone process and HVAC system, a number of variables were identified as input variable candidates and they are shown in Table I. These variables will be selected for ANN modeling in the next section.

TABLE I
CANDIDATURE INPUT VARIABLES

| Variables | Description | Unit |
|---|---|---|
| Controllable variables | | |
| $CV$ | Chilled water valve opening level | °C |
| $SP$ | Setpoint temperature | °C |
| $WT$ | Chilled (hot) water temperature | °C |
| Uncontrollable variables | | |
| $OT$ | Outdoor temperature | °C |
| $FR$ | Chilled (hot) water flow rate | % |
| $T$ | Zone temperature | °C |

## III. MODELING

### A. Model Structure

Nonlinear auto-regressive models with eXogenous inputs (NARX models) are commonly used for classical system identification [15]. According to this NARX structure, for a single-input, single-output system, the dynamics can be expressed by the following equations:

$$\widehat{y}(t) = f[\phi(t), w] + e(t), \tag{4}$$

$$\phi(t) = [y(t-1)...y(t-n_a), u_1(t-k_1)...u_1(t-n_b-k_1+1), ..., u_i, (t-k_i)...u_i(t-n_i-k_i+1)], \tag{5}$$

where $i$ is the number of input variables, $k$ is the delay time of input variables, $n_a$ to $n_i$ are the orders of input variables, $f$ is an approximated nonlinear function, $w$ is the weighting factor, and $e(t)$ is the error caused by unknown factors. The delay time and inputs orders indicate the physical characteristic of a dynamic systems.

### B. Data Preparation

Data preparation is to arrange the input-output data in an appropriated order so that they can be directly used for model training. In this study, a data preparation method introduced in [16] was used. To build an initial model, two most relevant inputs variables, outdoor temperature and setpoint temperature were chosen to form the initial model structure. The data were prepared and stored in the following matrix:

$$\begin{bmatrix} \overbrace{ZT_r \ \cdots \ ZT_{r-n_a+1} \quad OT_r \ \cdots \ OT_{r-n_b+1} \quad SP_r \ \cdots \ SP_{r-n_c+1}}^{Input} & \overbrace{Zt_{r+1}}^{Output} \\ \vdots \quad \ddots \quad \vdots \quad \vdots \quad \ddots \quad \vdots \quad \vdots \quad \ddots \quad \vdots & \vdots \\ ZT_n \ \cdots \ ZT_{n-n_a+1} \quad OT_n \ \cdots \ OT_{n-n_b+1} \quad SP_n \ \cdots \ SP_{n-n_c+1} & Zt_{n+1} \end{bmatrix}$$

where $r$ is the maximum order of the input and output variables, and $n$ is the number of data used for training. After the data were prepared in this way, they can directly used for model training.

Since some of the candidate variables selected may be correlated, noisy and have no significant relationships with the outputs, a suitable input variable selection criterion is needed. To find out the best inputs combination, a feed-forward selection criterion is employed to obtain the best model structure and to investigate the relevance of each input variable [17]. This method is quite straightforward: the initial candidate input variables are chosen based on the prior knowledge of the system. The performance of the model is then maximized by changing the orders of input variables $r$. After the last optimization process is finished, the new candidature variables are added and the same process repeated again. The most important variables can then be identified when the whole process is finished.

### C. Model Creation

ANNs are mathematical models inspired by biology neural networks. They mimic humans neuron system in order to acquire learning ability. Learning from historical data, the networks adjust the connection weights among the neurons according to learning rules, so the trained networks can

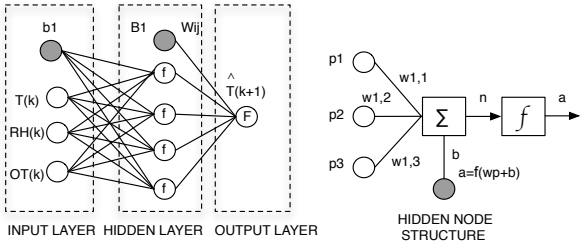


Fig. 4. Three-layer feedforward neural networks

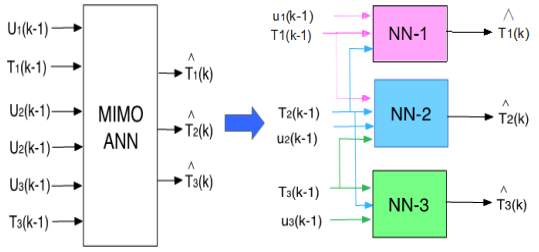


Fig. 5. ANN model for multi-zone modeling

generate correct outputs. The most commonly used ANN structure is Multi-layer-perceptrons (MLPs) based on back-propagation and it is also employed in this study.

AnANN with three layers of neurons and three input variables was first employed for training and its structure is shown in Fig. 4. In this model, the inputs from the previous layer are multiplied by the weights, summed up and added with a bias. The results pass an activation function at the hidden layer and then go to the next layer. The hidden layer uses a logistic sigmoid function as the activation function. Eq. (4) can therefore be rewritten as:

$$\hat{y}(t) = \sum_{i=1}^{n_h} W_{1j} logsig(\sum_{i=1}^{n_u} w_{ij} u_i + b_{j0}) + B_{10}, \quad (6)$$

where $w_ij$ and $W_ij$ are weights to the hidden layer and output layer, respectively. $B_ij$ and $b_ij$ are the corresponding bias. The weights and bias at the hidden layer were initialised using the Nguyen-Widrow method to keep the resulting model more consistent. Levenberg-Marquardt was employed to train the neural networks in 500 epochs, and the training process was terminated when the target mean square error (MSE) was reached.

### D. Multi-zone modeling

The thermal dynamics of a multi-zone building can be represented by a interconnected system of several zones. Fig. (6) shows the layout of the experimental areas used in this study. They can be classified into external zones which are directly connected to the ambient environment and interior zones which are in the middle of the building. Obviously, outdoor temperature affects the external zones through convection, conduction and radiation but not the interior zones. Considering this fact, a multi-zone temperature prediction should have the following rules:

- To predict the external zone temperatures, both outdoor temperature and their neighboring zone temperature should be considered as the input variable.
- To predict the interior zone temperatures, only their neighboring zone temperatures should be used as an input.
- External zone temperatures must be predicted first and then used as a input to predict interior zone temperatures.

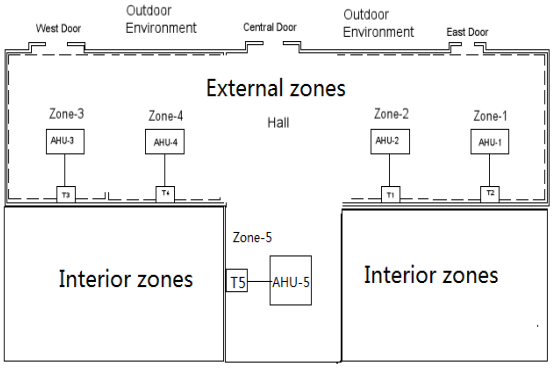


Fig. 6. Layout of the experiment areas

Based on the above rules, a multi-zone modeling method based on ANN is proposed. A example is given to illustrate this method. A three inputs, three outputs ANN model with the structure as shown in Fig. (5) is used to express the dynamic behavior of a three-zone process, where $u_1$ to $u_3$ are the input variables, $T_1$ to $T_3$ are measured zone temperatures and $\hat{T}_3$ is the predicted zone temperature. Following the rules set above, this model can be decoupled into three individual multiple-inputs, single-output (MISO) models. Each MISO model represents the thermal characteristic of a single zone, but still maintains connection with its neighboring zones. The availability of this method on a real building will be tested in the following section.

## IV. EXPERIMENT RESULTS AND DISCUSSIONS

Once the ANN model are determined using the method described above, the model is tested under real building environment. The experimental data used in this study were collected from a commercial building management system (BMS) at 10 minutes intervals during spring and summer season (Oct, 2012 to Feb, 2013 ) at terminal building of Adelaide airport. The outdoor temperature data is collected from a public weather forecast website. Several individual thermal zones, as shown in Fig. 6, were selected to test the modeling method. Each zone is installed with a temperature sensor to detect the zone temperature and controlled by individual AHUs. Mean of square errors (MSE) between measured temperature and predicted temperature is used to test the performance of the model:

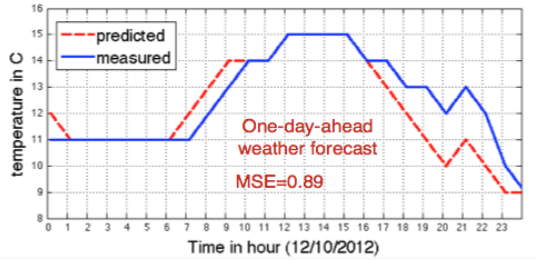


Fig. 7. Comparison of forecast outdoor temperature and real temperature

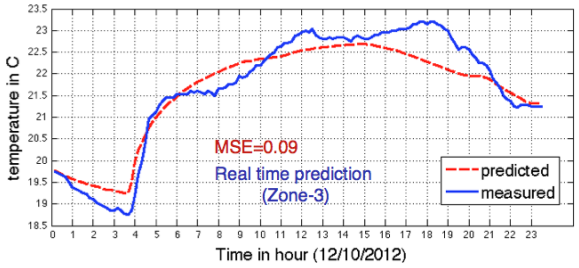


Fig. 8. One day ahead prediction result for Zone-3

$$MSE = \frac{\sum_{i=1}^{n}(\hat{y} - y)^2}{n}, \tag{7}$$

where y is measured output, $\hat{y}$ is the predicted output, and $n$ is number of data. Because the model developed in this study is used for predictive control (with a horizon of two or more), multiple steps ahead prediction accuracy should be concerned. To illustrate the problems, three different experiments were conducted and their results shown in the following sections.

### A. Single-zone prediction

The first experiment aims to investigate the real time prediction accuracies of a single-zone model. Real-time prediction means the model uses forecast outdoor temperature instead of the measured one as an input to predict indoor temperature. For this purpose, Zone-3 located at the west end of the building was selected as the experiment area. The heating system was operating during the day and the setpoint temperature was set to be 23 °C. Using the feed-forward input variable selection method mentioned , it was found that the ANN models with the following structure can generate the best prediction results for Zone-3:

$$\begin{aligned}\hat{T_3}(t) = f(&T_3(t-1), T_3(t-2), T_3(t-3), T_3(t-4),\\ &OT(t-1), OT(t-2), OT(t-3), SP(t-1)).\end{aligned} \tag{8}$$

where $f$ is the ANN nonlinear function. Eq. (8) shows setpoint temperature and outdoor temperature were the most important variables for indoor temperature prediction. Adding input variables such as chilled water temperature and chilled water flow rate inputs did not bring any improvement to ANN model. The reason is that these two variables are both influenced by the outdoor temperature, which has already been considered in the model. Fig. 8 shows that, using the weather forecast data, Zone-3 temperature can be predicted by the ANN model with a MSE less than $0.1°C$. This prediction result is accurate enough for the design of a MPC. Fig. 7 compares the one-day-ahead forecast temperature with the measured temperature on the test day, which shows a MSE of 0.89 between forecast temperature and recorded temperature. The largest weather forecast error happened at 19:00 pm, leading to a maximum error of $1°C$ at the same time .

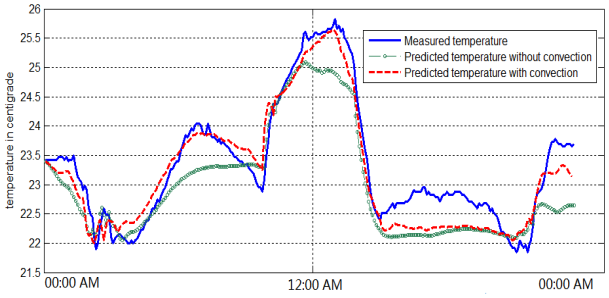


Fig. 9. Predicted Zone-1 temperature when Zone-2 temperature is used or not

### B. Thermal coupling investigation

The second experiment was designed to investigate the importance of thermal interactions between adjacent zones. To achieve this goal, Zone-1 and Zone-2 located at the east end of the building were selected for the test. The data was chosen from hot summer day on January, 2013. Two different types of model structures were used to predict Zone-1 temperature: one uses Zone-2 temperature as an input and the other did not. The simulation results were shown in Fig. 9. It is shown that by adding the Zone-2 temperature as an input, the prediction accuracy for Zone-1 was greatly improved. This indicates that interaction between zones caused by convection is important and the proposed model has revealed the significance.

### C. Multi-zone prediction

The third experiment was conducted to test the proposed multi-zone modeling method. Two adjacent zones, Zone-4 and Zone-5 were selected for this purpose. From Fig. (4), it can be seen that Zone-5 is not directly connected to the outdoor environment but to Zone-2 and Zone-4. According to the aforementioned modeling rule, to predict Zone-4 temperature, the outdoor temperature will be used as an input; To model Zone-5, Zone-4 temperature will be used as the inputs. In this way, both Zone-4 and Zone-5 temperatures can be predicted simultaneously. The following equations were obtained after model optimization:

$$\begin{aligned}\hat{T_4}(t) = f(&T_4(t-1), T_4(t-2), T_4(t-3),\\ &OT(t-1), OT(t-2), OT(t-3), SP_4(t-1)),\end{aligned} \tag{9}$$

$$\begin{aligned}\hat{T_5}(t) = f(&T_5(t-1), T_5(t-2), T_5(t-3), T_5(t-4)\\ &T_4(t-1), T_4(t-2), T_4(t-3), SP_5(t-1)).\end{aligned} \tag{10}$$

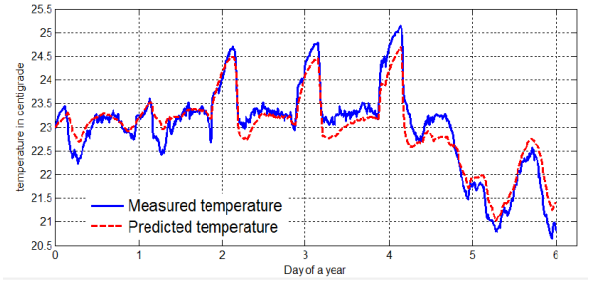


Fig. 10. Multi-zone prediction results for Zone-4

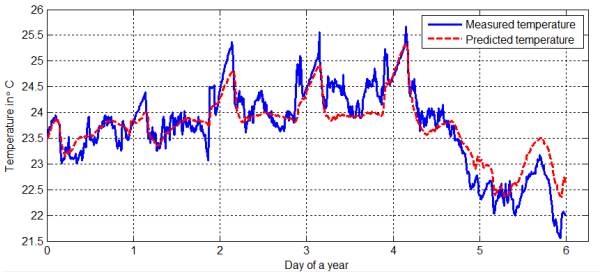


Fig. 11. Multi-zone prediction results for Zone-5

Using the model structure indicated in Eq. (9) and Eq. (10), ANN models were used to perform zone temperature predictions for both Zone-4 and Zone-5. Fig. 10 and Fig. 11 show that the ANN model can maintain prediction errors of less than 0.3 °C in both external and interior zones for successive 6 days. The prediction This proves that the proposed method is suitable to be used for multi-zone temperature prediction in real buildings. The MSE between measured values and prediction of Zone-4 is 0.15°C, while the error is about 0.25 °C for Zone-5. This error may be occurred because of increase in occupants number

## V. CONCLUSION AND FUTURE WORK

We propose an ANN based modeling method for multi-zone temperature prediction in commercial buildings. Using simple but reasonable input combinations, the proposed model is able to perform real time temperature prediction with good accuracies. The result of experiment-1 also shows the performance of the predictive model largely relies on the weather forecast accuracy. Another contribution is the use of proposed model to identify the significance of thermal convection between zones. The second experiment shows adding neighboring zone temperature as an input variable can improve the performance of the model, especially when the temperature difference between two zones is big. Based on this result, it is possible to build predictive models for both external zones and interior zones on the basis of outdoor temperature and control inputs within large commercial buildings. The results shown in Fig. 10 and Fig. 11 have also proved the availability of this method.

All the data used for modeling in this study were obtained from a commercial BMS system. This method is meaningful because predictive models can be built inside a built without the need to obtain too much knowledge about the system. As the future work, a robust test on the proposed models will be conducted before they are used for MPC design. If successful, the MPC can be designed for energy efficiency control in buildings.

## REFERENCES

[1] N. Nassif, S. Moujaes, and M. Zaheeruddin, "Self-tuning dynamic models of hvac system components," *Energy and Buildings*, vol. 40, no. 9, pp. 1709 – 1720, 2008.

[2] F. Oldewurtel, A. Parisio, C. N. Jones, D. Gyalistras, M. Gwerder, V. Stauch, B. Lehmann, and M. Morari, "Use of model predictive control and weather forecasts for energy efficient building climate control," *Energy and Buildings*, vol. 45, no. 0, pp. 15 – 27, 2012.

[3] N. Morel, M. Bauer, M. El-Khoury, and J. Krauss, "Neurobat, a Predictive and Adaptive Heating Control System Using Artificial Neural Networks," *Solar Energy Journal*, vol. 21, pp. 161–201, 2001.

[4] D. D. Massie, "Optimization of a building's cooling plant for operating cost and energy use," *International Journal of Thermal Sciences*, vol. 41, no. 12, pp. 1121 – 1129, 2002.

[5] T. Chow, G. Zhang, Z. Lin, and C. Song, "Global optimization of absorption chiller system by genetic algorithm and neural network," *Energy and Buildings*, vol. 34, no. 1, pp. 103 – 109, 2002.

[6] Y. Ma, F. Borrelli, B. Hencey, B. Coffey, S. Bengea, and P. Haves, "Model predictive control for the operation of building cooling systems," *Control Systems Technology, IEEE Transactions on*, vol. 20, no. 3, pp. 796 –803, may 2012.

[7] B. Tashtoush, M. Molhim, and M. Al-Rousan, "Dynamic model of an hvac system for control analysis," *Energy*, vol. 30, no. 10, pp. 1729 – 1745, 2005.

[8] G. Platt, J. Li, R. Li, G. Poulton, G. James, and J. Wall, "Adaptive hvac zone modeling for sustainable buildings," *Energy and Buildings*, vol. 42, no. 4, pp. 412 – 421, 2010.

[9] A. Mechaqrane and M. Zouak, "A comparison of linear and neural network arx models applied to a prediction of the indoor temperature of a building," *Neural Comput. Appl.*, vol. 13, no. 1, pp. 32–37, Apr. 2004.

[10] J. Yang, H. Rivard, and R. Zmeureanu, "On-line building energy prediction using adaptive artificial neural networks," *Energy and Buildings*, vol. 37, no. 12, pp. 1250 – 1259, 2005.

[11] A. Ruano, E. Crispim, E. ConceiA, and M. LAcio, "Prediction of building's temperature using neural networks models," *Energy and Buildings*, vol. 38, no. 6, pp. 682 – 694, 2006.

[12] T. Lu and M. Viljanen, "Prediction of indoor temperature and relative humidity using neural network models: model comparison," *Neural Computing and Applications*, vol. 18, pp. 345–357, 2009, 10.1007/s00521-008-0185-3.

[13] I.-H. Yang, M.-S. Yeo, and K.-W. Kim, "Application of artificial neural network to predict the optimal start time for heating system in building," *Energy Conversion and Management*, vol. 44, no. 17, pp. 2791 – 2809, 2003.

[14] J. W. Moon and J.-J. Kim, "Ann-based thermal control models for residential buildings," *Building and Environment*, vol. 45, no. 7, pp. 1612 – 1625, 2010.

[15] M. Mohammadzaheri, S. Grainger, and M. Bazghaleh, "Fuzzy modeling of a piezoelectric actuator," *International Journal of Precision Engineering and Manufacturing*, vol. 13, pp. 663–670, 2012. [Online]. Available: http://dx.doi.org/10.1007/s12541-012-0086-3

[16] M. Mohammadzaheri and L. Chen, "Double-command fuzzy control of a nonlinear cstr," *Korean Journal of Chemical Engineering*, vol. 27, pp. 19–31, 2010.

[17] H. Huang, L. Chen, M. Mohammadzaheri, and E. Hu, "A new zone temperature predictive modeling for energy saving in buildings," *Procedia Engineering*, vol. 49, no. 0, pp. 142 – 151, 2012, international Energy Congress 2012. [Online]. Available: http://www.sciencedirect.com/science/article/pii/S1877705812047790

## A.2 Conference-2

*Full citation*: Huang H., Chen L., Hu E., "Model predictive control for energy-efficient buildings: An airport terminal building study", In Control Automation (ICCA), 11th IEEE International Conference on, pp. 1025-1030, 2014.

This paper introduces a new simulation method to test developed MPC algorithms. In the simulation, an RNN model built with measured data is used to replace the actual building to provide feedback to the MPC. A linear MPC is tested under the simulation platform to demonstrate feasibility of this method. This simulation method is latter applied in *Paper-3* and *Paper-4*.

Huang, H., Chen, L. & Hu, E. (2014). Model predictive control for energy-efficient buildings: An airport terminal building study. *11th IEEE International Conference on Control & Automation (ICCA)*, 1025-1030.

NOTE:
This publication is included on pages 209 - 214 in the print copy of the thesis held in the University of Adelaide Library.

It is also available online to authorised users at:

http://dx.doi.org/10.1109/ICCA.2014.6871061

## A.3 Conference-3

*Full citation*: Huang H., Chen L., Hu E., "A hybrid model predictive control scheme for energy and cost savings in commercial buildings: Simulation and experiment", In American Control Conference (ACC), 2015, pp. 256-261, 2015.

This paper is a short-version of *Paper-3*.

Huang, H., Chen, L. & Hu, E. (2015). A hybrid model predictive control scheme for energy and cost savings in commercial buildings: Simulation and experiment. *2015 American Control Conference (ACC)*, 256-261.

NOTE:
This publication is included on pages 216 - 221 in the print copy of the thesis held in the University of Adelaide Library.

It is also available online to authorised users at:

http://dx.doi.org/10.1109/ACC.2015.7170745